

AN ABSTRACT OF THE THESIS OF

Asher Simmons for the degree of Master of Science in Electrical and Computer Engineering presented on November 7, 2013.

Title: A Frequency-Domain Approach to Simulating Wave Energy Converter Hydrodynamics

Abstract approved: _____

Mario E. Magaña

Wave energy converter (WEC) devices are complicated systems containing hydrodynamic, mechanical, and electrical elements. WEC design efforts are primarily focused in the time-domain, using frequency-based energy analyses and numerical problem solving approaches that are staples in hydrodynamic design efforts to form the basic information set used in these time-domain development models. These approaches, however, are a time-consuming and costly methodology choice that does not lend itself to rapid or large-scale hydrodynamic simulations. This thesis describes the technology proof-of-concept research into a frequency-domain approach that addresses these deficiencies. The approach being developed is constrained by the same restrictions that are applied to the time-domain approach, including the use of frequency-domain information as the fundamental base for development. Designers of communication systems have developed tools and approaches that exploit the benefits of frequency-domain analyses in their design approaches, and knowledge from that specialized domain is applied in the development of the methodology. The process used to develop and prove this approach is mathematically rigorous.

The research into the frequency-domain approach is proven to produce results that are comparable at a fraction of the simulation time. The advantages and disadvantages of the approach are discussed, as are the benefits conferred by the advantages. Some of the results are extrapolated further and shown to address the specific requirements of the WEC design process. Finally, additional developmental opportunities, including more in-depth analysis of the issues uncovered and methodology expansion possibilities are identified and documented.

©Copyright by Asher Simmons
November 7, 2013

All Rights Reserved

A frequency-domain approach to simulating wave energy converter
hydrodynamics

by
Asher Simmons

A THESIS

submitted to

Oregon State University

in partial fulfillment of
the requirements for the
degree of

Master of Science

Presented November 7, 2013
Commencement June 2014

Master of Science thesis of Asher Simmons presented on 7 November 2013

APPROVED:

Major Professor, representing Electrical and Computer Engineering

Director of the School of Electrical Engineering and Computer Science

Dean of the Graduate School

I understand that my thesis will become part of the permanent collection of Oregon State University libraries. My signature below authorizes release of my thesis to any reader upon request.

Asher Simmons, Author

ACKNOWLEDGEMENTS

The author expresses sincere appreciation to Professor Magaña and Professor Brekken for their excellent academic support; Dr. Margaret Simmons and Mr. Robert Simmons for their support, parental and otherwise; Mrs. Kelly Morris and other family for their timely reminders to 'breathe'.

TABLE OF CONTENTS

	<u>Page</u>
1 Introduction	1
1.1 Rationale for Research	1
1.2 Current State of Technology.....	2
1.2.1 Virtual, Rapid Prototyping.....	3
1.2.2 Wave Research.....	4
1.2.3 Wave Energy Research.....	5
1.3 Research Focus	6
1.4 Assumptions Guiding Ocean Wave Analysis.....	7
1.5 Organization of Research.....	8
2 Ocean Wave Energy – Concepts Behind Development.....	11
2.1 The Role of a Methodology in a Development Process.....	11
2.2 Wind Wave Basics	13
2.2.1 Wave Creation, Transformation, and Destruction	13
2.2.2 Mathematical Wave Descriptors.....	16
2.3 Understanding Energy in Wind Waves	17
2.3.1 Energy in Wave Amplitude.....	18
2.3.2 Sea State Data Sets.....	19
2.3.3 Spectral Descriptions of Wave Energy.....	20
2.3.4 Wave and Wave Energy Transport.....	23
2.4 PA-WEC Design Goals and Tools	24
2.4.1 Design for hydrodynamic Frequency Response	24
2.4.2 Tools for Calculating Hydrodynamic Coefficients.....	25
2.4.3 General Analysis Tools	26
2.5 Mathematical Description of PA-WEC Hydrodynamics	28
2.5.1 Equation of Motion.....	29
2.5.2 Formulation of Forces.....	29
2.5.3 Excitation Force.....	30
2.5.4 Radiation Force.....	31

TABLE OF CONTENTS (CONTINUED)

	<u>Page</u>
2.5.5 Coupled Radiation Force	32
2.5.6 Hydrostatic Stiffness Force	32
2.5.7 Viscous Friction Force	33
2.5.8 Mooring Forces	33
2.6 Understanding Wave Energy Farm Operation	33
2.6.1 WEF Function.....	34
2.6.2 Constraints on WEF Location.....	34
3 Methodology Development Process	36
3.1 Reference Frame and Motion Mode.....	37
3.2 WEC Model Input	38
3.2.1 Sea State Input.....	38
3.2.2 Generating the Sea State.....	39
3.3 WEC Model Coefficients.....	44
3.3.1 Simple Forces – Constants	44
3.3.2 Excitation Force	44
3.3.3 Radiation Force.....	46
3.3.4 Coupling Forces: Interactions Between Device Bodies	48
3.3.5 Mooring Forces	48
3.3.6 Power-Take-Off Force.....	48
3.4 WEC Models.....	48
3.4.1 Time-Domain	49
3.4.2 Frequency-Domain.....	50
3.5 WEC Model Scripts	55
3.5.1 Geometry Definition - Function	55
3.5.2 Impulse Response Calculation – Function	56
3.5.3 Calibration Simulation – Script	56
3.5.4 Single-WEC Single-Frequency Simulation - Script.....	57
3.6 WEC Model Output.....	58

TABLE OF CONTENTS (CONTINUED)

	<u>Page</u>
3.7 Development Approach	59
3.8 Ensuring Validity of Comparison	60
3.8.1 Sea State Creation Method.....	60
3.8.2 Composition of Hydrodynamic Forces	60
4 Research Results	62
4.1 Modeling Issues	62
4.1.1 Excitation Force Coefficients	62
4.1.2 Non-Causality of Excitation Force.....	64
4.1.3 Radiation Force Coefficients Source Data	64
4.1.4 Radiation Force Equation	64
4.1.5 Radiation Force Coefficients and Causality	65
4.1.6 IRF Calculations	66
4.1.7 Conflicting Sign Conventions.....	66
4.1.8 Modeling Issue Analysis.....	66
4.2 Force Component Calibration Results.....	67
4.2.1 Calibration of Excitation Force	67
4.2.2 Calibration of Radiation Forces.....	69
4.2.3 Calibration of Constants	71
4.2.4 Force Component Calibration Analysis	71
4.3 Single PA-WEC Comparisons	72
4.3.1 Simulation Result Comparisons.....	72
4.3.2 Simulation Speed Comparison.....	75
4.3.3 Single-Frequency Analysis.....	76
4.4 Single-WEC, Multiple Frequency	76
4.4.1 Regular, 0-Phase Shift, Input Wave	76
4.4.2 Random, Multi-Frequency Input Wave	79
4.4.3 Single WEC Simulation Result Analysis.....	84
5 Extrapolations, Observations and Conclusions.....	85

TABLE OF CONTENTS (CONTINUED)

	<u>Page</u>
5.1 Results-Driven Valuation and Extrapolation.....	85
5.1.1 Model Issues	85
5.1.2 Calibration.....	86
5.1.3 Simulation Times	87
5.1.4 Single-Frequency WEC Simulations.....	89
5.1.5 Multiple-Frequency Single Device Simulations.....	89
5.1.6 WEF Simulation Extrapolation.....	91
5.2 Methodology Viability	92
5.2.1 Methodology Advantages.....	92
5.2.2 Methodology Disadvantages.....	94
5.3 Advantage-Driven Benefits	94
5.4 Research Continuation and Expansion.....	96
5.4.1 Issues to Resolve	96
5.4.2 Future Research Topics for this Framework.....	98
5.5 Final Comments	99
6 Appendix A: Time-Domain Model.....	101
6.1 Scripts.....	101
6.1.1 Define geometry function	101
6.1.2 Impulse response function	104
6.1.3 Simulation run script.....	107
6.2 Schematics.....	113
6.2.1 Top Level.....	113
6.2.2 Excitation	114
6.2.3 WEC Dynamics	115
6.2.4 Body 1 Dynamics.....	116
6.2.5 Body 2 Dynamics.....	117
6.2.6 Coupling.....	118
6.2.7 Mooring.....	119

TABLE OF CONTENTS (CONTINUED)

	<u>Page</u>
7	Appendix B: Frequency-Domain Model.....
7.1	Model Derivation
7.2	Calibration.....
7.2.1	Excitation Force Calibration Script
7.2.2	Radiation Force Calibration Script
7.2.3	Excitation Force Calibration Schematic
7.2.4	Radiation Force Calibration Schematic
8	References.....

TABLE OF FIGURES

Fig. 2.1: Example of Sea Surface Representation.....	14
Fig. 2.2: Particle motion in Deep Water	15
Fig. 2.3: Particle Motion in Shoaling and Surf zones	17
Fig. 2.4: Wave ESD from NDBC Buoy 46229.....	22
Fig. 2.5: Hydrodynamic Analysis Coordinate System.....	27
Fig. 2.6: Simplification due to Axisymmetry.....	28
Fig. 3.1: Wave Energy Spectra Generated using TMA Methodology	40
Fig. 3.2: Example Sea Elevation Time Series.....	43
Fig. 3.3: Body 1 Simulink™ Model	50
Fig. 3.4: Fr, p Calibration Simulink™ Model.....	57
Fig. 4.1: $Fe, 1$ IRF Comparison	63
Fig. 4.2: Body 1 Fe Calibration Values	67
Fig. 4.3: Body 2 Fe Calibration Values	68
Fig. 4.4: Excitation Force Amplitude Calibration Errors.....	68
Fig. 4.5: Body 1 Fr Calibration Values	69
Fig. 4.6: Body 2 Fr Calibration Values	70
Fig. 4.7: Radiation Force Amplitude Calibration Errors.....	70
Fig. 4.8: Acceleration Amplitude Results for Body 1	72
Fig. 4.9: Acceleration Amplitude Results for Body 2	73
Fig. 4.10: Error in Acceleration Amplitude with Calibration Included	74
Fig. 4.11: Error in Acceleration Amplitude without Calibration	74
Fig. 4.12: Results Comparison, Multi-Frequency Simulation, Body 1.....	77

TABLE OF FIGURES (CONTINUED)

<u>Figure</u>	<u>Page</u>
Fig. 4.13: Results Comparison, Multi-Frequency Simulation, Body 2.....	78
Fig. 4.14: Amplitude Differential Due To Simulation Method	78
Fig. 4.15: Random Wave Energy Spectra.....	79
Fig. 4.16: Random Wave Spectra, Amplitude and Phase.....	80
Fig. 4.17: Body 1 Acceleration Comparison, 10 Minutes, Random Wave	81
Fig. 4.18: Body 2 Acceleration Comparison, 10 Minutes, Random Wave	81
Fig. 4.19: Body 1 Acceleration Output Comparison, 700 Data Points	82
Fig. 4.20: Body 2 Acceleration Output Comparison, 700 Data Points	83
Fig. 4.21: Method Acceleration Differentials, Random Wave	83
Fig. 5.1: Simulation Run Time Comparison.....	88
Fig. 5.2: Relative Velocity Comparison, Random Wave	90
Fig. 5.3: Frequency-Domain Method Input/Output Energy Comparison.....	91

TABLE OF TABLES

<u>Table</u>	<u>Page</u>
Table 3.1: Example AQWA™ Output - Added Mass.....	47
Table 3.2: Example AQWA™ Output - Damping Matrix.....	47

A frequency-domain approach to simulating wave energy converter hydrodynamics

1 Introduction

1.1 Rationale for Research

The fact that world-wide energy requirements are increasing is currently common knowledge in the industrialized world. Additionally, data-driven knowledge of environmental issues caused by current electricity generation technologies has a growing influence on public perceptions and governmental policies. These combined factors have resulted in a significant amount of research into alternative energy sources that are renewable and have a low impact on the environment. One of these energy sources that may be tapped by converters is ocean waves.

Wave energy conversion is an emerging technology and, like any new technology, is complicated by an uncertain path forward. Its adoption is further confounded by its infrastructure requirements, financial structures embedded in power delivery systems, conflict surrounding the need for clean energy systems, and the expense surrounding the invention of new technologies. The number of conversion device architectures being investigated world-wide number in the tens, and none has emerged as a technology leader. There is some literature that compares architecture types, such as the compilation found in [1] and the book [2 ch. 4, pp 45-136].

It is clear that a subset of these architectures requires multiple-device deployment to reach commercial-scale power production [1]. The multiple-device requirement imposes additional infrastructure components that are also being investigated and reported in the literature, such as array-level production and loading [1], optimal device separation [3], and transmission systems [4]. These research efforts are necessarily restricted by device uncertainty, and while developers can learn valuable lessons from the wind and solar industries, the

A frequency-domain approach to simulating wave energy converter hydrodynamics unique issues related to commercial scale wave energy require innovative development approaches.

This thesis describes the development of a prototype simulation methodology that generates statistically accurate motion information for use as an input to power take-off (PTO) electromechanical architectures. The methodology uses standard sea-state information as source data and processes the data with well-known physical oceanography algorithms. A second set of methodology inputs describing the hydrodynamic properties of the energy converter are extracted from industry-standard modeling software. The methodology is applicable to individual devices or arrays of devices.

Section 1.2 describes the most fundamental aspects of the current technology state that are applicable to WEC design. This is followed by a section describing the research focus. Section 1.4 details the assumptions applied during the experiments and analyses. Finally, the chapter ends with an overview of the remainder of the thesis.

1.2 Current State of Technology

Investigation of ocean waves as a renewable energy resource has caused a significant increase in the cross-functional diversity of researchers and developers. Scientists and engineers from many disciplines are forming collaborations specifically structured for advancing the technology. A side benefit of these collaborative efforts is the knowledge transfer between disciplines. This research reflects the cross-discipline nature of the field, presenting results that require knowledge of electrical, mechanical, and civil engineering as well as physical oceanography.

A frequency-domain approach to simulating wave energy converter hydrodynamics

1.2.1 Virtual, Rapid Prototyping

Designers in any scientific-based field are familiar with the concepts embodied by the term ‘prototype’, even if their specific jargon uses a different term.

Prototyping is defined by [5, p 290] as

a hardware and software development technique in which a preliminary version of part or all of the hardware or software is developed to permit user feedback, determine feasibility, or investigate timing or other issues in support of the development process

The rapid increase in inexpensive computational power caused by continual technological development in the semiconductor industry has enabled one such development approach: virtual rapid prototyping. The term ‘virtual’ is defined by [5, p. 403] to be “pertaining to a functional unit that appears to be real, but whose functions are accomplished by other means.” The same standard defines ‘rapid prototyping’ as “a type of prototyping in which emphasis is placed on developing prototypes early in the development process to permit early feedback and analysis in support of the development process” [5, p.296]. All of these definitions are applicable to the development of wave energy as a renewable energy source. Researchers and engineers developing wave energy can learn a significant amount from prototype approaches used in the design and development of other complex systems.

The methodology developed during this research project outlines a virtual rapid prototyping approach for the development of wave energy conversion devices and farms. The methodology uses virtual representations of the sea and device, enabling designers to quickly vet the hydrodynamic properties of multiple body types in identical statistically realistic environments. It also enables the controlled separation of the hydrodynamics from the power harvesting mechanism, creating a path for parallel device development efforts. Finally, it

A frequency-domain approach to simulating wave energy converter hydrodynamics

enables designers to determine the output of an array of devices in realistic ocean conditions, data which is useful for grid integration and financial studies.

1.2.2 Wave Research

Wave research applicable to harvesting wave energy is primarily conducted by either physical oceanographers or civil engineers. The research can be loosely classified as either wave or wave-structure studies.

Wave studies begin with the collection of research and analysis of data in ocean waves. This data is then used to create numerical representations of the development, propagation, and dissipation of the waves that are validated in laboratory or field studies. The first-order approximation, (a linear representation), of wave theory was first derived by G. B. Airy in 1845. G. G. Stokes followed him with a higher-order theory in 1847. These representations, referred to as “Airy waves” or “first order Stokes waves” respectively [6, ch. 3, p. 55], form the fundamental theory used in the initial analysis of waves, including the energy they contain. (A brief history of these equations can be found in chapter 5 of [7].) In the last ten years, Airy wave theory has been used in studies regarding the prediction of ocean waves [8, 9], hydrodynamic analysis of waves [10], the impact of wave energy harvesting on coastal environments[11], and modeling of the ocean surface [12-14].

Wave-structure interaction studies follow an empirical approach similar to that of the wave studies, and are primarily conducted in the laboratory or in the field. The study of wave energy converters, or WECs, is unique among energy converters in that the hydrodynamic response of the device in the presence of an energy conversion mechanism is not well understood. Laboratory efforts, whether in a real or virtual wave tank, are using advanced sensing techniques and scaled WEC models in single-device and arrayed-device interaction studies. The data collected in the laboratory is then correlated with data collected from

A frequency-domain approach to simulating wave energy converter hydrodynamics

in-situ deployment of prototype or production devices. The information gathered from the real-world data are then used to enhance the original simulations and prototype efforts, eventually reaching an empirically derived design appropriate for a particular wave climate. The aggregate data sets can also be used to evaluate other designs for the original wave climate or the same design for other wave climates. Research reported since 2001 includes topics such as hydrodynamic device modeling [15, 16], array and array element spacing analyses [3, 17], farm site characterizations [1, 18], and mooring studies [19].

1.2.3 Wave Energy Research

Although the concept of harnessing wave energy has been present since 1799 [20, ch. 1, p. 2], it has only been recently that technologies have advanced sufficiently to enable practical, commercial-scale wave energy harvesting. Power electronics, developed from advances made in the semiconductor industry, have successfully separated generation output from grid requirements. This advance has enabled cost-effective energy harvesting from sources that are uncontrollable, such as wind, wave and solar [21]. New lightweight, corrosion-resistant materials have been developed[22] that protect electricity generation and conditioning hardware from the harsh environment of the ocean. Large size permanent magnets with high magnetic field densities can be manufactured, replacing the electromagnets and simplifying the generator mechanical design [23].

WEC development is in the prototyping stage and the architectures are still being invented, which accounts for the wide diversity of devices: No single architecture, or even sub-architecture, has been proven to be better than the others. WECs are generally classified into four categories based on their energy conversion technologies. These classes are labeled: Overtopping, Attenuator, Oscillating Water Column, and Point Absorber. A concise description of each class

A frequency-domain approach to simulating wave energy converter hydrodynamics

along with commercial examples can be found in [24]. Research published since the year 2000 includes the development and evaluation of control algorithms [25-29], power take-off mechanisms [30, 31], and modeling methods [32-34].

Yet, with all these innovations, few WEC architectures are likely to be commercially viable as stand-alone devices. Developers are planning to create wave energy plants that are an aggregate of one or more type of WECs that share a common grid connection. These plants are referred to as Wave Energy Farms (WEFs). They are a system of WECs that are physically connected through the use of power electronics to interface to a grid at one physical location, in a manner similar to a solar farm or a wind farm. Research into WEF infrastructure issues is increasing even though WEC architectures are still being developed. Studies on the impact the WEF configuration has on power production [35], ocean ecology and ocean wave climate [36] are being conducted. Some studies, such as investigations of grid connection, can build on concepts developed for wind- or solar-power plants [37]. Other studies target issues that have no simple counterpoint in existing research, such as optimal mooring structures for an array of WECs [38].

1.3 Research Focus

Wave energy devices and farms are complicated systems with many of their details still unknown. The development costs are expensive in money and time. Costs can be reduced by implementing virtual rapid prototyping methodologies, where the system is modeled in several different ways [22]. Each system representation is useful for developing a particular aspect or component of the whole system. For example, the hydrodynamics of the device can first be represented in a software (virtual) model, and then in scaled physical prototypes, before being applied to the final design. This partitioned approach, when done correctly, allows designers to reduce the risk of device failure during the

A frequency-domain approach to simulating wave energy converter hydrodynamics

development process. Good examples from three case studies of this development approach can be found in [39].

This research is focused on the *point absorber* class of WEC (PA-WEC). The devices in this class are typically smaller than other WEC classes, both in physical size and power capability. They often convert only the vertical wave motion into electricity [24], and have a maximum power production capability limited to kilowatts. As such, none of the point absorber architectures has the capability of being commercially viable as a stand-alone device. Instead, developers plan to deploy multiple PA-WECs in a particular area, creating a WEF, similar to the farms of wind machines that can be seen across the world. Although WEF developers will likely deploy only one type of PA-WEC for cost purposes, there is no technical roadblock to a single WEF containing multiple types of PA-WECs.

The results of this research enable three aspects of wave energy device design. The first aspect is the hydrodynamic response of the device in realistic sea conditions. The methodology described herein details how to create a statistically realistic time-series of sea elevations at a specific location. The second aspect is the design of the power take-off mechanism (PTO) of the PA-WEC. The methodology details how to create a WEC simulation model that generates a meaningful time-series at the input of the PTO that is based on the hydrodynamic response of the physical design. The third design aspect enhanced is the WEF design. The methodology describes how to create a virtual WEF that contains detailed WEC hydrodynamic responses located in a statistically representative wave climate.

1.4 Assumptions Guiding Ocean Wave Analysis

The ocean surface, the source of the energy targeted for harvest, is difficult to describe mathematically. The total equation describes an inherently complex and non-linear process which is very difficult to incorporate in developmental

A frequency-domain approach to simulating wave energy converter hydrodynamics

research. However, there are a number of constraints and assumptions that can simplify the description resulting in a set of equations that are suitable for the initial stages of system analysis. The constraints and assumptions imposed on the total equation include:

- The relationship between wave height (H) and ocean depth (h) is well defined [40, ch. 3.4, pp. 57-58].
- Sea water is an incompressible, ideal fluid [41, ch. 4, p. 58].
- The three dimensional problem (x, y, z) is reduced to two dimensions (x, z) [6, ch. 3.1, p. 54].
- Wave solution created for waves travelling in the x -direction identically applicable for waves travelling in y -direction due to device symmetry[41, ch. 5.6.4, p. 166].
- Viscous and turbulent stresses are ignored, rendering the ocean irrotational [6, ch. 3.1, p. 54].
- Wave height is significantly smaller than the wave length (λ) [6, ch. 3.1, p. 54].

The wave solution resulting from these simplifications is often referred to as *linear waves, small-amplitude water waves, Airy waves, or first order Stokes waves* [6, ch. 3.1, p. 55]. This solution is widely used in the oceanographic, mechanical engineering and civil engineering communities. It is incorporated in many industry research tools developed for the design of structures in the marine environment. It is also the solution that is employed in this research.

1.5 Organization of Research

Chapter 2 discusses the basic concepts behind ocean wave energy. Section 2.1 discusses how methodologies impact complex system development. This is followed by a synopsis of wind-sourced waves. Section 2.3 is devoted to energy

A frequency-domain approach to simulating wave energy converter hydrodynamics

contained in waves: how it is described, historical records, and transport from one place to another. A description of WEC design tools is in Section 2.4, and Section 2.5 develops the mathematical hydrodynamic model. Chapter 2 is closed with a short discussion on WEFs

Chapter 3, which defines the process used to develop the frequency-domain methodology, begins with a discussion of references used to anchor the analyses. This is followed by a description of the model input, including what the input is and how it is generated for the virtual environment. Section 3.3 details the force components of the models. Next, Section 3.4 describes how the force components are combined to create the actual models used in the experimental process. The software code, functions and scripts are explained next. Finally, the WEC model outputs are covered in Section 3.6. The remainder of Chapter 3 is focused on the approach used to develop the frequency-domain methodology (Section 3.7) and the steps taken to ensure the experimental results will be valid (Section 3.8).

Using the development approach discussed in Section 3.7 as an outline, the majority of Chapter 4 presents the research results. Section 4.1, however, was not anticipated when the development approach was defined. It discusses issues that are relevant to the experimental models that were identified during the development process. Results associated with the direct comparison of the model components occupy Section 4.2. Single WEC comparisons begin in Section 4.3 and carry through the remainder of the chapter.

Chapter 5 is devoted to discussing the results in a variety of contexts, all of which are outside the experimental framework. Comments regarding, but not directly included, in the experimental results are presented in Section 5.1. This is followed by a discussion of the viability of the proposed methodology (Section 5.2) and benefits derived from using the approach (Section 5.3). Section 5.4 highlights factors associated with continuing the development of the

A frequency-domain approach to simulating wave energy converter
hydrodynamics

methodology. Finally, Section 5.5 provides a summary and some concluding remarks.

A frequency-domain approach to simulating wave energy converter
hydrodynamics

2 Ocean Wave Energy – Concepts Behind Development

The methodology developed in this research is designed to enable virtual rapid prototyping of PA-WECs and WEFs. Understanding the methodology and its applications first requires understanding the physics governing the environment and the device operation.

The ocean wave energy concepts described in this chapter are a focused set of those important to developers of wave energy. The system being examined has a description of the sea state as for the input. The system output is the motion input to the PTO mechanism of the PA-WEC. The system contained by these boundaries is the hydrodynamic response of the WEC.

2.1 The Role of a Methodology in a Development Process

The term ‘methodology’ is defined in [5, p. 222] as “a system of practices, techniques, procedures, and rules used by those who work in a discipline.” Teams of product designers are rarely successful in their development efforts without relying on some methodologies to frame their work. At a minimum, individuals working together unconsciously form norms and routines that define acceptable work practices – methodologies. Savvy senior developers and project managers use methodologies to improve the product design efforts with respect to the development goals. And, they can be reluctant to change their existing methods without clearly understanding the net positive benefits of the change.

The development process used to transform an idea into a viable product is, by necessity, unique to that product. Fortunately, there are many sources of product development templates or paradigms for designers to use as starting points for customization. These templates often contain a single, overarching methodology that is applied at multiple places in the development process. Device simulations, for example, happen many times during development. Each time, however,

A frequency-domain approach to simulating wave energy converter hydrodynamics

certain methodological attributes are changed to fit the particular development step. A prudent product developer will examine the development template and customize it for the particular project. This customization should include discarding dated methods and incorporating new methods.

However, developing the evidence supporting the case for a methodology change can be a nearly insurmountable task. This is especially true when the new method has been examined and discarded in the past. The methodology advocate must develop evidence with a clearly defined process and present that evidence in a transparent manner. The reasons for discarding the approach in the past should be directly reflected in the experimental design. The experiments should also deliver evidence regarding the viability of using the new method and lead to recommendations for further investigation. It is important to understand that the output of this type of experiment will not be a methodology that is production-worthy, but one requiring more in-depth development. This research process can be referred to as a ‘proof-of-concept’.

A proof-of-concept approach is applied to the frequency-domain methodology research. The experiments have been designed to demonstrate the correlation of the results between the time- and frequency-domain approaches, as well as the time needed for particular tasks. Discoveries made during the investigation have been recorded. Finally, recommendations regarding the fit of the frequency-domain method into the WEC and WEF development are made. Ideally, these results will be sufficient to either discard the approach or develop it further into a product.

The proof-of-concept approach forces the developer to understand the system targeted for revision. In this case, the system includes the energy source (which waves matter and why), emulation of the energy source (creation of representative sea states), and purposes of existing methods (what is the time-

A frequency-domain approach to simulating wave energy converter hydrodynamics

domain used for). The system also includes understanding the needs (satisfied and not) of the industry that are being addressed by the proposed approach. This understanding is used to ensure the experiments in the investigation are pertinent.

2.2 Wind Wave Basics

The gravity wave is the only wave that is of interest to PA-WEC developers. This section describes the lifecycle of these waves and defines some of the basic equations that embody their behavior.

2.2.1 Wave Creation, Transformation, and Destruction

Energy in ocean waves that is harnessed by point absorbers is a concentrated form of solar power. Solar radiation hitting the earth heats the different biosphere components according to the thermal properties of the component. For example, water heats at a rate that is different than land. This causes a temperature (energy) differential, an unstable natural state, at the abutting boundaries. The system automatically tries to correct this instability (equalize the temperature/energy) by moving air with high temperatures to regions with low temperatures. The observable part of this process is wind.[2, ch. 1, p. 1]

A similar balancing process causes the development of wind-generated waves. As wind moves over a flat sea, turbulence at the wind/sea interface causes random pressure variations in the water. The wind turbulence transfers some of its energy to the ocean causing some water molecules to move faster than others, making waves with short wavelengths, small amplitudes, and high frequencies – tiny waves. The wind continuing to push on the tiny waves makes them grow exponentially through an inherently unstable positive-feedback situation described by the Bernoulli Principle. The waves also interact with each other,

A frequency-domain approach to simulating wave energy converter hydrodynamics

with energy from short, high-frequency waves combining to create low-frequency waves [42, ch. 16.4, p. 288].

The low-frequency waves are functions of both space and time. Each wave has a unique set of characteristics: amplitude, spatial and temporal repetition, and phase[42, ch. 16.3, pp. 278-279]. Their combination results in the complicated sea surface profile observable in deep waters. This surface, as illustrated in Fig. 2.1, is inherently non-linear. For the remainder of this chapter, the word *wave* refers to a component wave with a single frequency (time and space) and phase, not the resultant surface profile.

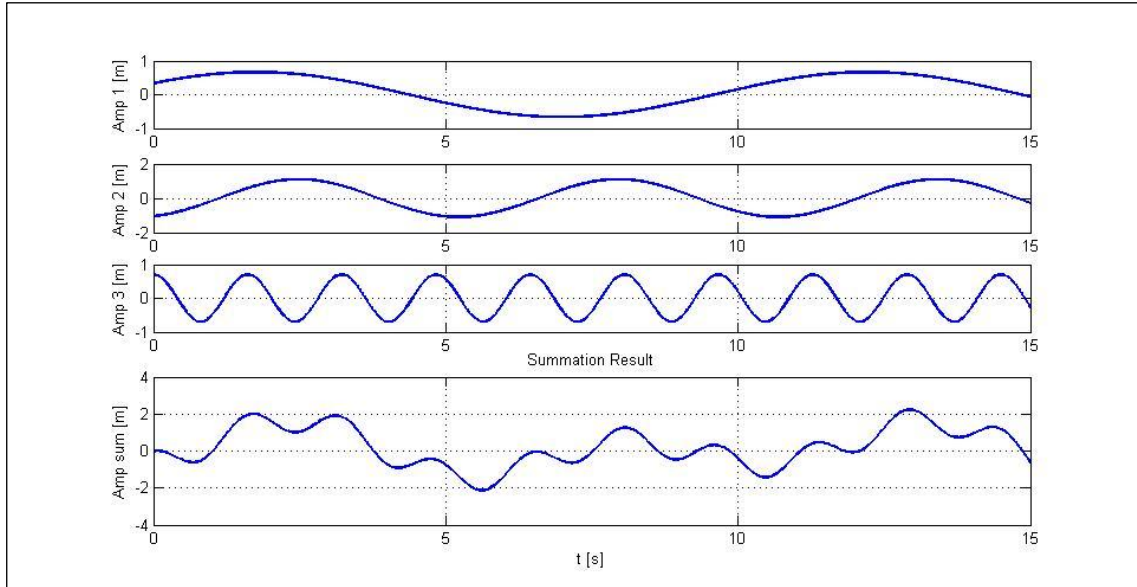


Fig. 2.1: Example of Sea Surface Representation

Water, having a higher density than air, requires more energy per unit volume to move than air, so the wind energy is naturally concentrated as it is transferred. The transferred energy is stored in the wave oscillation, being converted from potential energy at the wave crest and trough to kinetic energy at the wave slopes. The oscillation is maintained by the force of gravity, giving rise to the name gravity waves [41, ch.3, p. 44]. The amount of energy that can be absorbed

A frequency-domain approach to simulating wave energy converter
hydrodynamics

from the wind and stored by the sea is limited by the physical properties of the sea water, the length of unobstructed sea surface, and the depth of the sea floor.

Once captured by the ocean, this concentrated wind energy can travel huge distances without loss because the energy is propagated through the water without displacing the actual water mass. The water molecules move in a set of circular paths as seen in Fig. 2.2. Each orbit is largely stationary, with the water molecules experiencing little lateral displacement over time as the molecule paths are closed orbits. The circular orbits decrease in diameter exponentially as the depth below the surface increases, rapidly becoming negligible.

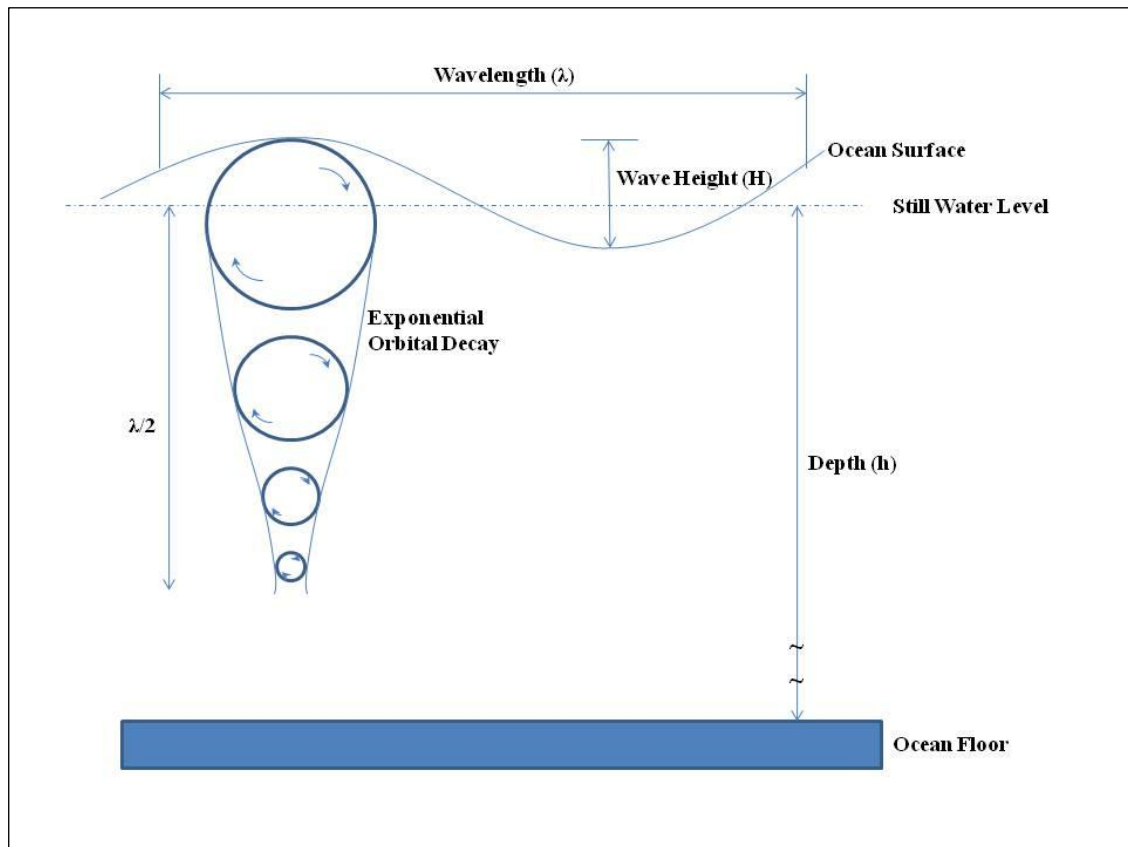


Fig. 2.2: Particle motion in Deep Water

A frequency-domain approach to simulating wave energy converter
hydrodynamics

2.2.2 Mathematical Wave Descriptors

The assumption of linear wave theory forces a relationship between the wavelength, wave period and the depth of the water that is referred to as the dispersion relation. This relationship connects the angular frequency (ω) and the wave number (k) of the wave and is written as [6, ch. 3.2, p. 61]:

$$\omega^2 = g \cdot k \cdot \tanh(k \cdot h) \quad [\text{rad}^2/\text{sec}^2] \quad (2-1)$$

where g is the gravitational acceleration constant and h is the depth of the still water level. Note the relation cannot be solved analytically, as k appears both inside the argument of the hyperbolic tangent function and as a multiplier of that same hyperbolic function. Instead, the solution must be found via the use of an iterative numerical approach [43, ch. 5, p. 90].

Using the definition of the wavelength, λ

$$\lambda = \frac{2 \cdot \pi}{k} \quad [\text{m}] \quad (2-2)$$

and that of ω

$$\omega = \frac{2 \cdot \pi}{T} \quad [\text{rad/sec}] \quad (2-3)$$

where T is the period of the wave, Eq. (2-1) can be re-written as

$$\lambda = \frac{g \cdot T^2}{2 \cdot \pi} \tanh(k \cdot h) \quad [\text{m}] \quad (2-4)$$

This representation provides clarity to the relationship between λ and the combination of T and h [6, ch. 3.2, p. 69].

At depths greater than or equal to one-half the wavelength, $k \cdot h$ becomes large enough that the hyperbolic tangent function is approximately unity. This defines the *deep water* condition, where λ is only a function of T and is depth-in [6, ch. 3.2, p. 69].

As waves pass through regions of depth less than half the wavelength, a portion of the wave energy is permanently converted to kinetic energy and

A frequency-domain approach to simulating wave energy converter hydrodynamics

invested in moving mass (see Fig. 2.3). Wave behavior in this region of the ocean, called the *shoaling zone*, is difficult to quantify due, in part, to non-linear nature of the energy transformations. This is the region where $\tanh(k \cdot h)$ is between unity and the value $k \cdot h$, and the hyperbolic function has a large impact on the λ - T - d relationship.

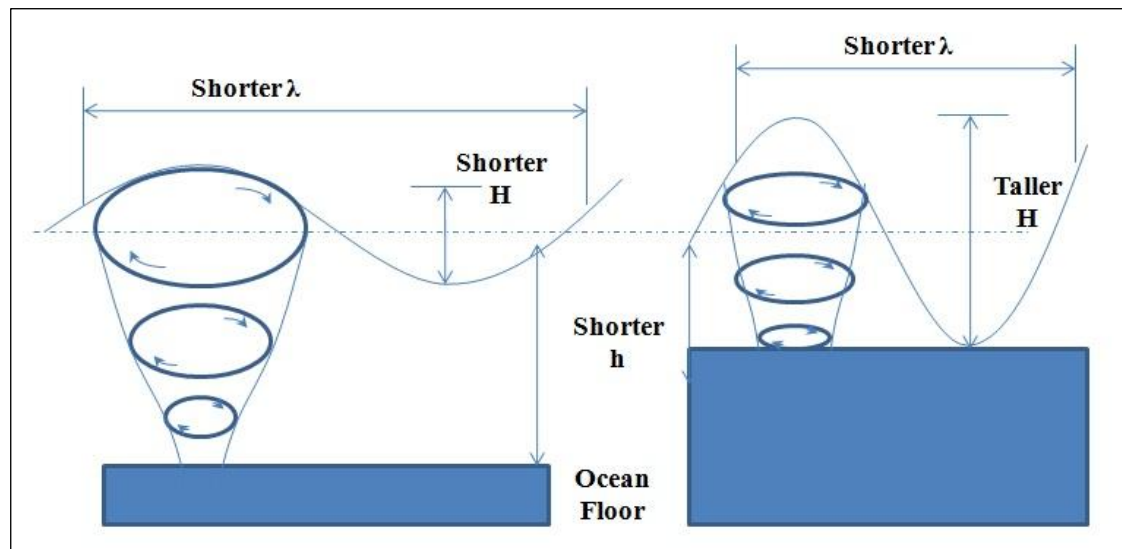


Fig. 2.3: Particle Motion in Shoaling and Surf zones

By the time the waves reach depths of a quarter wavelength or less, they have been transformed to a wave with a fixed T that is a function of the h only. The transformed waves are still combined, through superposition, to create a single wave of varying amplitude and constant frequency. Wave energy in this region, called the surf zone, is completely dissipated in the motion of water molecules and the ocean floor [42, ch. 17.1, pp. 293-296].

2.3 Understanding Energy in Wind Waves

Real ocean waves are the result of physical processes that are stochastic, so past behavior of the ocean surface cannot be used to predict the future behavior. However, statistics can be used to predict the likelihood of a particular behavior

A frequency-domain approach to simulating wave energy converter hydrodynamics

and statistical tools can be employed to describe behavioral characteristics. This section details real physical relationships, representative quantities, and statistical tools used to define energy in the ocean.

2.3.1 Energy in Wave Amplitude

The amount of energy contained in a deep-water ocean wave has been well-documented in texts by many researchers, including, in part, the authors of [2, ch. 2.1, p. 13], [6, ch. 4.2, pp. 207-213], [40, ch. 4.7, pp. 93 - 97], and [41, ch. 3.3, p. 48]. To simplify understanding how the wave energy is related to the wave characteristics, the equations are developed on a per unit basis, where the unit is either an area on the free surface of the ocean or a length along the wave crest. The reader must determine which unit is appropriate based upon the context of use. For further simplicity, the periodicity of the base sinusoidal equations is removed by averaging the equations in time and space [41, ch. 3.3, pp.46 - 47].

In this type of wave, energy is constantly oscillating between the potential form and the kinetic form. During any single oscillatory period of the wave, the energy is all potential energy (at the crest or trough of the wave), all kinetic energy (at the nominal water surface elevation) or some combination of the two energy types. The total energy in the wave at any one point in time and space is the sum of the kinetic portion and the potential portion.

$$E = 2 \cdot E_P = 2 \cdot E_K = E_P + E_K \text{ [J]} \quad (2-5)$$

E_P denotes the potential energy and E_K denotes the kinetic energy. According to [44, ch. 4.13, p. 89],

$$E_P = \frac{1}{4} \cdot \rho \cdot g \cdot A^2 \text{ [J]} \quad (2-6)$$

with ρ being the density of seawater and A being the amplitude of the wave. In the case of SI units, with a surface area bounded by one meter in the direction of

A frequency-domain approach to simulating wave energy converter
hydrodynamics

propagation and one meter in the direction of the wave crest, the total energy per unit area becomes [44, ch. 4.13, p. 89]

$$E_{tot} = \frac{1}{2} \cdot \rho \cdot g \cdot A^2 [J] \quad (2-7)$$

Furthermore, the equation:

$$A = \frac{H}{2} [m] \quad (2-8)$$

can be used to express E_{tot} as a function of H , the distance from trough to crest [43, ch. 5.1, p. 88]:

$$E_{tot} = \frac{1}{8} \cdot \rho \cdot g \cdot H^2 [J] \quad (2-9)$$

This equation clearly shows that the energy in a wave is proportional to the square of the wave height. The total energy found in a real sea can be found by applying this equation to the individual components and summing the results:

$$E_{tot, wave} = \frac{1}{8} \cdot \rho \cdot g \cdot \sum_{all} H^2 [J] \quad (2-10)$$

2.3.2 Sea State Data Sets

The real surface profile of the ocean is naturally random being the result of many random processes, including solar or lunar gravitational forces and non-local weather systems. However, the temporal periodicity is sufficiently accurate for about an hour and spatial periodicity is valid for a few tens of kilometers [42, ch. 16.3, p. 280]. As a result, a data record with an hourly sample rate and from a specific geographic location is sufficiently accurate for use in describing the sea climate for an area as large as 100 km² or more.

There are several national and international sources for the data records. The primary source in the United States is the National Data Buoy Center (NDBC). The (NDBC) is a part of the National Weather Service (NWS). NDBC designs, develops, operates, and maintains a network of data collecting buoys and coastal stations in

A frequency-domain approach to simulating wave energy converter hydrodynamics

the ocean off the coasts of the United States. About 90 of the buoys are owned and operated by the NDBC. Approximately 160 additional stations, owned by the members of the U.S. Integrated Ocean Observing System (IOOS), use the NDBC as their data assembly center. The majority of these stations record sea and atmospheric data on an hourly basis from a variety of instruments. The freely-available data is used for a variety of purposes including weather forecasting, shoreline erosion, and planning for sea-bound commercial and private enterprises [45].

Using the time-series data sampled at the measurement buoy as the source, the NDBC records the significant wave height (H_s), dominant period (T_d) and, frequently, dominant direction (*theta*) data sets for a specific buoy location every hour. H_s is defined as

$$H_s = 4\sqrt{M_0} = 4 \cdot H_{RMS} \text{ [m]} \quad (2-11)$$

where the 'RMS' sub-script refers to the Root Mean Squared value of H. T_d is the center frequency of the frequency window that has the largest amplitude without considering any direction-driven effects. Finally, *theta* is the dominant direction of the buoy from true North in a clockwise direction, reported in degrees [46].

2.3.3 Spectral Descriptions of Wave Energy

Describing the sea surface as characteristics that are functions of frequency naturally encourages researchers to visualize the data in the frequency domain, typically in a representation defined as a spectral description. The characteristics are arranged according to monotonically increasing frequencies forming a spectrum (plural) or spectra (singular). According to [40, ch. 7.3.1, pp. 194-195],

The procedure of extracting spectra from wave records is an evolving field... Of primary importance is the fact that the use of computers in time-series analysis has made it far more convenient to deal with digitized [sampled] data and spectral analysis is usually done by the fast Fourier transform (FFT) technique, popularized by

A frequency-domain approach to simulating wave energy converter hydrodynamics

Cooley and Tukey (1965). It should be noted parenthetically that almost all our knowledge about spectral analysis comes to the ocean engineers via the electronic and communications fields.

Characteristics that are continuous functions of time are converted to the frequency domain by application of the Fourier Transform¹. For example, the transformation of each component of Eq. (2-10) results in a set of energy-per-frequency versus frequency data for each component. By plotting this data set, researchers gain a clear picture of the frequency-based energy profile, or energy density *spectrum*. The specific energy spectrum is represented by $S(f)$ in equations.

A more practical method for generating the frequency-based data set has been made possible by the advances in computing. Computers today are inexpensive, fast, and readily able to manipulate large quantities of data. Scientists can now collect measurements at set time intervals (a time-series) that are hundreds or thousands of data points long. After the time-series is collected, scientists apply a computer algorithm, known as a Fast Fourier Transform (FFT), series, resulting in the frequency-series. The entire process is now dominated by the time it takes to gather and validate the data, not the time needed to manipulate the data for analysis. This is the process used by the NDBC to generate spectra for buoy locations.

An example of an energy density spectrum (also known as the Energy Spectral Density, ESD) for the NDBC buoy Umpqua Offshore is shown in Fig. 2.4. The vertical axis represents the energy value over a discrete frequency step. The horizontal axis delineates the actual frequencies. A careful examination of the vertical axis label shows that the value plotted is not strictly energy, but is

¹ It is assumed that the reader is familiar with Fourier-based frequency

A frequency-domain approach to simulating wave energy converter
hydrodynamics

instead H^2 . This is an appropriate, and common, representation of Eq. (2-10) where H^2 is the only variable.

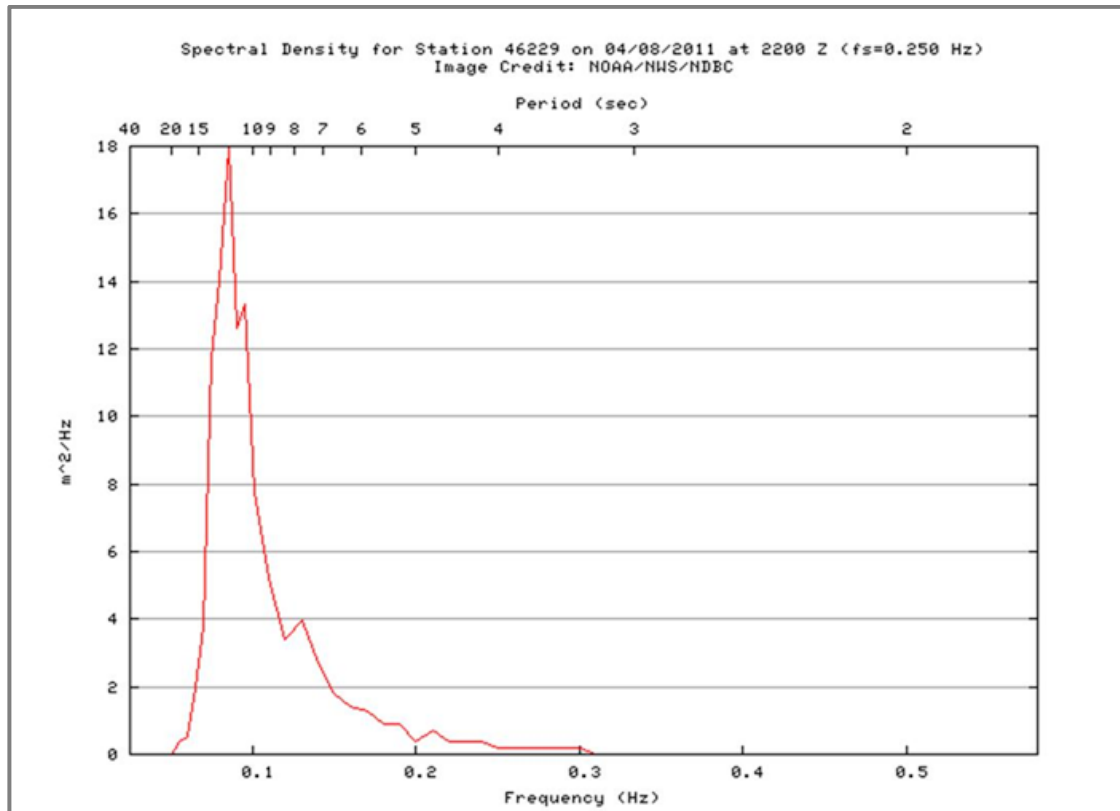


Fig. 2.4: Wave ESD from NDBC Buoy 46229

Physical oceanographers also use empirically-derived spectral functions to describe the ocean surface in theoretical research efforts. The equations are built from analysis of directly measured ocean and wind characteristics and enhanced with laboratory data. They have continued to evolve over time as measurement and calculation technologies have advanced. These spectra are typically referenced by a name that is derived from the names of the researchers or the name of the study that gathered the original data. Many of these spectra have been used in ocean wave modeling software tools such as SWAN (Simulating

A frequency-domain approach to simulating wave energy converter
hydrodynamics

WAves Nearshore) and WAM (WAve prediction Model) as well as in the calculation of wave power density [34].

2.3.4 Wave and Wave Energy Transport

The stochastic nature of the sea surface highlights a real sea characteristic that complicates wave energy development efforts: *The future sea state cannot be predicted* [6, ch. 3.4, p. 115] on an instantaneous basis. However, the deep-water wave set components have a temporal periodicity typically between five and twenty seconds. In terms of frequency, the upper end of this limit is the five-second wave. Waves with periods shorter than five seconds, usually created by local wind, are energy-poor and are of little interest to wave energy conversion. Waves with periods longer than 20 seconds also occur. However they are the result of tides, storms, or seismic activity and are also of little interest to wave energy conversion [2] [42, ch. 4].

For the condition of deep water, the hyperbolic tangent function in Eq. (2-1) is approximately unity, simplifying the dispersion relation to :

$$\omega = \sqrt{g \cdot k} \text{ [rad/s]} \quad (2-12)$$

This simplification is used in the definition of the velocity of small-amplitude water wave propagation known as *phase velocity* (v_p) or *celerity* (c) to show the velocity is a function of k .

$$v_p \equiv c \equiv \frac{\omega}{k} = \sqrt{g/k} \text{ [m/s]} \quad (2-13)$$

A second velocity description called the group velocity, v_g , plays an important role n wave energy development. This velocity

$$v_g = v_p/2 \text{ [m/s]} \quad (2-14)$$

describes the propagation speed of the energy flux and associated wave amplitude variations [41, ch. 3.2, pp. 45-46].

A frequency-domain approach to simulating wave energy converter hydrodynamics

2.4 PA-WEC Design Goals and Tools

Proceeding with the knowledge that the target wave energy is contained in the surface motion, PA-WEC designers must create devices that capture the motion and translate it to electricity. These two concepts define the major sub-systems of the PA-WEC. The first sub-system labeled here is known as the hydrodynamic response. As the name suggests, the hydrodynamic describes the WEC motion that is a result of the device being hit by the gravity wave. The output of this sub-system is the motion caused at the input of the second sub-system. Section 2.4.1 describes the hydrodynamic sub-system.

The second sub-system is labeled here as the PTO mechanism. This sub-system defines the electromechanical processes that are used to convert WEC motion into raw electricity, which is then delivered to the WEF. Because this research is focused on accurately and effectively modeling the input to the PTO mechanism, and not the conversion method employed by the sub-system, detailed descriptions are not provided.

2.4.1 Design for hydrodynamic Frequency Response

The hydrodynamic response is a complicated function of the body shape and mass of each WEC device, the interactions between the device bodies, the incident wave at all its component frequencies, and the impact caused by the PTO mechanism. For example, a donut-shaped body moves in the water differently than a pencil-shaped body. Combining the two shapes results in a third motion profile that is not necessarily a simple linear combination of the individual motion responses. Fortunately, development tools combined with computational power can be employed to calculate the hydrodynamics of a particular body shape. Especially because these tools primarily operate in the frequency domain.

The most convenient, intuitive description of the energy in the sea surface is the ESD. It defines where the energy exists in terms of the oscillatory motion, the

A frequency-domain approach to simulating wave energy converter hydrodynamics

frequency. The frequency range defined by the ESD also defines the wave response specification of the PA-WEC design. For example, Fig. 2.1 shows that the wave energy at NDBC Site 46229 is confined to frequencies between 0.04 and 0.32 Hertz. The physical design of the device for that location must move in response to excitations at the same frequencies in order to capture any of the wave energy. In fact, the degree to which a hydrodynamic response matches the surface ESD is a good indicator of how well the device will deliver energy to the electricity generation portion of the architecture.

2.4.2 Tools for Calculating Hydrodynamic Coefficients

Any model of the hydrodynamic response of the PA-WEC depends on the developer's ability to accurately determine the component forces of the equation being modeled. Each force is a coefficient combined with a motion descriptor, where the coefficient is determined from non-analytical methods. One common method is the use of boundary-element-method (BEM) calculation software. However, even with the use of the best software on the market, the task is a non-trivial one.

In general, software for computer-aided design of physical structures is used to create a three-dimensional representation of the device. This representation is limited to the external surface of the device. This model is loaded into the hydrodynamic analysis program and combined with other device parameters such as mass, length, and amount of body submerged. Once the PA-WEC device is sufficiently described for the stage of development it is in, it is 'hit' with a virtual water wave. The virtual wave is a monochromatic ideal sinusoid of unity amplitude at frequency f and with the physical characteristics of the fluid. The hydrodynamic responses are analytically or numerically calculated and reported. Repetition of this process at different incident wave frequencies results in a set of coefficients useful in other modeling platforms.

A frequency-domain approach to simulating wave energy converter hydrodynamics

AQWA™ and WAMIT™ are two of the commercial-grade BEM software packages used by PA-WEC designers. AQWA™ is a product of the ANSYS Corporation. It has been offered by ANSYS since 2005, although it has been offered by other companies since the mid 1980's [48]. WAMIT, Inc has been providing the WAMIT™ platform as commercial product since 1999 [49]. Either program can be used to create the hydrodynamic coefficients required for this methodology. It is important to note that the best results are obtained when all of the device rigid bodies are included in a single BEM analysis, although the results are reported on a per-body basis.

2.4.3 General Analysis Tools

PA-WEC designers use analysis tools and paradigms that are based in the fields of classical fluid mechanics and linear algebra as a framework for their development. These tools include a Cartesian reference frame complete with definitions for motion modes. They also include state space analysis, and matrix mathematics.

Six modes of motion are used to describe the total motion of the device with respect to a fixed reference, as seen in Fig. 2.5. These modes are defined as (1) surge, (2) sway, (3) heave, (4) roll, (5) pitch, and (6) yaw. Modes 1-3 represent translational motion in a three-dimensional Cartesian reference frame. Modes 4-6 define rotational motion about the axes in the same reference frame. Motion in one mode is in of motion in a different mode although the analysis methodology is identical for each motion type. Each of the motion modes are modeled as single oscillators, resulting in six oscillators for every rigid body in the system.

A frequency-domain approach to simulating wave energy converter
hydrodynamics

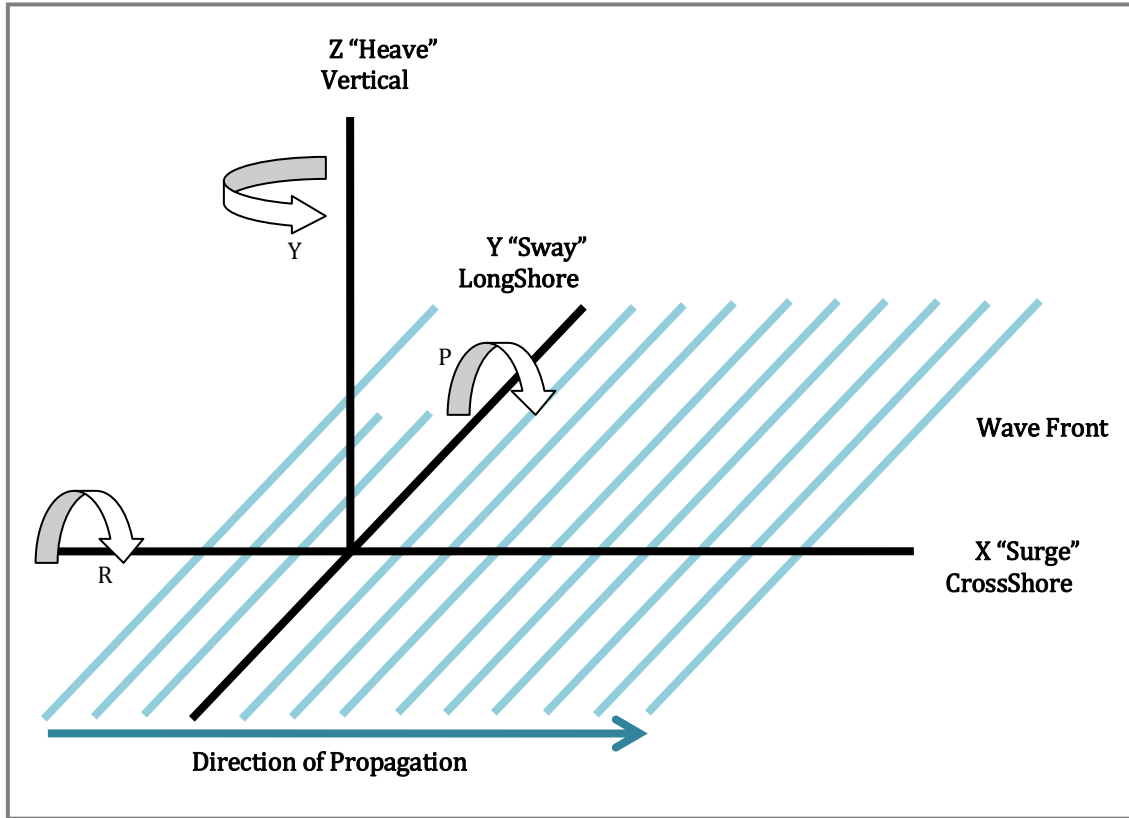


Fig. 2.5: Hydrodynamic Analysis Coordinate System

Designers also use carefully selected system simplifications to focus their attention on the most fundamental aspects of the system development. For example, a PA-WEC that is designed to be axisymmetric in the x-y plane can be modeled in a two-dimensional (x,z) Cartesian frame, because the direction of the incident wave has no bearing on the device operation (see Fig. 2.6). However, this simplification cannot be made if the device is not axisymmetric about the x-y plane as waves coming from the x-direction cause a different motion than waves incident from the y-direction. The equations describing the device motion are on the incident wave direction, forcing the analysis into the three-dimensional framework [41].

A frequency-domain approach to simulating wave energy converter hydrodynamics

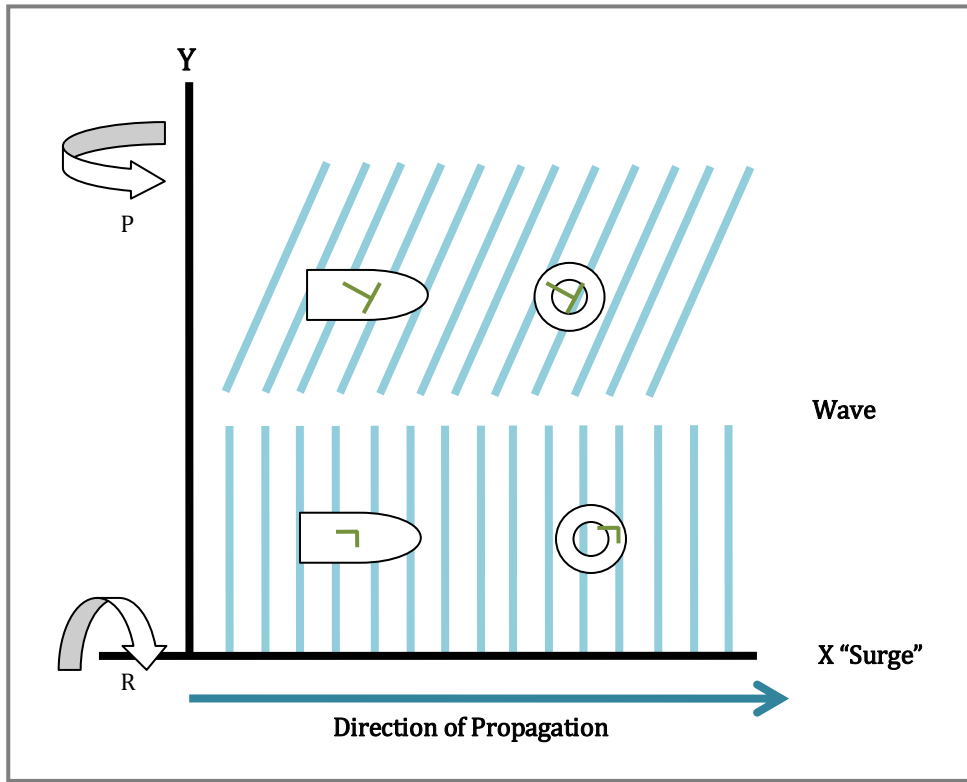


Fig. 2.6: Simplification due to Axisymmetry

2.5 Mathematical Description of PA-WEC Hydrodynamics

It is tempting to believe that PA-WEC modeling is used in a manner similar to other marine hydrodynamic models. Although the physics behind both model sets are the same, the purposes of the model are quite different. Hydrodynamic models used for evaluating sea conditions to a fixed or floating structure are focused on understanding the effects of the incident wave forces on the body structure. The design goal is focused on useful longevity. Hydrodynamic models are used to understand the continual performance of the device, which is the effective transfer of motion from the incident wave to the power generation mechanism. Loading is of secondary importance in PA-WEC device design, and is addressed only after the hydrodynamic performance of the design is understood [50].

A frequency-domain approach to simulating wave energy converter
hydrodynamics

2.5.1 Equation of Motion

The equation of motion that describes the hydrodynamic is the Newtonian dynamic equation for an oscillating body. For a body in an ideal fluid

$$F_{TOT,p} = F_{HYDRO,p} + F_{EXT,p} \quad [N] \quad (2-15)$$

where

- $F_{TOT,p}$ is the total force acting on the body
- $F_{HYDRO,p}$ is the hydrodynamic force acting on the body
- $F_{EXT,p}$ is the external force acting on the body
- p is the body reference number, and is omitted from reference when the PA-WEC has only a single body.

In this representation, the two last terms represent the aggregate impact of the fluid forces or the external forces. The derivations of the component elements of $F_{HYDRO,p}$ and $F_{EXT,p}$ are non-trivial and are not included here, but can be found in several publications, including the books [2, 41, 51]. Instead, the derivation results, taken from [41, 50] are incorporated in the following sections.

2.5.2 Formulation of Forces

For a PA-WEC moving in heave only, the hydrodynamic force governing motion is defined as:

$$F_{HYDRO,p} = F_{e,p} + F_{r,p} + F_{cr,p} + F_{b,p} + F_{v,p} + F_{f,p} \quad [N] \quad (2-16)$$

where

- $F_{e,p}$ is the excitation force
- $F_{r,p}$ is the radiation force
- $F_{cr,p}$ is the coupled radiation force
- $F_{b,p}$ is the hydrostatic stiffness force
- $F_{v,p}$ is the viscous force
- $F_{f,p}$ is the friction force

A frequency-domain approach to simulating wave energy converter hydrodynamics

Although the friction forces are unavoidable in real systems, it is often ignored in early analysis efforts, as it is considered to be negligible [41, ch. 5.9, pp. 181 - 183]. Therefore, no equation for $F_{f,p}$ is given.

The external force governing the PA-WEC motion is defined as:

$$F_{EXT,p} = F_{PTO,p} + F_{Moor,p} \quad [N] \quad (2-17)$$

where $F_{PTO,p}$ is the force on the body due to the PTO mechanism and $F_{Moor,p}$ is the force on the body due to the device mooring [52].

The forces described in this section are all functions of time, although the time-dependencies of each may vary. At a minimum, each force is defined with a time-dependency related to the position, velocity or acceleration of the rigid body. Some of the forces are related to multiple time- motion descriptors. Thus, in order for Eq. (2-15) to have meaning, $F_{EXT,p}$ must have “the same time dependency” [50, ch. 3.4.2, p. 58] as the $F_{HYDRO,p}$ components. This relationship is in of the analysis domain, as long as the domain is consistent between the forces. The PTO force included in this experiment is a placeholder for the generator model. It is currently modeled as a proportional constant applied to the relative velocity of the device bodies. This is a simplistic representation for true WEC development, and appropriate only for early development efforts.

2.5.3 Excitation Force

$F_{e,p}$ is the source of the PA-WEC movement and is known as the *excitation-force vector*. It is caused by the oscillatory motion in the incident wave front and is defined as

$$F_{e,p} = F_{FK,p} + F_{d,p} \quad [N] \quad (2-18)$$

where $F_{FK,p}$ is the *Froude-Krylov force vector* and $F_{d,p}$ is the *diffraction force vector*. The Froude-Krylov force vector describes the force placed on the PA-WEC body by the incident wave if the body does not move. According to [41, ch. 5.6.3,

A frequency-domain approach to simulating wave energy converter hydrodynamics

p. 163], it may be a decent approximation to $F_{e,p}$, especially “if the extension of the immersed body is very small compared with the wavelength” of the incident wave. $F_{FK,p}$ is found by direct integration of the known pressure from the incident wave over the body surface that is made wet from that wave. As a result, $F_{FK,p}$ is unique for any given combination of body surface shape and incident wave combination.

The diffraction force vector exists to satisfy the homogeneous boundary condition on the wet surface of the PA-WEC rigid bodies. It is function of both the incident wave and the shape of the body. $F_{d,p}$ cannot be analytically determined for practical body surfaces. Instead, it is numerically calculated through application of well-understood mathematical techniques from the fields of naval hydrodynamics and offshore engineering [50, ch. 3.4, p. 56].

2.5.4 Radiation Force

The *radiation force*, $F_{r,p}$, is the force associated with the creation of waves when a rigid body oscillates on the surface of a fluid. According to linear theory it is proportional to the amplitude of the oscillation displacement, and it is defined as

$$F_{r,p}(\omega) = -\{(\mathbf{AM}_p) \cdot (\text{acceleration}) + (\mathbf{B}_p) \cdot (\text{velocity})\} [N] \quad (2-19)$$

Every term to the right of the equation is a function of frequency, and commonly references $\omega \left[\frac{\text{rad}}{\text{s}} \right]$. \mathbf{AM}_p , called the *added mass coefficient*, represents the portion of the oscillatory energy that is stored in the wave being created in the fluid. The *damping coefficient*, \mathbf{B}_p is the restriction on the oscillation caused by the fluid. Taken together, \mathbf{AM}_p and \mathbf{B}_p form the frequency-dependant radiation-impedance matrix \mathbf{Z}_p :

$$\mathbf{Z}_p = \mathbf{R}_p + i \cdot \mathbf{X}_p = \mathbf{R}_p + i \cdot \omega \cdot \mathbf{AM}_p [\text{kg/s}] \quad (2-20)$$

A frequency-domain approach to simulating wave energy converter hydrodynamics

\mathbf{R}_p is called the radiation-resistance matrix and \mathbf{X}_p is the radiation-reactance matrix. For a system with a single rigid body, \mathbf{Z}_p is a square matrix composed of complex elements $\mathbf{Z}_{ii',p}$. In a single-body system, \mathbf{Z}_p is a 6x6 matrix and the subscripts i and i' reference the impedance between any two of the six oscillators in the system. In a system with N multiple rigid bodies, \mathbf{Z}_p becomes a matrix of 6x6 matrices, resulting in a matrix that contains $6N^2$ elements. Like $F_{d,p}$, the elements of \mathbf{Z}_p must be calculated numerically [50, ch. 3.4, p. 56].

2.5.5 Coupled Radiation Force

The *coupled radiation force*, $F_{cr,p}$, is the force that the movement of one body places on the second body. The equation governing this force is currently not well defined, although it is an inescapable component of the overall motion. For the purpose of this research, $F_{cr,p}$ is defined as the negative of an added mass times a velocity. The added mass term is the lesser of the two maximum frequency values provided in the AQWA output. The velocity is the speed of the opposing body. For example,

$$(F_{cr} \text{ Body 1}) = -(AM) \cdot (\text{body 2 velocity}) [N] \quad (2-21)$$

2.5.6 Hydrostatic Stiffness Force

The *hydrostatic stiffness force*, $F_{b,p}$, is the restorative force placed on the body by the water when it is pushed into the water surface. It is also called the buoyancy force. It is a direct result of the hydrostatic pressure acting on the surface of the body, and is equal to the weight of the fluid displaced by the body. $F_{b,p}$ is only applicable in the positive vertical direction (\hat{z}) and acts through the center of gravity of the displaced fluid. F_b is described by

$$F_{b,p} = -(S_{b,p}) \cdot (\text{body position}) [N] \quad (2-22)$$

A frequency-domain approach to simulating wave energy converter
hydrodynamics

where $S_{b,p}$ is the *buoyancy coefficient*. For linear theory, $S_{b,p}$ is a constant with respect to time and derived from the mass and shape of the body [41, ch. 5.9, pp. 181-182]. $S_{b,p}$ can be described as a function of position without violating any of the constraints or assumptions.

2.5.7 Viscous Friction Force

Although all the equations for this approach assumed an ideal fluid which, would not have $F_{v,p}$, these non-zero loss forces are introduced as practical correction factors. $F_{v,p}$ is defined as

$$F_{v,p} = -R_{v,p} \cdot (\text{body velocity}) [N] \quad (2-23)$$

2.5.8 Mooring Forces

Equations defining the mooring force are not well defined in the research to date. However, some sort of mooring structure is a fundamental requirement of a WEC, so $F_{Moor,p}$ is maintained in the EOMs. It is defined as

$$F_{Moor} = -R_{mb} \cdot (\text{body velocity}) - R_{mk} \cdot (\text{body position}) [N] \quad (2-24)$$

Currently, the mooring is affixed to only one of the WEC bodies and impacts the other body through the body-to-body coupling forces.

2.6 Understanding Wave Energy Farm Operation

The Wave Energy Farm, or WEF, is the term used in reference to a collection of co-located PA-WECs that share a common infrastructure. Such collections are currently an economic necessity, as the infrastructure costs for a single device overwhelm the profits from the output of an individual device. However, the infrastructure-to-device cost ratio decreases as the number of devices increase. There are limits to this ratio as with any real world system. Likewise, there are possibly discontinuities in the device to cost ratio plot due to any number of reasons, including WEF aspect ratio, array geometry, and bathymetry. However,

A frequency-domain approach to simulating wave energy converter hydrodynamics

there are no peer-reviewed publications that report research in this area. This may be due to the relative newness of the technology or to the corporate confidentiality requirements of the developers.

2.6.1 WEF Function

The WEF is the system that aggregates power from individual devices into a commercially viable quantity and delivers it to the electrical grid. The WEF components include individual devices, infrastructure, and several levels of programmable control. It uses the infrastructure, which includes PA-WEC output aggregation, power storage and conditioning, and grid connection, to perform these functions. The WEF programmable controls are software that include automatic monitoring, communication, and control functions. These software components are tied into each individual device, storage facility, and conditioning/delivery equipment. The WEF can be conceptually partitioned into two components. The first component is labeled the WEC-side and describes the characteristics of each array element. The second component is labeled the Grid-side. This component contains descriptions of all the elements that transform individual PA-WEC outputs into the single grid interface.

2.6.2 Constraints on WEF Location

While there are many constraints on WEF location, the information found in sections 2.2.1 and 2.3.1 clearly shows that the water depth, or bathymetry, has an important impact on the energy available for harvest. This translates to a constraint on the location of the WEF. Placing the WEF in deep water, where the available wave energy is at a maximum, may push the infrastructure and maintenance costs beyond sustainability. An attempt to minimize infrastructure costs by placing the WEF close to shore would reduce the amount of energy per WEC available for harvest. Any bathymetry within the WEF boundaries that

A frequency-domain approach to simulating wave energy converter
hydrodynamics

decreases the water depth to a point meeting the definition of the shoaling zone decreases the amount of harvestable energy. Thus, from the perspective of cost-effective harvestable energy, the ideal placement for the WEF is on the deep side of the shoaling zone. The placement may be further refined by clearly understanding the amount of energy removed from the wave front as it passes through the farm, as energy attenuation pushes the deep-water boundary line closer to shore.

The sea state characteristics throughout the year, or in periodic abnormal years (like as El Nino) versus normal years, can also impact WEF location. A wide variation in the site sea elevations through the course of a year can force an increase in device development and maintenance costs. An excessive cost increase versus the energy harvested can render the site location economically unsound. Likewise, a significant period of low elevations can result in low farm output. The same low output could also be the result of excessively high sea surface elevations which force the devices into a shut-down state for survivability.

A frequency-domain approach to simulating wave energy converter hydrodynamics

3 Methodology Development Process

The traditional time-domain approach to simulations or emulations implements all of the governing equations in the time-domain. This means that every calculation that is performed is a function of time. The equations that form the model are solved in a step-wise manner and each solution is associated with a particular instant in simulation time. As a consequence, the number of calculations required increases as the model increases in complexity. In addition, the basic choices of how the model is implemented in the environment can also cause the calculation complexity to increase. These issues result in the simulations being time and compute intensive, limiting the usefulness of the simulation approach. Still, the time-domain approach is currently the commonly used development method, so any meaningful exploration into other methods must be related to the standard.

The methodology defined in this research judiciously applies a frequency-domain analysis, developed in MATLAB™, to the hydrodynamic portion of the WEC design. This converts the analysis from a time-domain, step-wise simulation to a series of mathematical equations applied to arrays. Both approaches have a time-series of motion information, per device body, as their outputs. This motion information is ideal as the input source to a time-domain simulation of the power-generation portion of the WEC.

Proving that two approaches produce comparable results requires that one approach is used as a reference for the other. The reference frame is the time-domain approach. The reference model used is one that was developed at Oregon State University (OSU) by graduate student Kelley Ruehl. Her methods and approach are detailed in [53]. The model was further enhanced and maintained by Bret Bosma, also an OSU graduate student. Finally, the model was modified to

A frequency-domain approach to simulating wave energy converter hydrodynamics

facilitate the accurate comparison with the frequency-domain approach. Places where these modifications were made are noted in the following descriptions.

The reference model itself is a Simulink™ model driven by a MATLAB™ script. Detailed descriptions of this model, including development and use, are found in [53]. Finally, the reference model has several run-time options that define the WEC geometry and the source of the sea elevation model. The WEC geometry is restricted to one that had the most development, although the majority of the results are protected under confidentiality agreements with the private developer. However, it is important to note that methodology is applicable to any WEC device that fits the constraints detailed in Section 1.4, assuming that BEM data can be provided.

Finally, the sea elevation models used are developed from the measured data as described in Section 3.2.2. The time-domain version of the sea surface is merely the frequency-domain version that has been transformed using a Fourier Transform approach.

3.1 Reference Frame and Motion Mode

The concepts and definitions of the general reference frame and motion mode are detailed in Sections 2.4.2 and 2.4.3. This research defines the reference frame as a two-dimensional Cartesian framework, with axes in the x and z directions. Therefore, a plot of the incident wave elevation will have a horizontal axis of time, a vertical axis of elevation, and data points that represent the elevation at a single x location. This simplified formulation is possible because the device is under consideration is axisymmetric. For devices that are asymmetric, the reference frame must be three-dimensional, and all the equations related to device motion must be developed as vectors within the horizontal (x-y) plane.

In addition, this research focuses on motion mode 3 only. This reduces the state space matrices to scalar values for each body in the PA-WEC device.

A frequency-domain approach to simulating wave energy converter
hydrodynamics

Separate matrices may still be employed to delineate multiple bodies in the device. The methodologies discussed are in of the mode representation.

3.2 WEC Model Input

The most fundamental components of the hydrodynamic WEC model are two base information sets that inform the model of the simulation specifics. The first information set defines the conditions of the ocean at a specific location. The second set defines the hydrodynamic properties of the device being modeled. These sets are described in the following sections.

3.2.1 Sea State Input

The sea elevation input is the data set that represents the ocean wave field incident to the PA-WEC device being simulated. The simplest way obtain the incident wave field is to use an actual time-series record from a buoy station. However, this would require special recording buoys, as the overwhelming majority of data stations do not store the actual time-series record. Another way to obtain the incident wave is to create it using well-defined statistical methods developed by oceanographers. This is the most likely and useful method for providing realistic input to a hydrodynamic model.

Regardless of the source, the virtual sea profile must have the following characteristics in order to generate useful simulation results:

- 1) Statistically identical to the real sea state at the proposed WEF location.
- 2) Randomized, enabling the use of statistical methods for the selection of states to model.
- 3) Repeatable, allowing for accurate device comparisons and simulation debug.

The virtual sea elevation profile is generated through a process defined in [12]. This procedure uses a fundamental wave equation to create an elevation

A frequency-domain approach to simulating wave energy converter hydrodynamics

time-series from an energy spectrum. The source energy spectrum is developed from buoy data by applying a process defined in [54]. There are several applications of this process that employ different buoy data sets. The oceanography community differentiates between them by including the reference to the data set in the spectrum name. The process used here is referred to as the TMA spectrum as it was built from the TEXEL, MARSEN, and ARSLOE data sets. This particular application uses a sea state description as data values for its input variables. The implementation of the process follows the detail found in [55].

3.2.2 Generating the Sea State

A description of the sea state, consisting of H_s , T_d , and *theta*, is obtained from a NDBC buoy near the desired farm site. T_d is used to select the frequency (γ) and directional width (n) parameters from guidelines published by [56]. These additional parameters further characterize the range of frequencies and directions that contain the wave energy. The complete sea state description and the additional parameters are applied to Equation 10 of [54], resulting in a frequency-domain spectral representation of the wave energy. The spectrum is built of i discrete bins, each a finite frequency-range Δf wide. Every bin is characterized by a center frequency - f_i , amplitude - S_i , and direction - θ_i . An example of a resultant spectrum is shown in Fig. 3.1.

A frequency-domain approach to simulating wave energy converter
hydrodynamics

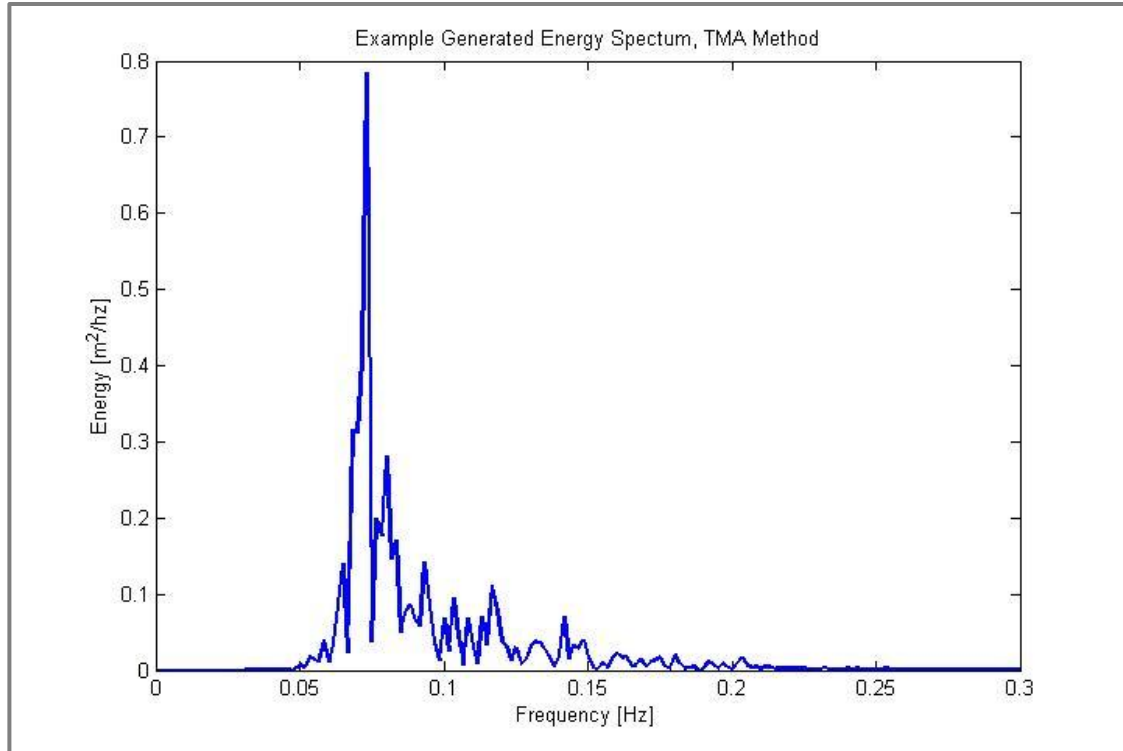


Fig. 3.1: Wave Energy Spectra Generated using TMA Methodology

A traditional Cartesian coordinate system² is defined as the reference point for generating the sea surface. The sea surface elevation η is a function of the location (x, y) and the time. It is represented by

$$\eta = \sum_{all\ i} A_i \cdot \cos(k_i \cdot x \cdot \cos \theta_i + k_i \cdot y \cdot \sin \theta_i - 2 \cdot \pi \cdot f_i \cdot t + \epsilon_i) \ [m] \quad (3-1)$$

- A_i is the component amplitude
- k_i is the component wave number

² The positive x-direction points East (to the right), the positive y-direction points North (up), and when used, the positive z-direction is out of the page pointing to the sky.

A frequency-domain approach to simulating wave energy converter
hydrodynamics

- θ_i is the component direction
- f_i is the component frequency
- ϵ_i is the component phase
- i is the number of frequencies used to describe the wave energy spectrum
- (x, y) is the location of η with respect to the defined coordinate system

The first variable is the amplitude of the i^{th} component. It is derived from the i^{th} bin in the representative spectrum. The area of each bin is the area of a rectangle that is as tall as the spectrum amplitude and as wide as the frequency range. This area becomes the amplitude of the wave component at the center frequency by application of

$$A_i = 2\sqrt{S_i(f_i, \theta_i) \cdot \Delta f \cdot \Delta \theta_i} \quad [m^2/\text{Hz}] \quad (3-2)$$

where $S_i(f_i, \theta_i)$ is the spectral amplitude as a function of the frequency and direction.

The θ_i direction value for each bin is assigned “using the directional distribution function as a proxy for a probability density function for wave direction. The method insures a homogeneous directional wave field with no artificial spatial wave grouping” [55].

Two of the remaining component variables, frequency and wave number, used in Eq. (3-1) are functions of the component frequency. This frequency is defined as the center frequency of the i^{th} spectral bin. The first variable, f_i , is simply the frequency itself. This frequency is also applied to a reordered dispersion relation, Eq. (3-3), along with the depth at the location, to generate the second variable, k_i . A numerical procedure is used to determine k_i because the associated λ_i is unknown. The reordered dispersion relation is

$$k_{n+1} \cdot h_{n+1} = \frac{h \cdot \omega^2}{g} \cdot \coth(k_n \cdot h_n) \quad (3-3)$$

A frequency-domain approach to simulating wave energy converter hydrodynamics

The first value in the iteration is given by setting the value kh to infinity, causing the hyperbolic cotangent function to be equal to one.

The formulation of Eq. (3-1) specifically enables attenuation of the sea surface elevation due to the location depth. This is especially important in the case where the location depth and incident wavelengths define a shoaling region, a likely occurrence for a WEF.

The final component variable, phase, is a number representing a phase offset. It is usually created by multiplying a random number by 2π . The random number is the result of a computer algorithm that chooses a value from the uniformly distributed open interval (0-1). There is one phase per frequency for each time window simulated. Using the randomly generated wave forms early in the development cycle helps developers compare different designs and identify gross errors in a specific design. This approach is also convenient for regression testing, where the simulation goal is to verify device operation in as broad a subset of normal operating conditions as possible. However, this approach is not convenient for detailed development testing because it is not repeatable. The repeatability issue is resolved by providing the ability to load a saved phase set instead of generating one. This gives the designer repeatability of the random state, a crucial tool during many of the development phases.

The last two variables, (x, y) describe the elevation series location with respect to the coordinate system. The variables have a unit designation of meters, and their values are an arbitrary choice for a single η . The most mathematically convenient location is the origin of the coordinate system, $(x = 0, y = 0)$, and is assigned to a particular WEC in the WEF. This eliminates the inner cosine and sine functions. It also eliminates the wave number. The resulting equation is

$$\eta(x = 0, y = 0, t) = \sum_{all \ i} A_i \cdot \cos(-2 \cdot \pi \cdot f_i \cdot t - \epsilon_i) [m] \quad (3-4)$$

A frequency-domain approach to simulating wave energy converter hydrodynamics

This equation represents the sea state for individual WEC device simulations. The more general form of this equation, Eq. (3-3) is used to create the sea state for each point in a WEF array that represents a single WEC device.

The Eqs 3-3 and 3-4 are functions of frequency – that is, they exist in a frequency-domain frame of reference. They are used in the frequency-domain methodology as they are described. However, they must be transformed from functions of frequency into functions of time for the time-domain approach. These transformations are accomplished through the application of an Inverse Fourier Transform. An example elevation time-series generated by this process for a single WEC is shown in Fig. 3.2.

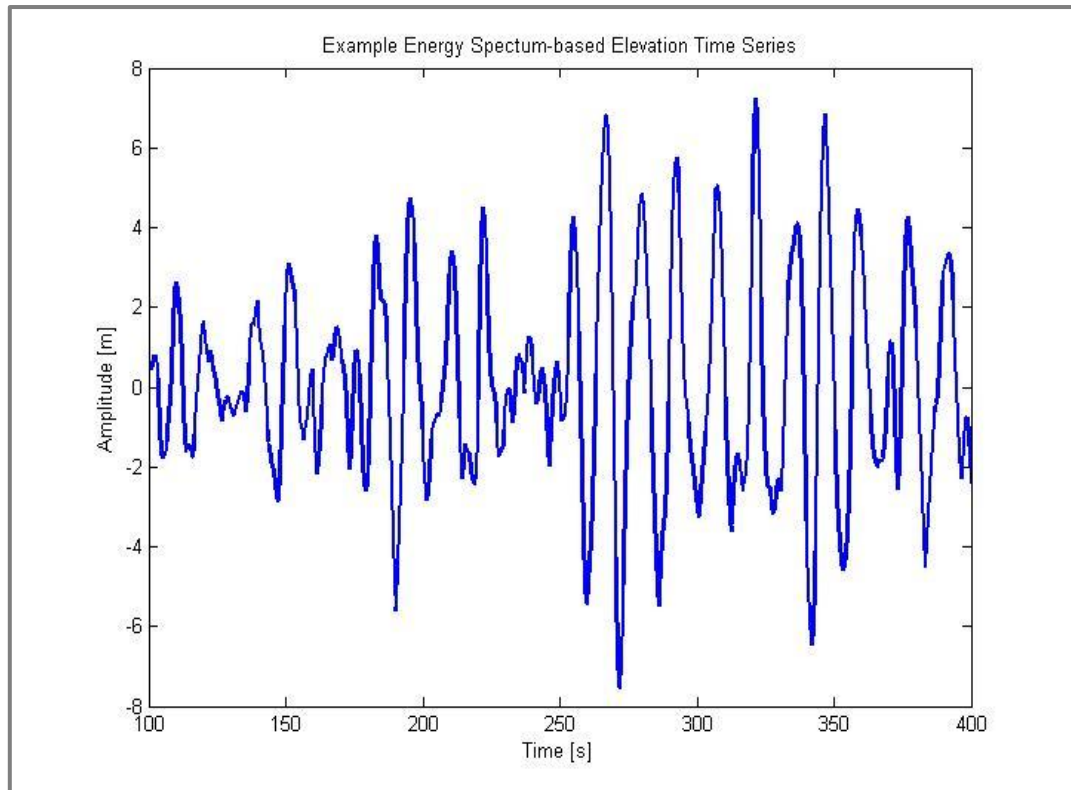


Fig. 3.2: Example Sea Elevation Time Series

A frequency-domain approach to simulating wave energy converter
hydrodynamics

3.3 WEC Model Coefficients

The process for developing the hydrodynamic forces described in Section 2.5 is demonstrated using the output of the AQWA-line product from ANSYS, BEM simulation environment. The input to this simulation is quite complex, and is not explained here. A full description of the input requirements may be found in a combination of AQWA™ reference materials. The processing that converts the AQWA™ output and physical device characteristics into the component forces described in this section.

3.3.1 Simple Forces – Constants

According to Eq. (2-16), the coefficients for the forces $F_{b,p}$, $F_{v,p}$, and $F_{f,p}$ are constants, in of the choice of domain.

The *hydrostatic stiffness force*, described in Section 2.5.6, is formulated as:

$$F_{b,p} = -(S_{b,p}) \cdot (\text{body position}) = -(Khs_p) \cdot (\text{body position}) \quad (3-5)$$

The coefficient, Khs_p , is

$$Khs_p = \rho_{sw} \cdot g \cdot A_p \quad (3-6)$$

The *viscous friction force*, described in Section 2.5.7, is formulated as:

$$F_{v,p} = -R_{v,p} \cdot (\text{body velocity}) = -(bv_p) \cdot (\text{body velocity}) \quad (3-7)$$

The coefficient bv_p is determined numerically, and adjusted with values from experiments.

3.3.2 Excitation Force

The information source for $F_{e,p}$ is a table in the AQWA™ output file labeled “FROUDE KRYLOV + DIFFRACTION FORCES-VARIATION WITH WAVE PERIOD/FREQUENCY”. An example of the table is found in Table 3.1.

A frequency-domain approach to simulating wave energy converter
hydrodynamics

FROUDE KRYLOV + DIFFRACTION FORCES-VARIATION WITH WAVE PERIOD/FREQUENCY									
PERIOD	FREQ	X		Y		Z		AMP	PHASE
		AMP	PHASE	AMP	PHASE	AMP	PHASE		
63.87	0.098	1.47E+03	90	7.10E-03	8.61	8.37E+04	0		
30.37	0.207	3.26E+03	90	4.85E-03	32.87	8.26E+04	-0.01		
19.92	0.315	5.51E+03	90	7.72E-03	133.5	8.07E+04	-0.02		
14.82	0.424	8.62E+03	90	9.34E-03	108.4	7.82E+04	-0.05		
11.8	0.533	1.29E+04	90.02	1.46E-02	73.93	7.49E+04	-0.11		

Table 3.1: Example AQWA™ results for Fe source data

The data within the table reports one amplitude and phase pair for each frequency analyzed. A representation of the excitation at each frequency can be displayed by applying the equation

$$Q = Q_0 \cdot \cos(-\omega \cdot t + \varphi) \quad (3-8)$$

where Q_0 is the amplitude, φ is the phase, and ω is the angular frequency [57, p.2]. The negative sign applied to the ωt term is slightly confusing. The trigonometry identity [58]

$$\cos(\theta) = \cos(-\theta) \quad (3-9)$$

is applied and Eq. (3-7) becomes

$$Q = Q_0 \cdot \cos(\omega \cdot t - \varphi) \quad (3-10)$$

The number of amplitude-phase pairs in the AQWA™ output is limited to 50 for each run. In addition, those 50 points are equally spaced between the start and end frequencies.

The amplitude and phase data is extracted from the AQWA™ output. The data is expanded via interpolation to a frequency-series with an incremental step size of 0.01 rad/s. The data are then converted to a single complex number per positive frequency. The complex-valued frequency-series represents the $F_{e,p}$ transfer function. No further processing of the information is needed for the frequency-domain solution.

A frequency-domain approach to simulating wave energy converter hydrodynamics

The time-domain analysis, however, does require additional processing. The set of frequency-series are converted to time-domain values through the application of an inverse Fourier Transform integral across all frequencies. The resultant values form the coefficients of a direct finite-impulse-response filter. The application of this filter is described in Section 3.4.1.

3.3.3 Radiation Force

Two additional outputs of AQWA-line are used for the creation of $F_{r,p}$. These are the Added Mass Table 3.1 and the Damping Table 3.2. The data in these tables is reported as a single real value per frequency per motion mode. The motion mode is reported as a two-digit subscript, and for this research, the '33' mode data is extracted. The values from the Added Mass table, column M33, become the imaginary part of Eq. (2-20), without further manipulation. The values from the damping table, (column C33), report a standard hydrodynamic variable 'C', where:

$$\mathbf{C}_n = \mathbf{R}_n / (2 \cdot \pi \cdot f_n) \quad (3-11)$$

However, since \mathbf{Z}_p requires \mathbf{R}_p and not \mathbf{C}_p , Eq (3-11) is solved for \mathbf{R}_p . Once these values are obtained, \mathbf{Z}_p is constructed according to Eq. (2-20) and used directly in the frequency-domain approach.

A frequency-domain approach to simulating wave energy converter
hydrodynamics

Table 3.1: Example AQWA™ Output - Added Mass

ADDED MASS-VARIATION WITH WAVE PERIOD/FREQUENCY						
PERIOD	FREQ	M	M	M	M	
(SECS)	(RAD/S)	11	22	33	44	
63.87	0.098	3.58E+03	3.58E+03	1.88E+05	5.25E+05	
30.37	0.207	3.58E+03	3.58E+03	1.88E+05	5.25E+05	
19.92	0.315	3.58E+03	3.58E+03	1.88E+05	5.25E+05	
14.82	0.424	3.58E+03	3.58E+03	1.88E+05	5.25E+05	
11.8	0.533	3.58E+03	3.59E+03	1.88E+05	5.25E+05	
9.8	0.641	3.59E+03	3.59E+03	1.88E+05	5.25E+05	
8.38	0.75	3.59E+03	3.59E+03	1.88E+05	5.26E+05	

Table 3.2: Example AQWA™ Output - Damping Matrix

DAMPING-VARIATION WITH WAVE				PERIOD/FREQUENCY	
PERIOD	FREQ	C	C	C	C
(SECS)	(RAD/S)	11	22	33	44
63.87	0.098	2.52E-04	2.53E-04	-4.85E-03	-9.44E-05
30.37	0.207	3.14E-03	3.14E-03	1.22E-01	1.34E-03
19.92	0.315	1.87E-02	1.87E-02	3.10E+00	1.77E-02
14.82	0.424	9.14E-02	9.16E-02	2.49E+01	1.43E-01
11.8	0.533	3.60E-01	3.60E-01	1.15E+02	8.65E-01
9.8	0.641	1.05E+00	1.05E+00	3.43E+02	3.87E+00

For the time domain, \mathbf{Z}_p is further manipulated before implementation. In the realm of pure physics, Eq. (2-20) is not guaranteed to have a closed solution, because the added mass at infinity term does not converge to zero. Following [41], \mathbf{Z}_p is decomposed into the frequency-dependent transfer function \mathbf{K}_p , where

$$\mathbf{K}_{p,n} = \mathbf{Z}_{p,n} - i \cdot \omega \cdot m(\infty) = \mathbf{R}_{p,n} + i \cdot \omega \cdot m - i \cdot \omega \cdot m(\omega = \infty) \quad (3-12)$$

The time-domain filter coefficients are calculated by applying an inverse Fourier Transform to the transfer function $\mathbf{K}_{p,n}(\omega)$. The full time-domain $F_{r,p}$ is then constructed according to:

A frequency-domain approach to simulating wave energy converter
hydrodynamics

$$F_{r,p} = -k * (\text{body velocity}) - m(\omega = \infty) \cdot (\text{body acceleration}) \quad (3-13)$$

3.3.4 Coupling Forces: Interactions Between Device Bodies

There is no well-defined industry process for determining the interactions between bodies that has been applied to WEC design in the literature. The frequency-domain transfer function is assumed to be a constant. It is set equal to the negative of the lesser of the maximum added mass values derived by AQWA for the two device bodies.

$$Kc_{p,n}(\omega) = -\min(\text{added mass}_p(\omega = \infty)) \quad (3-14)$$

Because this is a constant, the full time-domain $Fc_{r,p}$ is then constructed according to Eq. (2-19).

3.3.5 Mooring Forces

The *mooring forces*, described in Section 2.5.8, are formulated:

$$\begin{aligned} F_{Moor} &= -R_{mb} \cdot (\text{velocity}) - R_{mk} \cdot (\text{position}) \\ &= -(Moorb) \cdot (\text{velocity}) - (Moork) \cdot (\text{position}) \end{aligned} \quad (3-15)$$

The coefficients *Moorb* and *Moork* are designer assigned values in the reference model. The same values are used in the frequency-domain formulation.

3.3.6 Power-Take-Off Force

$F_{PTO,p\mp}$ represents the force applied to the PTO mechanism. It is modeled as:

$$F_{PTO,p\mp} = \pm \text{damping} \cdot (\text{body 1 velocity} - \text{body 2 velocity}) \quad (3-16)$$

The coefficient *damping* is arbitrarily assigned a real constant value.

3.4 WEC Models

The fundamental focus of this research is the comparison of two different modeling approaches for WEC devices. The next sections describe the WEC model for each approach.

A frequency-domain approach to simulating wave energy converter hydrodynamics

3.4.1 Time-Domain

The time-domain model is developed by implementing Eq (2-15) in the Mathworks Simulink™ environment. An example of this is found in Fig. 3.3 which shows the formulation of the Body 1 motion.

The output of the skinny rectangle to the upper left is the total force. This total force is divided by the body mass, creating the body acceleration. Acceleration is integrated to achieve velocity which is integrated to achieve position. The integrator functions are represented by the rectangular icons containing $\frac{1}{s}$. These three motion descriptors form the output of the model for this body. They also form the basic time-dependencies for the different forces that are calculated in the model. Forces with constant coefficients are applied as gains and implemented in the triangular icons. The icons contain the coefficient variable names. Forces with time/frequency coefficients are found in the rectangular boxes labeled $\frac{\text{num}(z)}{1}$. These icons represent direct-form filters with coefficients generated as described in Section 3.3. The mathematical function they perform is a convolution between the impulse response function and the motion descriptor.

Forces that are direct feedback from the Body 1 motion variables are implemented in this schematic. They are $F_{v,2}$, $F_{r,2}$, and $F_{b,2}$. The remaining forces ($F_{e,2}$, $F_{cr,2}$, $F_{m,2}$, and $F_{PTO,2}$) are inputs to this schematic, created in other schematics using similar techniques. Finally, the rectangular boxes with inputs only and captions of ‘To Workspace’ capture the values of the signal routed to them as a vector. These vectors are available in MATLAB™ for further analysis. A full set of model schematics can be found in Appendix A: Time-Domain Model.

A frequency-domain approach to simulating wave energy converter hydrodynamics

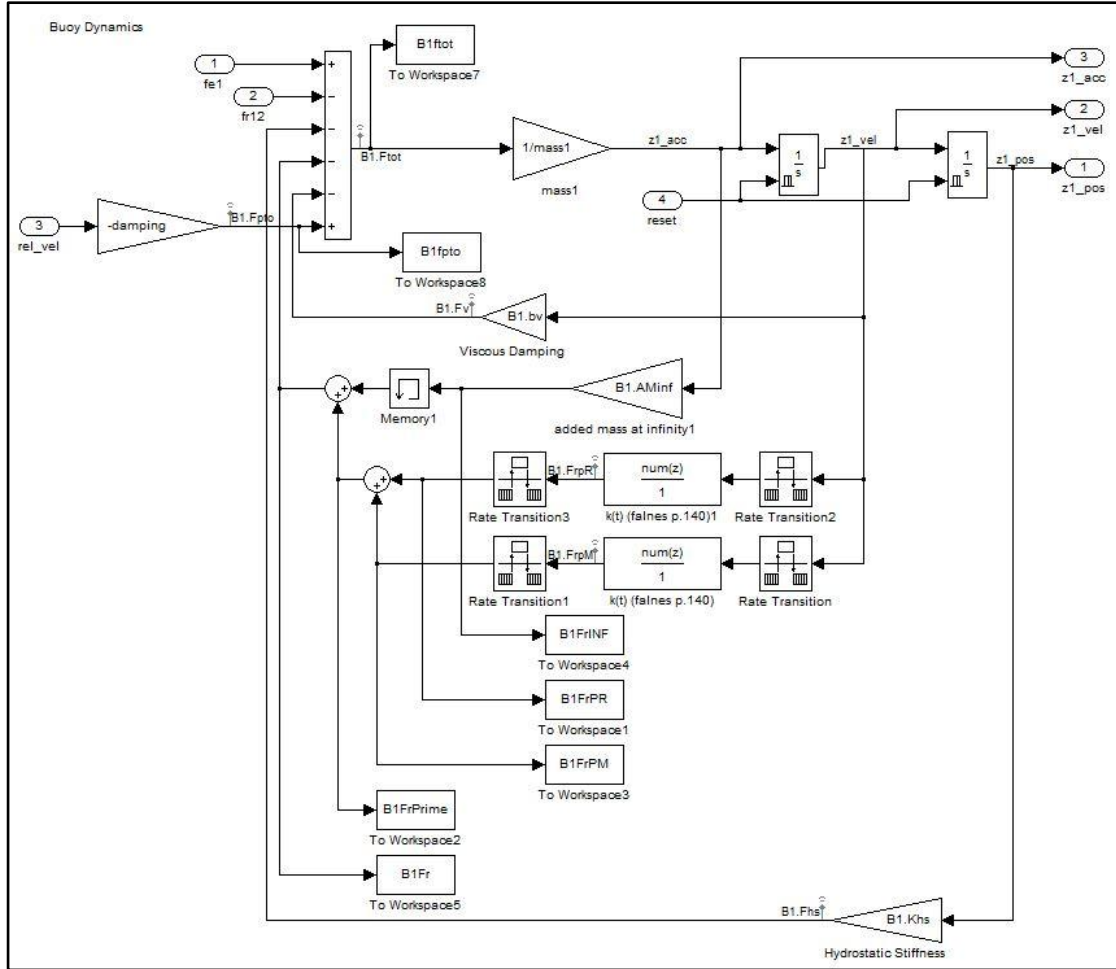


Fig. 3.3: Body 1 Simulink™ Model

3.4.2 Frequency-Domain

The simulation approach developed here performs all of the equation manipulation in the frequency domain, only converting anything to the time-domain after solving for the desired inputs. This section describes the solution derivation as a series of steps, outlining the mathematical steps and presenting significant equations. The detailed derivation is found in Appendix B: Frequency-Domain Model.

A frequency-domain approach to simulating wave energy converter
hydrodynamics

Body 1 of the WEC device, the float, is described by the specific representation of the EOM, where the individual force components are replaced with their specific coefficient/motion term combination. These time-domain component equations are listed below. The variable $z1$ represents the position descriptor of WEC body 1 (position, velocity, or acceleration) as noted in each subscript. Each term, being a force, has units of Newtons [N].

$$f_{tot} = (\text{mass1}) \cdot (z1_{acceleration}) \quad (3-17)$$

$$fe_1 = (\eta) * (B1fe_{filt}) \cdot (u) \quad (3-18)$$

$$fr_{12} = (z2_{acceleration}) \cdot \text{mass}(\omega = \infty) \cdot (u) \quad (3-19)$$

$$fb_1 = (z1_{pos}) \cdot (B1khs) \cdot (u) \quad (3-20)$$

$$fr_1 = (z1_{vel}) * (B1fr_{filt}) \cdot (u) \quad (3-21)$$

$$fv_1 = (z1_{vel}) \cdot (B1bv) \cdot (u) \quad (3-22)$$

$$fpto_1 = -(z1_{vel} - z2_{vel}) \cdot (\text{damping}) \cdot (u) \quad (3-23)$$

Eq (2-15) is then re-written, incorporating these combinations and isolating $z1$ terms to the left side:

$$\begin{aligned} & (\text{mass1}) \cdot (z1_{acc}) \cdot (u) \quad (3-24) \\ & + (z1_{pos}) \cdot (B1khs) \cdot (u) \\ & + (z1_{vel}) * (B1fr_{filt}) \cdot (u) \\ & + (z1_{vel}) \cdot (B1bv + \text{damping}) \cdot (u) \\ & = (\eta) * (B1fe_{filt}) \\ & - (z2_{acceleration}) \cdot BcAMinf \cdot (u) \\ & + (z2_{vel}) \cdot (\text{damping}) \cdot (u) \end{aligned}$$

The multiplier u , the unit step-function, is used to indicate the portions of the equation that are causal.

The sea surface elevation, η , is written in the form defined in Eq (3-1). Because the system is constrained to be linear, the output motion terms (acceleration,

A frequency-domain approach to simulating wave energy converter
hydrodynamics

velocity, position) are also written in this form. Finally, the velocity and position variables are re-written in terms of the acceleration through use of calculus. The resulting equation is:

$$\begin{aligned}
 & \sum_{n=1}^{\infty} Z1_n \{ (mass1) \cdot (\cos(2 \cdot \pi \cdot f_n + Z1\varphi_n)) \cdot (u) \cdot \\
 & \quad + (B1khs) \cdot \left[\frac{-1}{(2 \cdot \pi \cdot f_n)^2} \cdot \cos(2 \cdot \pi \cdot f_n + Z1\varphi_n) + (C1V_n) \cdot (t) + C1P_n \right] \cdot (u) \\
 & \quad + \left(\left[\frac{1}{2 \cdot \pi \cdot f_n} \cdot \sin(2 \cdot \pi \cdot f_n + Z1\varphi_n) + C1V_n \right] \cdot (u) \right) * (B1fr_{filt}) \\
 & \quad + (B1bv + damping) \cdot \left[\frac{1}{2 \cdot \pi \cdot f_n} \cdot \sin(2 \cdot \pi \cdot f_n + Z1\varphi_n) + C1V_n \right] \cdot (u) \} \\
 & = \sum_{n=1}^{\infty} (A_n) \cdot \cos(2 \cdot \pi \cdot f_n + \varphi_n) * (B1fe_{filt}) \\
 & \quad - \sum_{n=1}^{\infty} Z2_n \{ (BcAMinf) \cdot \cos(2 \cdot \pi \cdot f_n + Z2\varphi_n) \cdot (u) \\
 & \quad - (damping) \cdot \left[\frac{1}{2 \cdot \pi \cdot f_n} \cdot \sin(2 \cdot \pi \cdot f_n + Z2\varphi_n) + C2V_n \right] \cdot (u) \}
 \end{aligned} \tag{3-25}$$

Next, the equation is transformed from the time-domain to the frequency-domain by the application of the following Fourier Transforms [59, ch. 3.3, p.107]:

- Ideal Cosine with a phase shift (α):

$$\begin{aligned}
 \cos(2 \cdot \pi \cdot f \cdot t + \alpha) &= \frac{1}{2} \cdot (\cos \alpha) \cdot [\delta(f + f_0) + \delta(f - f_0)] \\
 &\quad - \frac{i}{2} \cdot (\sin \alpha) \cdot [\delta(f + f_0) - \delta(f - f_0)]
 \end{aligned} \tag{3-26}$$

- Causal Cosine with a phase shift (α):

A frequency-domain approach to simulating wave energy converter
hydrodynamics

$$\begin{aligned}
 & \cos(2 \cdot \pi \cdot f \cdot t + \alpha) \cdot (u) \\
 &= (\cos \alpha) \cdot \frac{1}{4} \cdot (\delta(f + f_0) + \delta(f - f_0)) + \frac{i \cdot 2 \cdot \pi \cdot f \cdot (\cos \alpha)}{(2 \cdot \pi \cdot f_0)^2 - (2 \cdot \pi \cdot f)^2} \\
 &\quad - (\sin \alpha) \cdot \frac{1}{i \cdot 4} \cdot (\delta(f + f_0) - \delta(f - f_0)) - \frac{i \cdot 2 \cdot \pi \cdot f_0 \cdot (\sin \alpha)}{(2 \cdot \pi \cdot f_0)^2 - (2 \cdot \pi \cdot f)^2}
 \end{aligned} \tag{3-27}$$

- Causal Sine with a phase shift (α):

$$\begin{aligned}
 & \sin(2 \cdot \pi \cdot f \cdot t + \alpha) \cdot (u) \\
 &= (\cos \alpha) \cdot \frac{1}{i \cdot 4} \cdot (\delta(f + f_0) - \delta(f - f_0)) - \frac{i \cdot 2 \cdot \pi \cdot f_0 \cdot (\cos \alpha)}{(2 \cdot \pi \cdot f_0)^2 - (2 \cdot \pi \cdot f)^2} \\
 &\quad + (\sin \alpha) \cdot \frac{1}{4} \cdot (\delta(f + f_0) + \delta(f - f_0)) + \frac{i \cdot 2 \cdot \pi \cdot f \cdot (\sin \alpha)}{(2 \cdot \pi \cdot f_0)^2 - (2 \cdot \pi \cdot f)^2}
 \end{aligned} \tag{3-28}$$

- Heaviside Step Function:

$$u(t) = \frac{\delta(f)}{4} - \frac{i}{2 \cdot \pi \cdot f} \tag{3-29}$$

These equations are inserted into Eq. Error! Reference source not found., like terms are grouped, and denominators rationalized. At this point in the derivation, the time/frequency force coefficients are represented by variables. Each variable corresponds to a frequency-series vector where the vector entries are complex numbers describing the amplitude and phase of the force at that frequency. This is very similar to the native output of AQWA. The excitation force variables are $B1FE_n$ and $B2FE_n$. The radiation force variables are $B1Z_n$, $B2Z_n$, $BC12Z_n$, and $BC21Z_n$. The forces are created by multiplication with the motion descriptors, rather than the time-domain convolution.

To make solving this equation easier, it is broken into four separate equations: Positive Frequency, Negative Frequency, No Frequency, and All Frequencies. This is possible because these divisions are orthogonal to each other, and the

A frequency-domain approach to simulating wave energy converter
hydrodynamics

approach is likened to solving a complex variable by separating it into a real part and an imaginary part. For this methodology, the No- and All- frequency equations are unexamined. This is a valid approach for this research, as the focus is on the steady-state motion, not positional offsets (described by the No Frequency equation) nor the instantaneous position shifts caused at the start of time. However, it is important to note that these conditions cannot be ignored during the complete system design. The resulting equation for the positive frequency component, after algebraic manipulation, is:

$$\begin{aligned}
 & \sum_{n=1}^{\infty} Z1_n \cdot (\text{mass1}) \cdot [\delta(f - f_n)] \cdot [\cos(Z1\varphi_n) + i \sin(Z1\varphi_n)] \\
 & - \sum_{n=1}^{\infty} Z1_n \cdot \left(\frac{B1Khs}{(2 \cdot \pi \cdot f_n)^2} \right) \cdot [\delta(f - f_n)] \cdot [\cos(Z1\varphi_n) + i \sin(Z1\varphi_n)] \\
 & + \sum_{n=1}^{\infty} Z1_n \cdot \left(\frac{B1Z_n + B1bv}{2 \cdot \pi \cdot f_n} \right) \cdot [\delta(f - f_n)] \cdot [-i \cdot \cos(Z1\varphi_n) + \sin(Z1\varphi_n)] \\
 & + \sum_{n=1}^{\infty} Z1_n \cdot \left(\frac{\text{damping}}{2 \cdot \pi \cdot f_n} \right) \cdot [\delta(f - f_n)] \cdot [-i \cdot \cos(Z1\varphi_n) + \sin(Z1\varphi_n)] \\
 & = \sum_{n=1}^{\infty} (A_n) \cdot (B1FE_n) \cdot [\delta(f - f_n)] \cdot [\cos(\varphi_n) + i \sin(\varphi_n)] \\
 & - \sum_{n=1}^{\infty} (Z2_n) \cdot (BcAMinf) \cdot [\delta(f - f_n)] \cdot [\cos(Z2\varphi_n) + i \sin(Z2\varphi_n)] \\
 & - \sum_{n=1}^{\infty} (Z2_n) \cdot \left(\frac{B1Z_n + \text{damping}}{2 \cdot \pi \cdot f_n} \right) \cdot [\delta(f - f_n)] \cdot [-i \cos(Z1\varphi_n) + \sin(Z1\varphi_n)]
 \end{aligned} \tag{3-30}$$

The Positive- and Negative- frequency equations are complex-conjugate versions of each other. While it is tempting to solve only the Positive equation, solving both provides the developer a validation of the solutions. This is

A frequency-domain approach to simulating wave energy converter
hydrodynamics

especially useful when the model being developed is not depicting a commonplace, well-known, and well understood process.

The method described for Body 1 of the WEC is also applied to Body 2, resulting in an additional two equations. The Positive frequency equations for the two bodies are used to solve for the motion variables Z1 and Z2. These variables are complex in nature, describing the amplitude and phase of the acceleration of each body. These equations are implemented in a MATLAB™ script.

3.5 WEC Model Scripts

There are several MATLAB™ scripts that perform key operations in the modeling environment. The key functionality of these scripts is explained here. In addition, the full scripts are included in Appendix A: Time-Domain Model and Appendix B: Frequency-Domain Model. The modeling environment that contains these scripts is a combined environment, ensuring that both simulation approaches use the same source data and allowing for easy comparison between their outputs. While this is not strictly necessary for single-frequency simulations, it is a convenient way to manage multiple-frequency simulations.

3.5.1 Geometry Definition - Function

The first script is a function called by other scripts. The function queries the user to determine which geometry will be used for the simulation, a one-of-four choice. It then extracts the device body base data from the appropriate AQWA™ output files and performs minimal processing functions. Also, the constant force-coefficient constants are defined in this file. The acquired data is passed back to the parent script through the return mechanism of the function.

A frequency-domain approach to simulating wave energy converter hydrodynamics

3.5.2 Impulse Response Calculation – Function

The second script processes the geometry and AQWA™ data, converting raw data into the time-domain impulse response functions (IRFs). These IRFs contain the coefficients used in the time-domain filter blocks performing the convolution functions. The script input is the body data determined by the geometry function and the simulation time-step. The script outputs the excitation, radiation, and coupled radiation frequency-domain transfer functions and their associated IRFs.

3.5.3 Calibration Simulation – Script

There are several calibration scripts that are used to match the time-domain results and the frequency-domain results to each other. While the frequency-domain calculations are very accurate, they do not automatically match the time-domain results. This is due, primarily, to simulation tool artifacts. The filters that are built for use in the time-domain solution are approximations and vary on their implementations. This calibration script performs a single-frequency regular wave simulation on the filter alone, performing the convolution with a unity-input cosine wave. The schematic used with $F_{r,p}$ is found in Fig. 3.4.

Amplitude and phase information is automatically captured and compared to the frequency-domain value. The difference between the two measurements is used to adjust the frequency-domain values to match the time-domain ones. This is, effectively, erasing the computational error that was inserted into the time-domain method.

A frequency-domain approach to simulating wave energy converter hydrodynamics

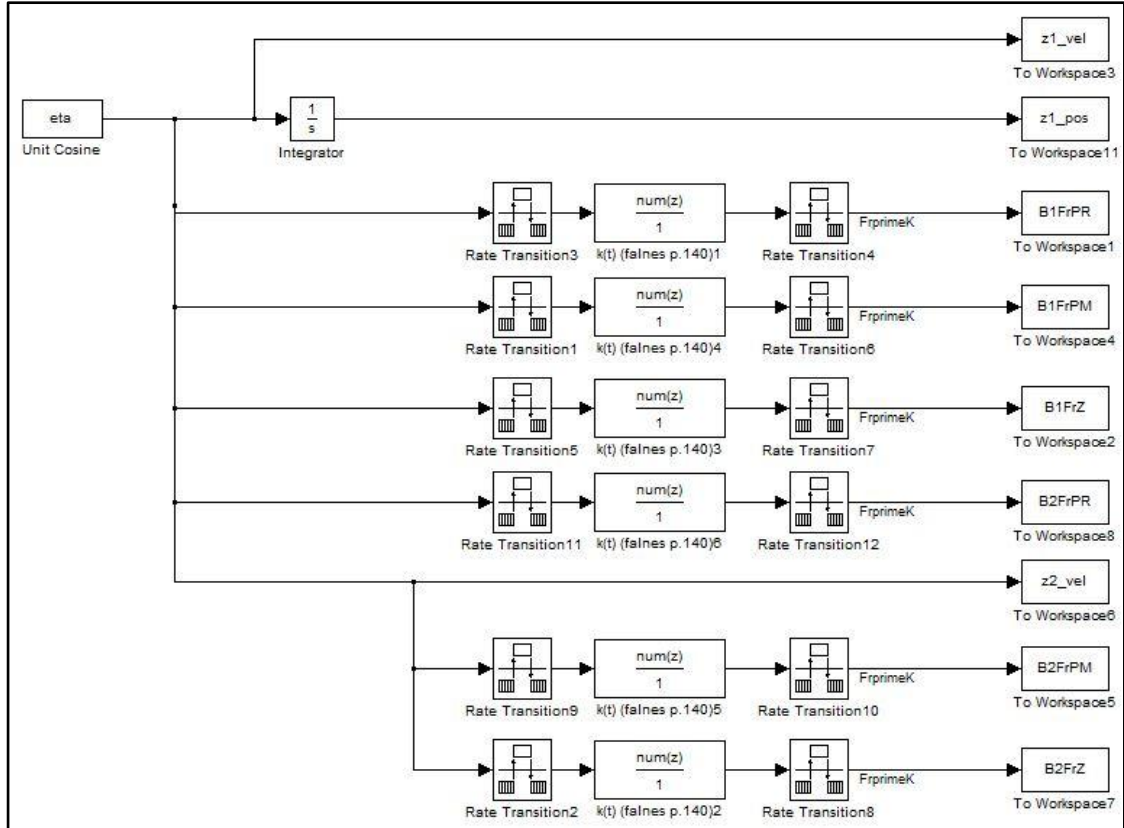


Fig. 3.4: $F_{r,p}$ Calibration Simulink™ Model

3.5.4 Single-WEC Single-Frequency Simulation - Script

There is a main script in the environment that manages a set of single-frequency simulations for a single WEC device. This script calls the functions described in Sections 3.5.1 and 3.5.2. After setting up the environment, the script enters a loop that is as long as the number of frequencies under examination. This quantity is determined in the impulse response function. The script runs a single time-domain simulation for every frequency with a regular wave at that frequency as input to the model. Once the simulation is done, the script records the amplitude and phase of the body accelerations and stores this in a vector. It

A frequency-domain approach to simulating wave energy converter hydrodynamics

also keeps a running summation of the input waves, so that a multiple (all) frequency simulation can be run as well.

After all the time-domain simulations are completed, the frequency-domain calculations are performed. The script also calculates an error term for each amplitude and phase. The amplitude error term is calculated according to:

$$\text{amp error}(\%) = 100 * \frac{(\text{time amp} - \text{frequency amp})}{\text{time amp}} \quad (3-31)$$

while the phase error is

$$\text{phase error}(\%) = 100 * \frac{(\text{time phs} - \text{frequency phs})}{2\pi} \quad (3-32)$$

This script is also used to perform *in-situ* verification of the model. The frequency-looping variable is set to a single value and the simulation is performed for that frequency. The time-domain output of individual force components is created by capturing the magnitude and phase of the component input and output. The output amplitude is divided by the input amplitude, creating a value that should match the frequency-domain amplitude. The component phases are similarly compared. This process ensures that the construction of the two models use the components in the same configurations.

3.6 WEC Model Output

The time-domain method produces the output time-series by recording the results of the simulation run. Specifically, a ‘To Workspace’ function is instanced in the Simulink™ model and configured to report the data as an array. Each acceleration, velocity, and position record for each WEC body is recorded in this manner.

The frequency-domain approach produces the output variables Z1 and Z2, which represent the acceleration of the two bodies. These variables have the form of a complex number written in the amplitude-phase lexicon.

A frequency-domain approach to simulating wave energy converter
hydrodynamics

The next step in the methodology is to return these output variable to the time domain. The general method for performing this conversion would be an inverse Fourier Transform. Because the motion descriptors have been completely described as cosine functions, the inverse Fourier Transform can be realized by constructing the cosine from the acceleration results. This process is mathematically described by

$$zP(t) = \sum_{n=1}^{\infty} (ZP_n) \cdot \cos(2 \cdot \pi \cdot f_n \cdot t + Z\varphi_n) \quad (3-33)$$

where ZP_n is the amplitude of the body motion and $Z\varphi_n$ is the phase of the body motion. The letter P is a placeholder for the WEC device body number.

The final step is to execute the summation in Eq. (3-33), thereby creating the time-series body acceleration, which is ready for use in the power take-off modeling of the WEC.

3.7 Development Approach

The comparison of the two approaches is not a single comparison, but rather a process of comparisons. The steps below list the comparisons that form the core of the development process, in the order they occur. Each step is completed before the next step is attempted. Also, each change to the formulation of either model is validated by re-running the previous step(s) comparison.

1. Force component, stand-alone
2. Single-frequency simulation, *in-situ*
 - a. Force component
 - b. $F_{e,p}, F_{v,p}, F_{b,p}, F_{moor}$, and $F_{PTO,p}$
 - c. $F_{r,p}$
 - d. $F_{cr,p}$
3. Multiple-frequency simulation: regular, 0-phase cosines.

A frequency-domain approach to simulating wave energy converter
hydrodynamics

4. Multiple-frequency simulation: random sea-state.

3.8 Ensuring Validity of Comparison

The validity of the comparison between the approaches is bolstered by the comparison setup. Both approaches are built upon the same equation of motion, hence the same basis and assumptions defined in the Airy waves solution. Likewise, they are both provided with the same sea state description as their fundamental inputs. There are, however, some fundamental differences between the two approaches, which have been erased through application-specific alterations. These alterations are described in the following paragraphs.

3.8.1 Sea State Creation Method

The first alteration concerns the creation of the elevation time-series from the sea state input. The inherent method used in [53] is based on the work described in [60], while the research described herein uses the approach defined by [12]. This discrepancy has been resolved for the comparison work by replacing the method from [53] by the method from [12].

3.8.2 Composition of Hydrodynamic Forces

The second alteration concerns the F_{HYDRO} component of the fundamental equation of motion as expressed in Eq. (2-15). F_{HYDRO} , repeated here

$$F_{HYDRO,p} = F_{e,p} + F_{r,p} + F_{b,p} + F_{v,p} + F_{f,p} \quad [N] \quad (3-34)$$

is composed of five forces. The time-domain methodology includes values for the first four forces, with the fifth ($F_{f,p}$) assumed to be zero. Likewise, the frequency-domain methodology does not include $F_{f,p}$.

- Frequency Range examined

A frequency-domain approach to simulating wave energy converter
hydrodynamics

Both simulations are performed in the MATLAB™ environment. The fundamental metric being compared between the two methodologies is simulation time, and is captured by the built-in MATLAB™ function ‘tic-toc’. The time measured is confined to the amount required to generate the elevation time-series and run the simulation that produces the PTO mechanism input time-series.

A frequency-domain approach to simulating wave energy converter
hydrodynamics

4 Research Results

There are several types of results to report regarding this research effort. They are grouped into the categories of modeling issues, WEC single-frequency simulation, and WEC multiple-frequency simulation. A brief analysis is included immediately after the reporting in each category. These analyses are comments regarding the quantifiable information indicated by the research results.

4.1 Modeling Issues

During development, the EOM frequency-domain force components were individually compared to their time-domain counterparts in two environments as detailed in Section 3.5.4. This process led to the discovery of several issues with the time-domain simulation. Each of these issues is explained in this section.

4.1.1 *Excitation Force Coefficients*

The comparison of $F_{e,p}$ between domains indicated that the time-domain signal was double the amplitude of the frequency-domain result. Exploration of the code that created the $F_{e,p}$ (IRF) revealed that the integration step was coded incorrectly. The original code is:

```

1. %% Calculate IRF from f-domain data
2. tmax = 25; % know that IRF~=0 for t>25s, so let tmax = 25s
3. t = -tmax:0.01:tmax;
4. for k = 1:length(t) % coeff 1/pi = because INT[0,inf], not INT[-
    inf,inf], Based on WAMIT Manual F2T and Falnes (2002,1995)
5.     Fe_b(k) = real(1/pi*trapz(omega,fe_b.*exp(1i*omega.*t(k))) );
6. end

```

The equation implemented in the for-loop is the fundamental Fourier Transform. However, the integration has been confined to the positive frequencies, as indicated in the line-4 comment and the definition of omega.

A frequency-domain approach to simulating wave energy converter hydrodynamics

According to the AQWA™ reference manual, the source data is to represent the amplitude and phase of a cosine, as defined in Eq (3-8). The integration in line-4 is transforming the values from frequency-domain to time-domain. This indicates that the complex variable fe_b is the frequency-domain version of the cosine function, namely Eq Error! Reference source not found.. Consequently, the fe_b variable should be divided by two.

The original code was changed to more accurately reflect the actual process taking place. The frequency amplitudes are divided by two. They are then converted to complex numbers by application of the phase angles. Those complex numbers are placed in a frequency-series matrix. The full frequency series is then constructed by including the negative frequency values. These full-frequency variables are transformed according to the unmodified Fourier Transform equation. A comparison of the results is found in Fig. 4.1.

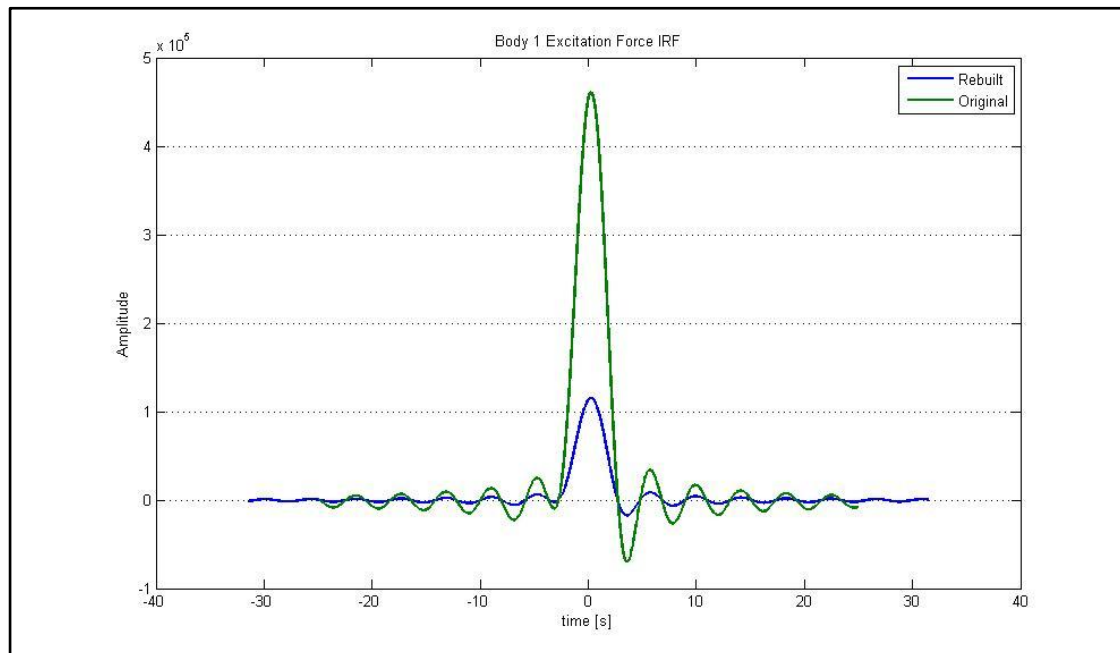


Fig. 4.1: $F_{e,1}$ IRF Comparison

A frequency-domain approach to simulating wave energy converter hydrodynamics

4.1.2 Non-Causality of Excitation Force

$F_{e,p}$ is a non-causal force, with future values of the input affecting the current value of the response. To account for this in the time-domain environment, the $F_{e,p}$ IRF is split into two sets of coefficients along time = 0. A shifted version of η is applied to the negative filter and the actual η is applied to the positive filter. The filter outputs are summed and the result becomes the source for the rest of the model.

This summation creates an output that is double the η input. This is not an artifact of building the filter, but rather an artifact of applying two versions of the η source: one shifted in time, one in real time, both with unity amplitude.

This issue was not addressed in this research, other than to ensure the frequency-domain and time-domain $F_{e,p}$ values were equal.

4.1.3 Radiation Force Coefficients Source Data

The calibration of $F_{r,p}$ revealed a vexing issue. The output of the $F_{r,p}$ filter returned a value that was completely nonsensical with respect to the composed transfer-function value. The equation used to create the coefficients for $k(t)$ as required for Eq. (3-13)

$$k(t) = \frac{2}{\pi} \cdot \int_0^{\infty} [R(\omega)] \cdot [\cos(\omega t)] \cdot d\omega \quad (4-1)$$

is the result of the application of the Kramers-Kronig relationship following [41]. It was finally determined that the $R(\omega)$ in the MATLAB™ script was, in fact, the $C(\omega)$ from the AQWA™ results. This was corrected according to Eq. (3-11)

4.1.4 Radiation Force Equation

The $F_{r,p}$ implemented in the original time-domain model had two characteristics, (excluding the C/R confusion addressed in Section 4.1.3), that made matching it to the frequency-domain representation difficult. The first of

A frequency-domain approach to simulating wave energy converter hydrodynamics

these is the choice of equation for $k(t)$ and the second is the implementation of the equation for $F_{r,p}$.

There are several different equations that can be used to determine $k(t)$, the IRF. Each of these equations produce mathematically identical results when used in a general application where the values being integrated are continuous functions of frequency and all frequencies are considered [41, ch. 5.3.1, pp. 140-141]. The original time-domain implementation used Eq (4-1) results could not be matched to the frequency-domain results with any degree of accuracy. Hence, the formulation of $k(t)$ was changed, matching the description found in Section 3.3.3.

$F_{r,p}$ is formed by following Eq (3-13), which creates the force by adding a value to $k(t)$. The time-domain model implements this by manipulating the EOM so that the added mass term is combined with the body mass in the creation of the acceleration. This method of implementation prevents an algebraic loop in Simulink™. However, it also prevents the direct *in-situ* comparison of $F_{r,p}$.

The model was changed to implement $F_{r,p}$ in a more direct manner. Instead of combining two components into a filter in MATLAB™ and moving the mass term in Simulink™, all three components are formed in Simulink™ and then combined.

4.1.5 Radiation Force Coefficients and Causality

$F_{r,p}$ is a causal force, occurring only in response to some other applied force. This is represented in the frequency-domain by the use of Eq. (3-27), the Fourier Transform representation of a causal cosine. Review of this equation clearly shows that the positive and negative frequency components are the time-domain amplitude divided by 4, whereas with the ideal cosine they are divided by two. This divisor was not applied in the original time-domain equation, resulting in a

A frequency-domain approach to simulating wave energy converter hydrodynamics

$F_{r,p}$ value that is 4x the frequency-domain value. The time-domain implementation was changed to match the mathematics.

4.1.6 IRF Calculations

The original IRF calculations chose a time span of 25 seconds. While this may be a valid value for truncating the tails of the IRF, it is insufficient for the actual coefficient calculations. The integration that creates the IRF is with respect to all frequencies, and the time vector of the integration must be long enough to account for the largest period (smallest frequency). As a consequence, the time span used for the IRF calculation was changed to be 31.4 seconds, as the shortest frequency evaluated is 0.18 rad/s.

4.1.7 Conflicting Sign Conventions.

The coupling force implemented in the time-domain model is a rough estimate described by Eqs. (2-21) and (3-14). Eq. (3-13) clearly shows that $F_{r,p}$ is a negative value with the $mass_p(\infty)$ term contributing to the amplitude in an additive manner. Logically, $F_{cr,p}$ should follow the same methodology. However, the original reference model implemented the $mass_p(\infty)$ term such that it reduced the amplitude of $F_{cr,p}$ rather than increasing it.

Because $F_{cr,p}$ is a rough estimate, following no experimentally derived result, the composition of the force was altered to match the method used for $F_{r,p}$.

4.1.8 Modeling Issue Analysis

The issues presented in Section 4.1 show that the process of building the frequency-domain framework exposed seven discrepancies with respect to the traditional time-domain approach. Each of these artifacts will ultimately result in suspect power calculations, undermining the perceived quality of the models. Five of the artifacts, such as the duplication of the input amplitude (Section 4.1.2)

A frequency-domain approach to simulating wave energy converter hydrodynamics

seem to have an obvious resolution. Determining the resolution of other artifacts, such as the divide by four in the frequency-transform (Section 4.1.5), do not have a clear resolution.

4.2 Force Component Calibration Results

The calibration process is designed to identify and offset known computational discrepancies, ensuring the accuracy of the result comparisons.

4.2.1 Calibration of Excitation Force

The excitation forces for both WEC bodies were calibrated using the procedure defined in Section 3.5.3. The figures below show the results of this calibration, both as real-number differentials (Fig. 4.2 and Fig. 4.3) and as a percentage of the time-domain value (Fig. 4.4).

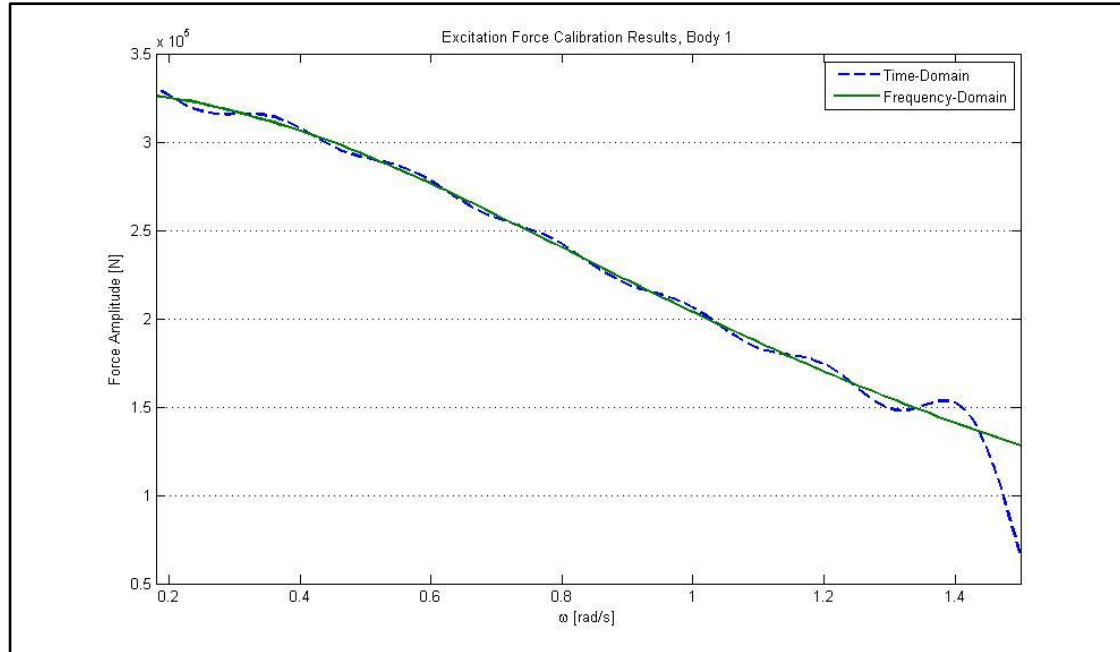


Fig. 4.2: Body 1 F_e Calibration Values

A frequency-domain approach to simulating wave energy converter
hydrodynamics

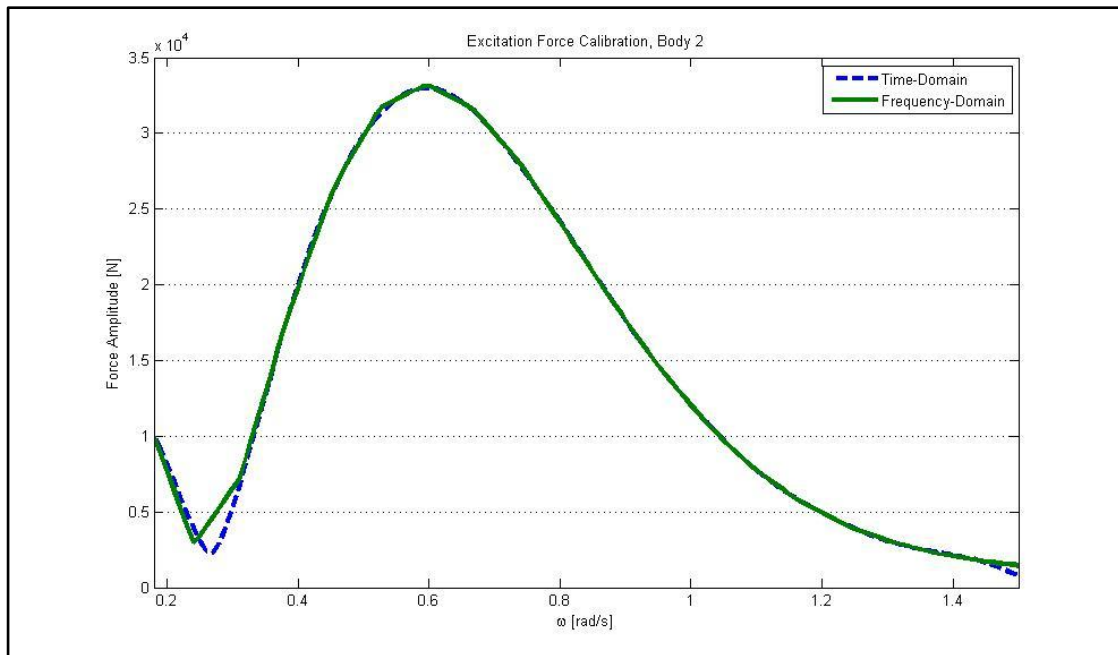


Fig. 4.3: Body 2 F_e Calibration Values

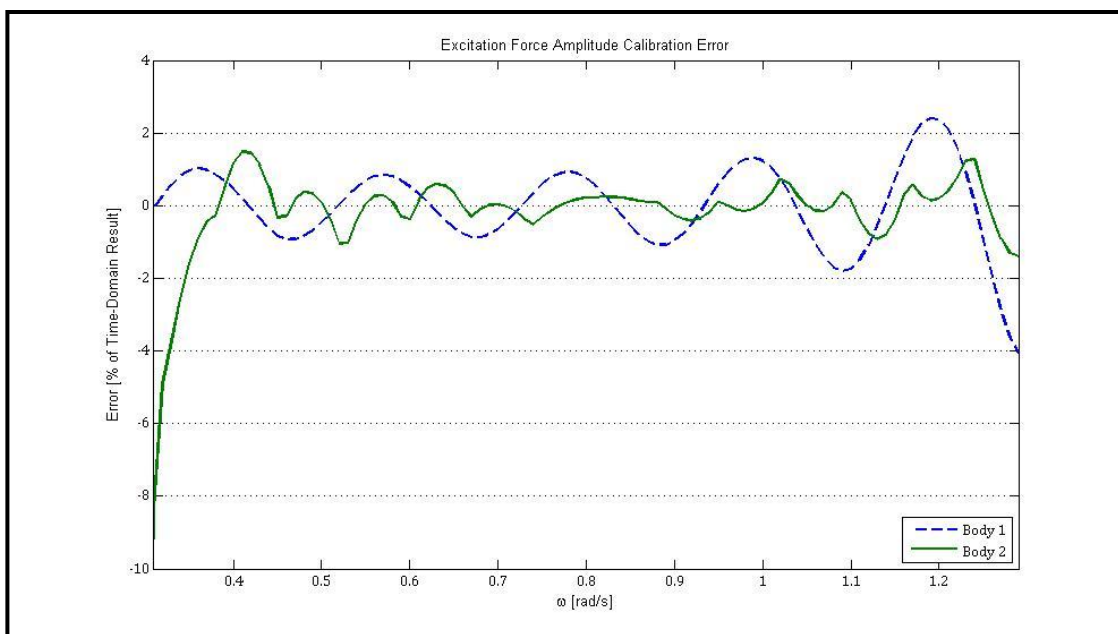


Fig. 4.4: Excitation Force Amplitude Calibration Errors

A frequency-domain approach to simulating wave energy converter hydrodynamics

4.2.2 Calibration of Radiation Forces

The radiation forces for both WEC bodies were calibrated using the procedure defined in Section 3.5.3. The figures below show the results of this calibration.

Fig. 4.5 and Fig. 4.6 display the actual amplitudes for Bodies 1 and 2 respectively. Fig. 4.7 graphs the differences between the methods as an error percentage of the time-domain value.

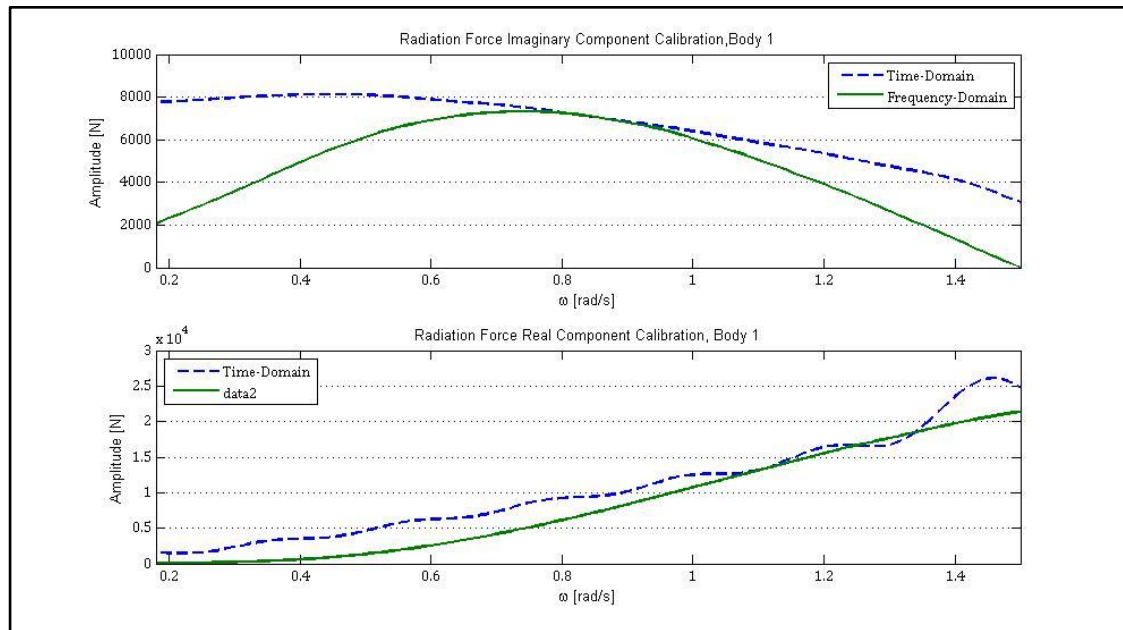


Fig. 4.5: Body 1 F_r Calibration Values

A frequency-domain approach to simulating wave energy converter hydrodynamics

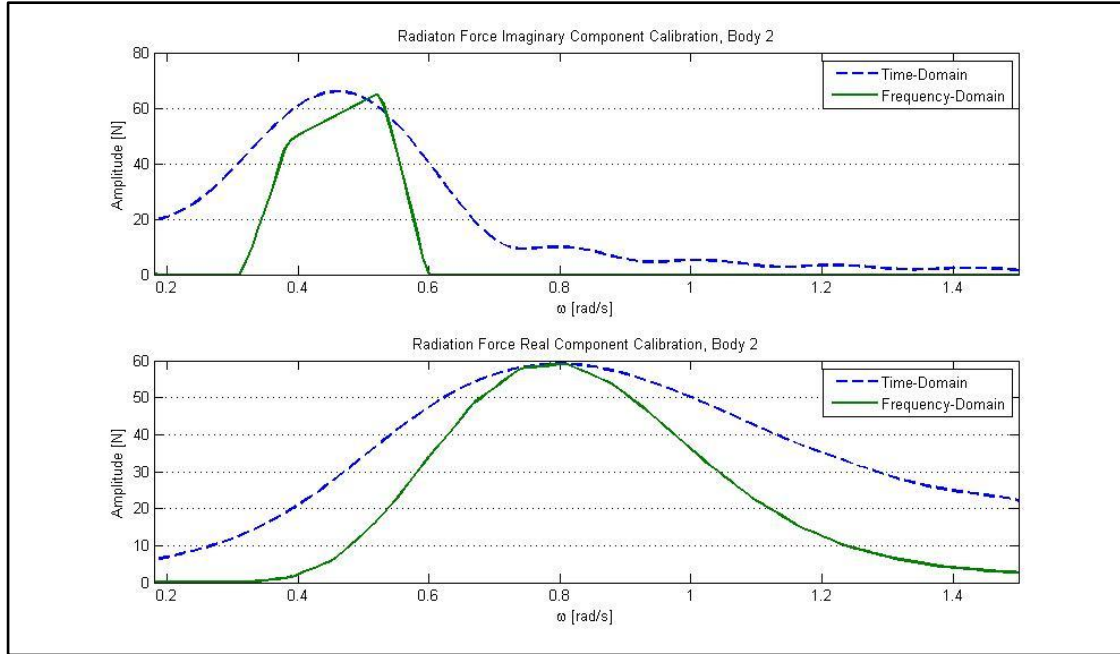


Fig. 4.6: Body 2 F_r Calibration Values

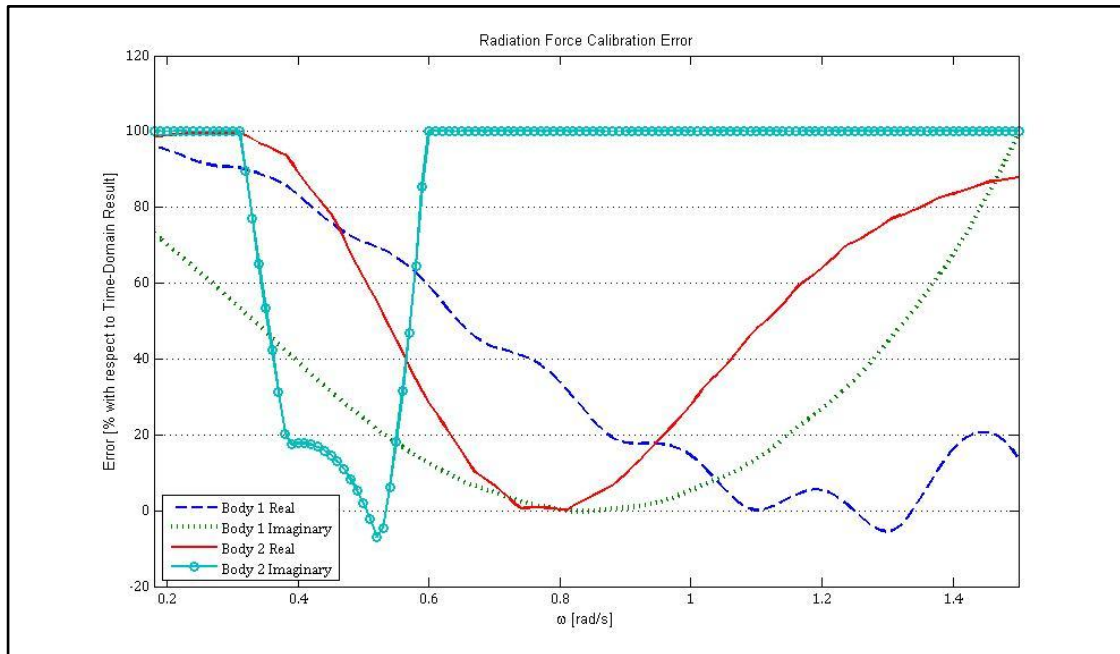


Fig. 4.7: Radiation Force Amplitude Calibration Errors

A frequency-domain approach to simulating wave energy converter
hydrodynamics

4.2.3 Calibration of Constants

It is true that the constant force coefficients do not need calibration, as there is no loss of information in performing a multiplication with them. However, there may be data corruption caused by how the constant is implemented in the time-domain model. An example of this is the added-mass at infinity term (AMinf) found in each body model and in the coupled dynamics model. Just after the gain icon, there is an icon labeled ‘Memory’. This icon breaks an algebraic loop by delaying the signal for one time-step. This delay is, effectively, a phase-shift equal to:

$$\begin{aligned} & \text{Memory Induced Phase Shift} \\ & = [2 \cdot \pi \cdot (1 \text{ time step})] / (\text{time steps in period}) \text{ [rad/s]} \end{aligned} \quad (4-2)$$

Because the time-step is constant, but the number of steps in the period is related to the frequency, the amount of error introduced increases with the frequency. This error can be corrected for by forcing the frequency-domain constant to be complex instead of real, thereby achieving the same delay as introduced in the time-domain simulation. This correction operation was not implemented in these results. Hence, the results have an intrinsic error that increases with frequency.

4.2.4 Force Component Calibration Analysis

As depicted in Sections 4.2.1 and 4.2.2, the calibration process clearly succeeded in exposing the model inaccuracies induced by the simulation tool restrictions and implementation choices. It is also clear that the differences in the results produced by the two domain methodologies are not all insignificant. It is unlikely that the tool and implementation artifacts cause these significant differences. The root cause of the differences has not been identified.

A frequency-domain approach to simulating wave energy converter hydrodynamics

4.3 Single PA-WEC Comparisons

This research effort involved developing a frequency-domain simulation methodology. The results of this approach were then compared to the results of the traditional time-domain methodology. The development centered on a single device simulation (one WEC body type), on the assumption that multiple device simulations are achieved in an additive manner. The results from the comparisons are detailed in the following sections.

4.3.1 Simulation Result Comparisons

It is known that the different frequencies present different results due to various simulation artifacts. To understand each of these differences, a set of single-frequency simulations were run on the single-device model. The comparison between the accelerations achieved at each frequency for WEC Body 1 is found in Fig. 4.8. The same comparison for Body 2 is found in Fig. 4.9.

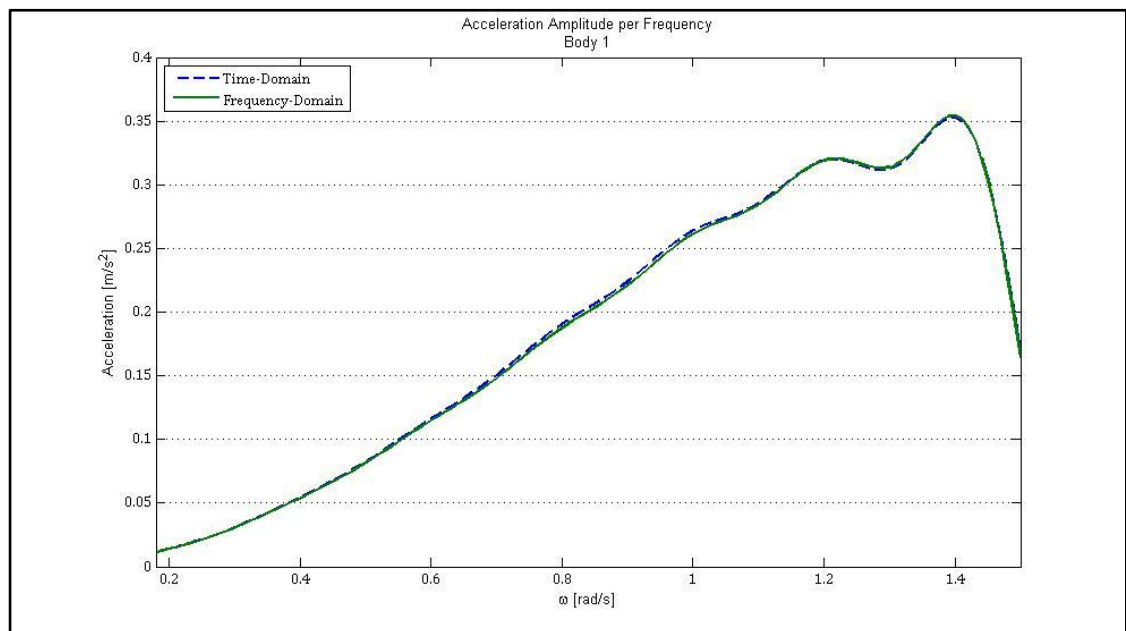


Fig. 4.8: Acceleration Amplitude Results for Body 1

A frequency-domain approach to simulating wave energy converter hydrodynamics

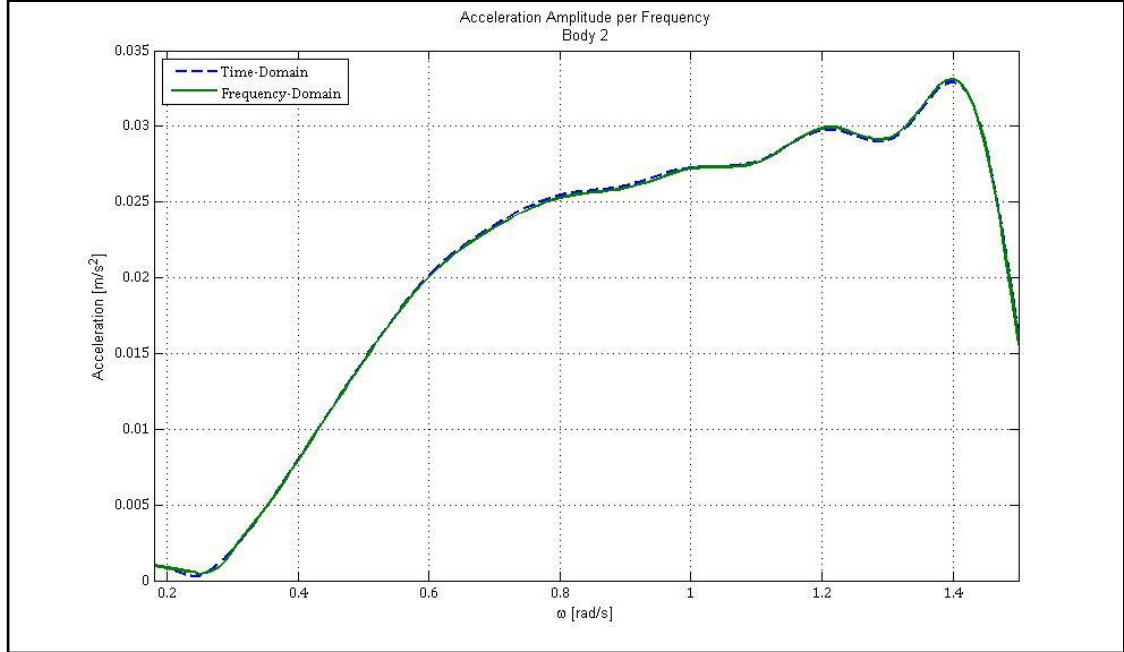


Fig. 4.9: Acceleration Amplitude Results for Body 2

The difference in the results between the domains is also graphed as an error term, with the reference being the time-domain result. Two comparisons were made. The first compares the final acceleration outputs using a calibrated frequency model. This is found in Fig. 4.10. The second compares these outputs when the force components are not calibrated. These results are displayed in Fig. 4.11.

A frequency-domain approach to simulating wave energy converter
hydrodynamics

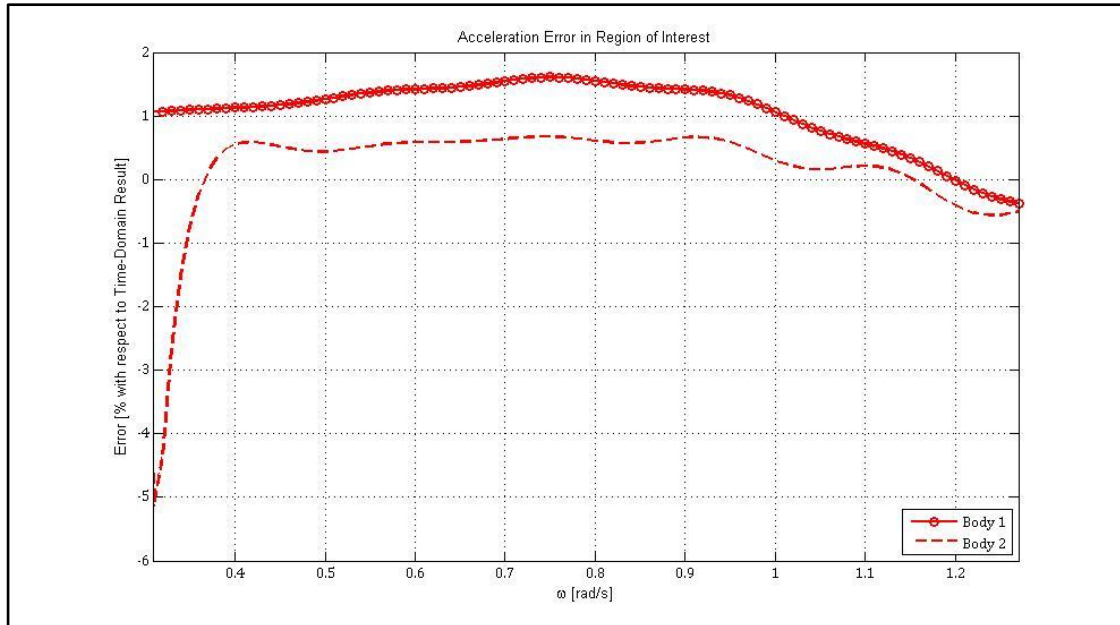


Fig. 4.10: Error in Acceleration Amplitude with Calibration Included

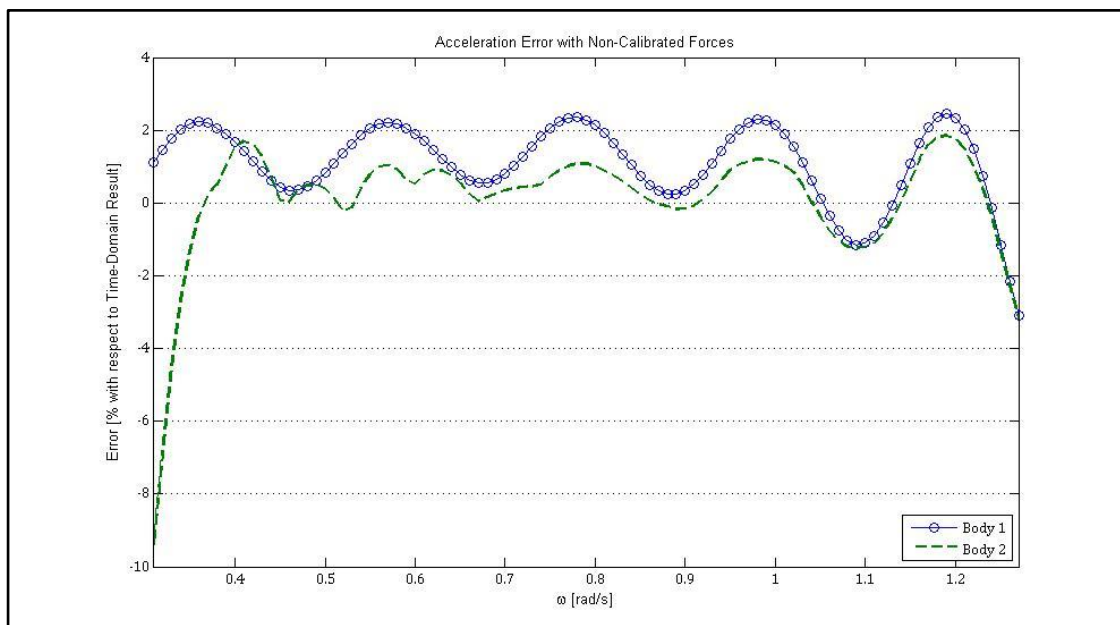


Fig. 4.11: Error in Acceleration Amplitude without Calibration

A frequency-domain approach to simulating wave energy converter
hydrodynamics

4.3.2 Simulation Speed Comparison

The time required for each simulation methodology is different, as are the other typical computational-related metrics, CPU time and memory requirements. The latter two have not been examined here. However, the time requirements for the simulations have been. This was accomplished through embedding the ‘tic’ and ‘toc’ MATLAB™ functions into the simulation environment. There were 133 frequencies included in the simulation. Increasing the number of frequencies will increase the simulation times.

In the time-domain, a simulation run has a setup time of 4.64 seconds. The most time-consuming part of the setup is the calculation of the IRFs, which take a total of 4.1 seconds to complete. In theory, this setup is run only one time for each body type, although the calculation of η_p must be run for every simulation. The simulation itself takes an average of 18.9 seconds per run and provides 600 seconds of valid data. It is important to note that 600 seconds of valid output data requires roughly 770 seconds of simulated time. This is due to the settling time required by the $F_{e,p}$.and $F_{r,p}$ filters.

In the frequency-domain method, the setup for a simulation run is 0.54 seconds. Like the time-domain approach, the setup can be run once for each body type, regardless of the number of simulations to be performed. And, like the time-domain method, the calculation of η_p occurs for every simulation. The calibration steps, done one time per body type, are also part of the total setup. The $F_{e,p}$ calibration takes 1291 seconds and the $F_{r,p}$ takes an additional 3318 seconds. Finally, generating 600 seconds of valid output data takes 1.9 seconds. In fact, the time required to perform the simulation is nearly independent of the simulation length.

A frequency-domain approach to simulating wave energy converter hydrodynamics

4.3.3 Single-Frequency Analysis

More direct evidence of the importance of the calibration process becomes evident with the single-frequency simulation amplitude comparison results. As seen in Fig. 4.4 and Fig. 4.7, the two simulation domains produce comparable results over the target frequency range. This process is primarily supported by the results displayed in Fig. 4.10 and Fig. 4.11. The significant differences between the two approaches noted in Section 4.2.4 are not present in the amplitude comparisons displayed in Section 4.3.1, having been corrected during the calibration process. This clearly demonstrates that there is an unresolved issue in the implementation of the IRFs.

The comparison of simulation time between the methods clearly indicates two points. The first point is that the frequency-domain methodology is clearly *slower* to establish than the time-domain approach. Assuming that both approaches perform the setup once and save the state to reuse, the frequency-domain approach is 4,610 seconds where the time-domain approach is 4.64 seconds. The ratio between the methods is about 1:1000. The second point made by the time comparison is that the frequency-domain methodology is clearly *faster* for the actual simulation than the time-domain method. The ratio between the methods is about 350:1.

4.4 Single-WEC, Multiple Frequency

As described in Section 3.7, a multiple-frequency simulation was performed in both methodologies in addition to the single-frequency simulations.

4.4.1 Regular, 0-Phase Shift, Input Wave

For the time-domain simulation, the sea state, η , was artificially created from a summation of unity-amplitude cosine functions, one for every 133 frequencies.

A frequency-domain approach to simulating wave energy converter hydrodynamics

The amplitude was then divided by 133 creating a unity-amplitude wave at the point when all the frequencies aligned.

In the frequency-domain, 133 individual acceleration amplitudes and phases for each WEC body were calculated. These complex numbers were then applied to Eq. (3-33). The resulting time-series was then divided by 133 and compared to the time-domain time-series. A plot of the Body 1 waveforms is found in Fig. 4.12. Fig. 4.13 contains the results for Body 2. Finally, a plot of the differential results is shown in Fig. 4.14.

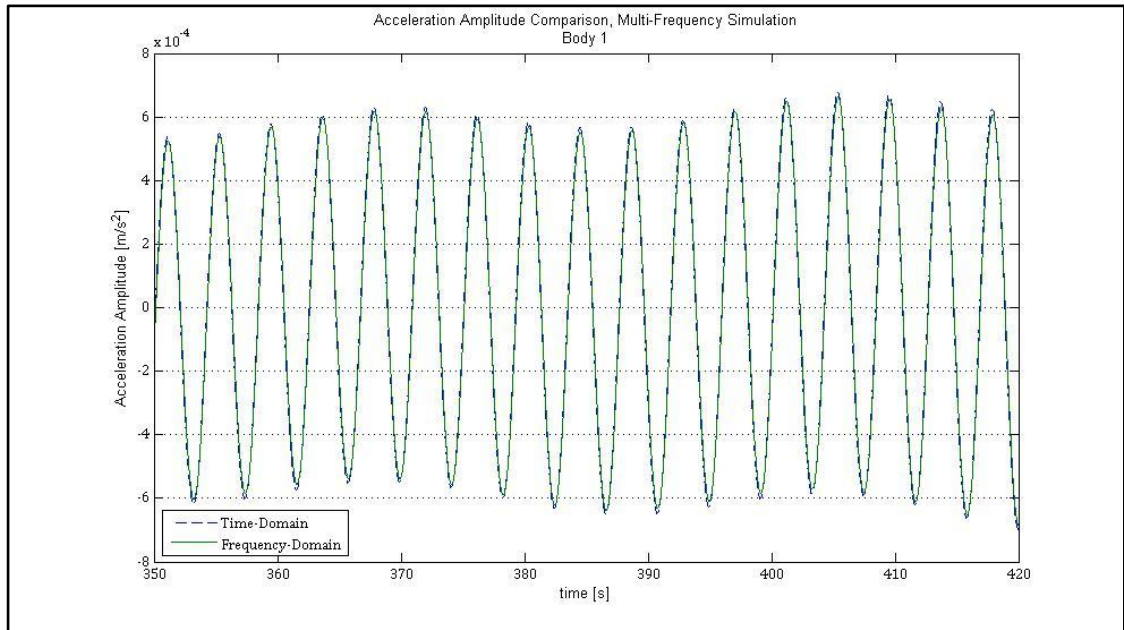


Fig. 4.12: Results Comparison, Multi-Frequency Simulation, Body 1

A frequency-domain approach to simulating wave energy converter
hydrodynamics

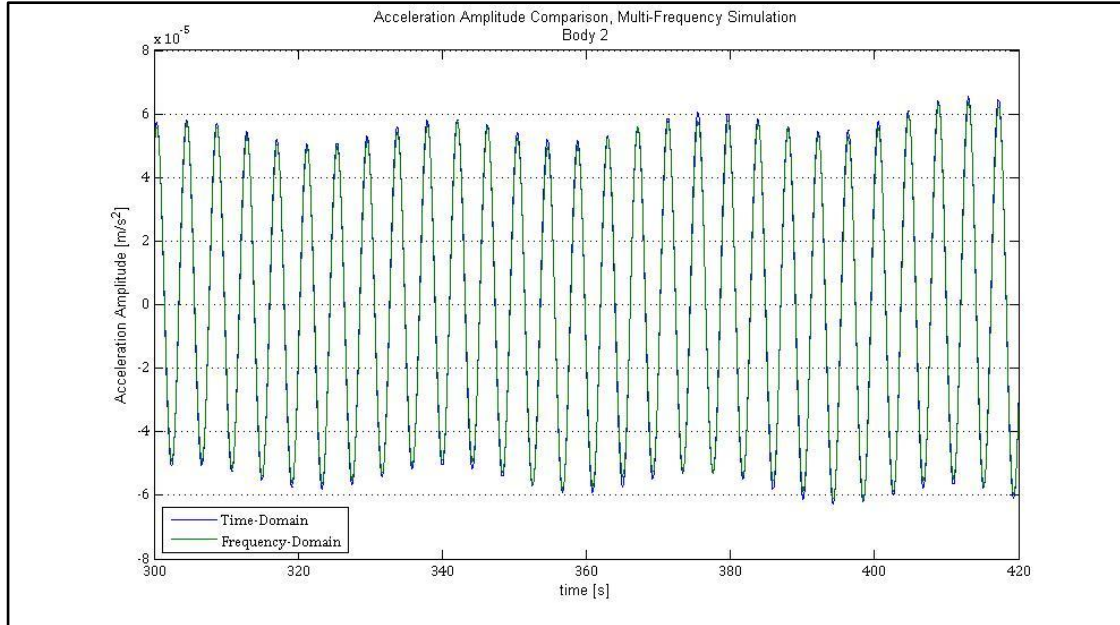


Fig. 4.13: Results Comparison, Multi-Frequency Simulation, Body 2

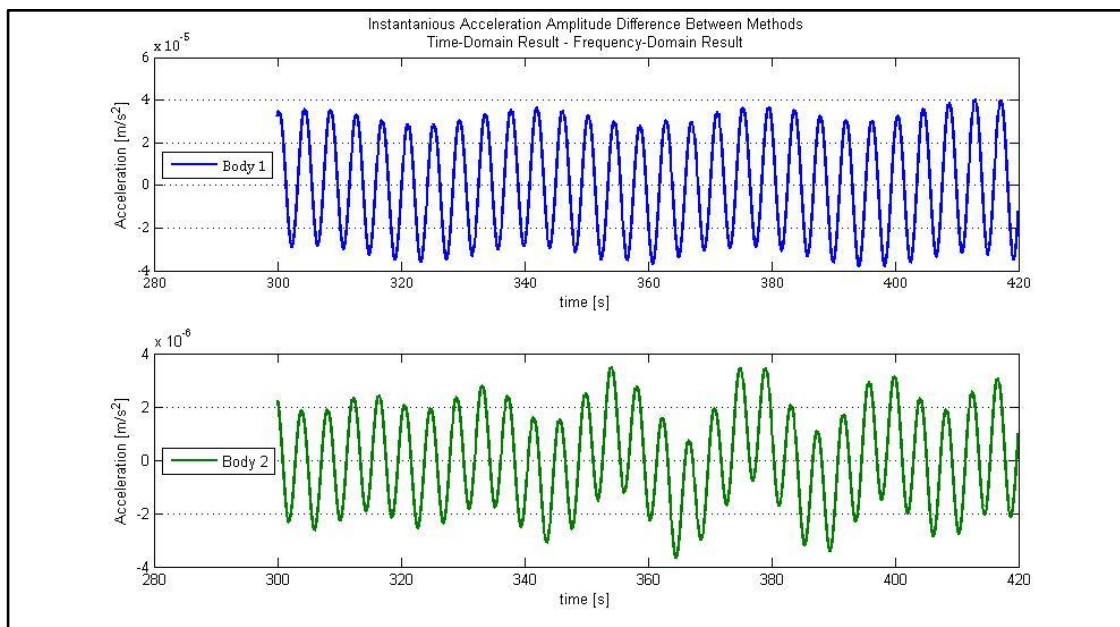


Fig. 4.14: Amplitude Differential Due To Simulation Method

A frequency-domain approach to simulating wave energy converter
hydrodynamics

4.4.2 Random, Multi-Frequency Input Wave

The two models cannot distinguish between a ‘regular’ and ‘random’ input wave. This means that a simulation and comparison of a random input wave is not strictly required. However, in this experiment it was used to validate the phase shifts between the two domains. While this could be accomplished with the multi-frequency regular wave simulation, it is a perceptual milestone to see the results generated from a simulation of a modeled sea state.

The sea state used to generate the input is described by a $H_s = 6.57m$, a $T_d = 13.79s$, and a $\theta = 257^\circ$. The energy spectra of the source, corresponding to Eq. (2-10), is shown in Fig. 4.15. Plots of the generated random state, amplitude and phase, are displayed in Fig. 4.16.

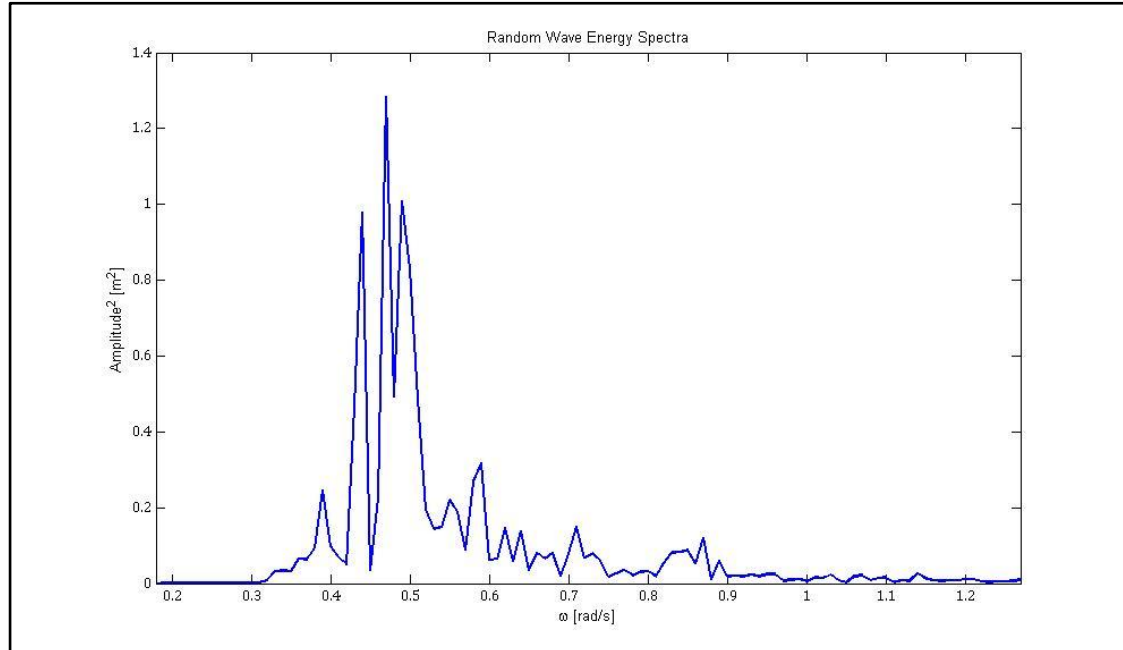


Fig. 4.15: Random Wave Energy Spectra

A frequency-domain approach to simulating wave energy converter
hydrodynamics

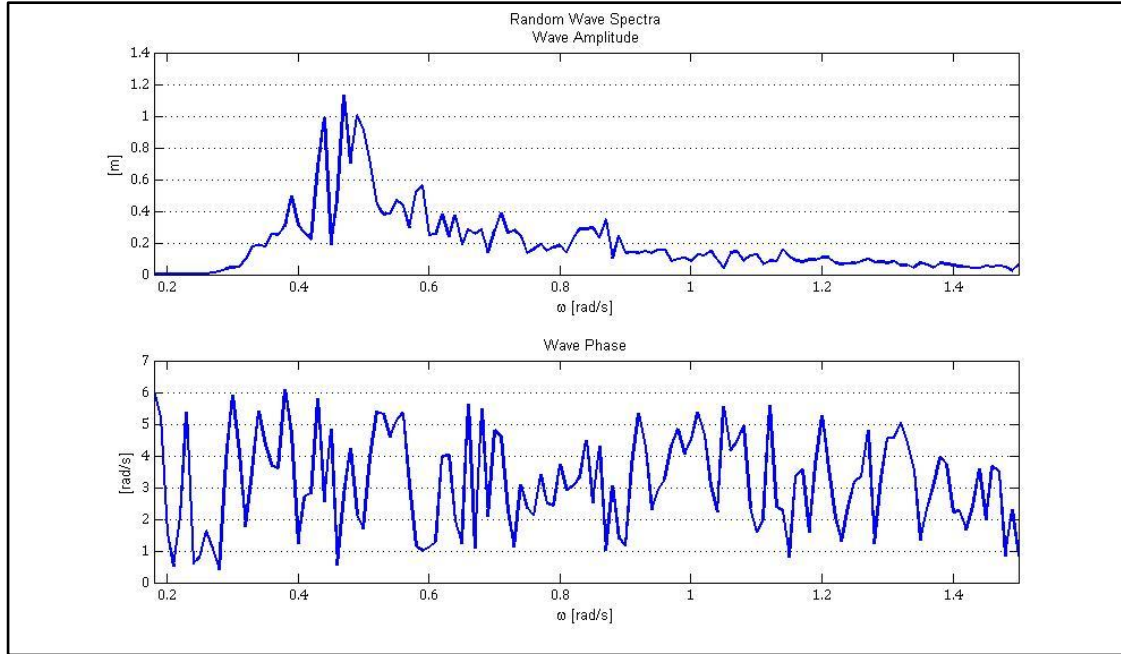


Fig. 4.16: Random Wave Spectra, Amplitude and Phase

Fig. 4.17 (Body 1) and Fig. 4.18 (Body 2) compare the simulated accelerations for each method over a 10 minute window. The time-step for this simulation is 0.01 seconds, which yields 60,000 data points. This shows that the two methods track each other well over time. Close-up comparisons of only 700 data points, in Fig. 4.19 and Fig. 4.20, show that there is a quantifiable difference. The instantaneous differential for each body is displayed in Fig. 4.21.

A frequency-domain approach to simulating wave energy converter
hydrodynamics

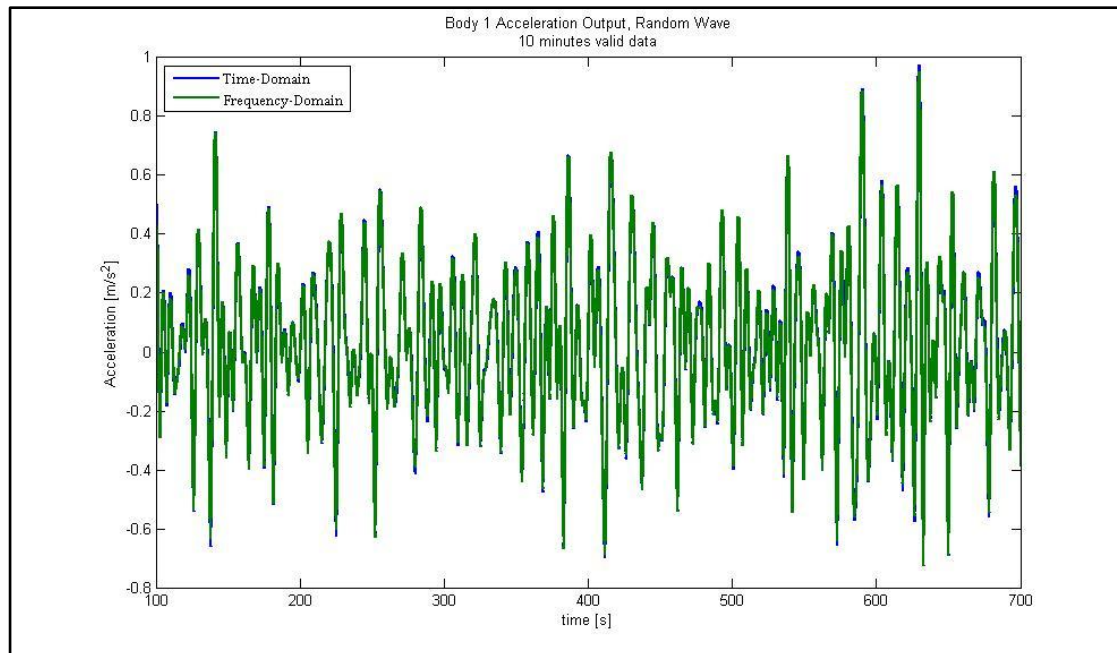


Fig. 4.17: Body 1 Acceleration Comparison, 10 Minutes, Random Wave

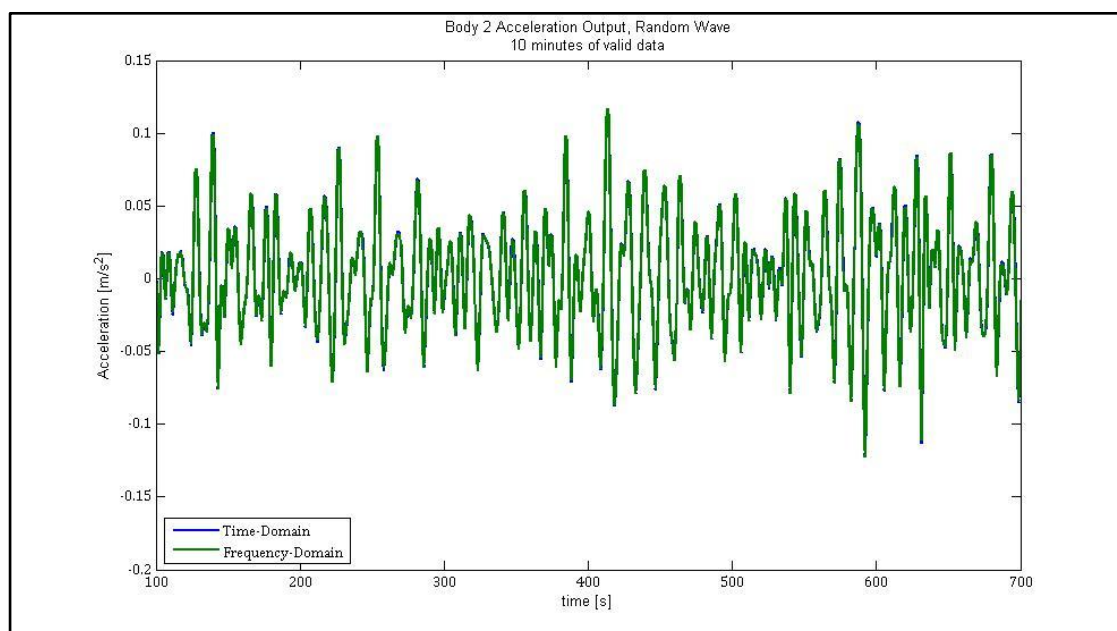


Fig. 4.18: Body 2 Acceleration Comparison, 10 Minutes, Random Wave

A frequency-domain approach to simulating wave energy converter hydrodynamics

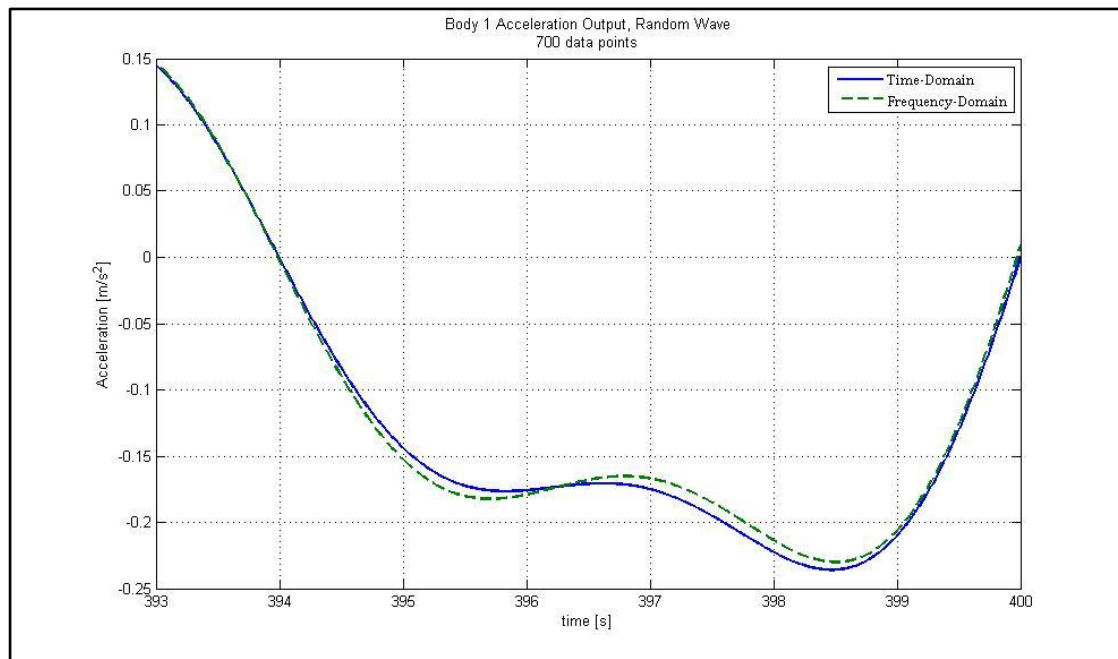


Fig. 4.19: Body 1 Acceleration Output Comparison, 700 Data Points

A frequency-domain approach to simulating wave energy converter
hydrodynamics

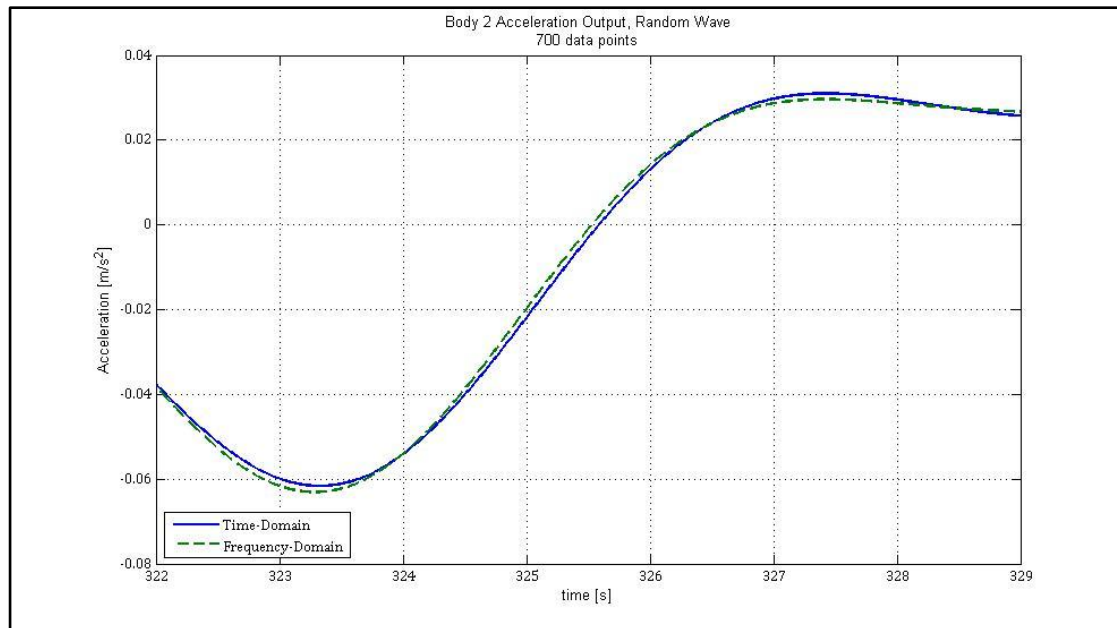


Fig. 4.20: Body 2 Acceleration Output Comparison, 700 Data Points

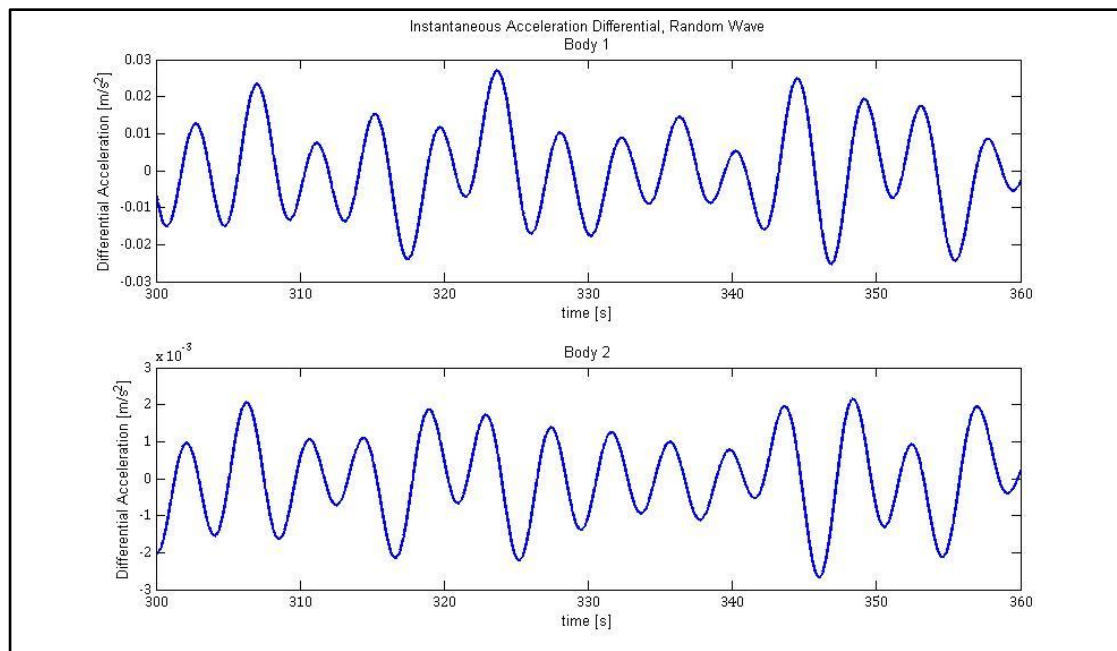


Fig. 4.21: Method Acceleration Differentials, Random Wave

A frequency-domain approach to simulating wave energy converter hydrodynamics

4.4.3 Single WEC Simulation Result Analysis

It is clear that the results presented in this section show that, while there are some differences in the output, the two simulation approaches produce comparable results. In fact, the frequency-domain results are close enough to the time-domain results as to be a replacement for them. This substitution can be made in any application that can effectively use the output data.

A frequency-domain approach to simulating wave energy converter
hydrodynamics

5 Extrapolations, Observations and Conclusions

Just as there were several levels of results presented, there are several levels of conclusions and observations regarding the research. The first of these is the valuation of the experimental results and any data-driven extrapolation of those results. The second addresses the fit of the frequency-domain approach to the current WEC development methodology. The third speculates on details observations made during the research process.

5.1 Results-Driven Valuation and Extrapolation

The results presented in Chapter 4, along with the brief analyses, provide data-driven evidence supporting the proposed frequency-domain simulation method. Thus far, it is an appropriate substitute for the current state-of-art time-domain method for simulating a hydrodynamic response.

Regardless of this conclusion, the process of developing and evaluating the frequency-domain approach was quite valuable. In fact, the comparison of the two simulation methodologies clearly exposed many areas of confusion that might otherwise have been missed. Each step in the research contributed to a deeper understanding of the development challenges and issues surrounding WEC creation, where operating under erroneous assumptions can preemptively exterminate a development project.

5.1.1 Model Issues

The issues presented in Section 4.1 are a reflection of how new the WEC development process is, at least in the public domain. They document serious discrepancies that should become high priority targets for additional development, as their resolution can only improve the reputation of academic

A frequency-domain approach to simulating wave energy converter hydrodynamics

research. Likewise, private developers would benefit from understanding these issues and ensuring they are not negatively impacted by them.

One specific example of this is clarification of the real output amplitude. The transform to the frequency-domain reduces the amplitude of the input source, as it places one-half of it in the negative frequency space. In the field of communications, designers can adjust for this by applying a gain to the filtered signal. This is not possible for the WEC model where the filters represent real physical processes that are not under the developer's control. However, understanding how to address this issue may require collaboration with physicists and mathematicians, or a physical experiment that compares reality to mathematically-derived results.

5.1.2 Calibration

The process of calibrating the individual force components exposed two other modeling issues that should be addressed. The first is that the correlation between the time-domain and frequency-domain is not well understood. [61] reports that the correlation between the two domains is not realistic above a frequency of 2 rad/sec given the current tools used for evaluation. This information was incorporated into the time-domain reference model. Therefore, correlation efforts for WEC development focused on frequencies below this limit.

The second issue is that the method used to create the IRF is vital to correlating the output results. The issue exists for both causal and non-causal IRF generation. It can be seen by applying the same frequency-domain transfer function description to two implementations of the transformation process and comparing the results. The fact that the input to the transformations is identical while the output is different indicates the implementation method is the root cause. Further investigation was not conducted, although the identification of a proven method would benefit developers.

A frequency-domain approach to simulating wave energy converter hydrodynamics

The investigation that discovered these issues pointed to an additional area of concern. It appears that either the relationship between time-domain and frequency-domain, or the WEC system, is not well understood. Multiple conversations occurred during this research effort that referred to including all frequencies in the transfer functions so as to not lose information. These conversations implied that one frequency contains information pertinent to another frequency when, in fact, frequencies are orthogonal.

This became very clear during the investigation of the radiation force implementation. The time-domain reference implemented a version of the function that was developed using the Kramers-Kronig relationships. This version was used because it is guaranteed to have a closed solution over the positive frequency range of zero to infinity. The choice to use this function resulted in a time-domain modeling approach that precluded the direct *in-situ* comparison of $F_{r,p}$, which was vital to the debug process.

In fact, the closed integral is guaranteed, by the system containing the WEC device. The ocean not only transports energy from one region to another, it also filters that energy as it is absorbed. The bounds of this filter with respect to a WEC are 0.31 rad/s and 1.26 rad/s, as described in Section 2.3.4. This is an even smaller range than the 2 rad/s range identified earlier in this section.

There may be a case made for including frequencies near to but outside this range in the frequency-domain to time-domain transformation process, as it may result in a better time-frequency domain correlation within the range. This was not investigated.

5.1.3 Simulation Times

The difference in simulation run-times between the two methodologies is so significant that an expanded analysis is worthwhile.

A frequency-domain approach to simulating wave energy converter hydrodynamics

The graph in Fig. 5.1, which extrapolates from the data presented in Section 4.3.2, provides further insight into this simulation-time advantage. This graph assumes that the length of valid output data produced by the simulation is 10 minutes. It also assumes that the setup is performed once per body/sea state combination, regardless of the simulation method. It clearly shows that the crossover point where the frequency-domain approach takes less time is 274 simulations for a single sea state. Expanding the setup to four sea states reduces the crossover number to 68. Finally, if the number of sea states is expanded to 12, the crossover is reduced to 23. The extrapolated data show that the frequency-domain methodology is a better choice than the time-domain approach when the number of sea states being simulated is increased. It also shows that, for a 12 sea state simulation suite, the time-domain approach will take about 19 hours, where the frequency-domain method will take about 3.2 hours.

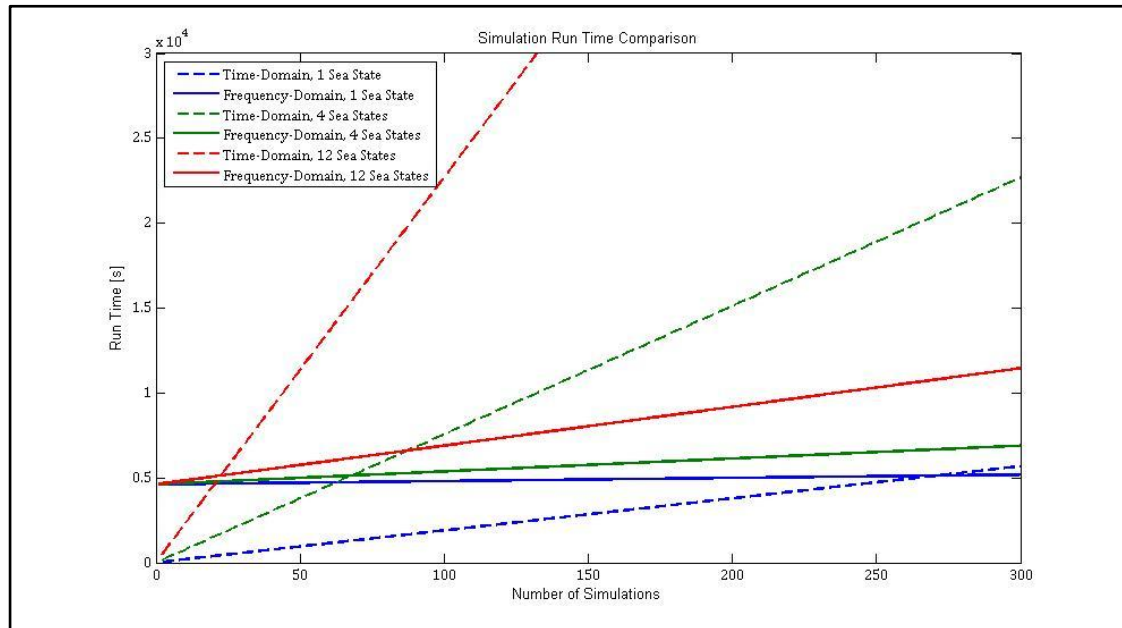


Fig. 5.1: Simulation Run Time Comparison

A frequency-domain approach to simulating wave energy converter hydrodynamics

5.1.4 Single-Frequency WEC Simulations

The single-frequency step in the research process proved to be valuable in teaching two key points. The first point is that the choice of implementing the time-domain model directly impacts the development of a comparable frequency-domain model. The best example of this was the implementation of the radiation force described in Section 5.1.2. The revised implementation, which consolidated the creation of $F_{r,p}$, was instrumental in ensuring the directionality of the phase-shifts, a surprisingly non-trivial effort.

The second point involved the number of frequencies required for the simulations. The desire to determine if addressing the calibration issues was a necessity resulted in a greater understanding of the total wave energy system. This led to understanding the ocean as an energy filter, which enabled a narrower development focus. It also reinforced the importance of clearly understanding the system boundaries when developing a product.

5.1.5 Multiple-Frequency Single Device Simulations

Two additional data representations can be made from slightly modified versions of the results presented in Section 4.4.2. The model output is the body acceleration. An integration process applied to the output results in data describing the velocity of each body. This is, perhaps, the most meaningful representation, as energy is often represented as a proportionality constant applied to a velocity. The plot found in Fig. 5.2 displays the relative body velocity from both domains.

A frequency-domain approach to simulating wave energy converter hydrodynamics

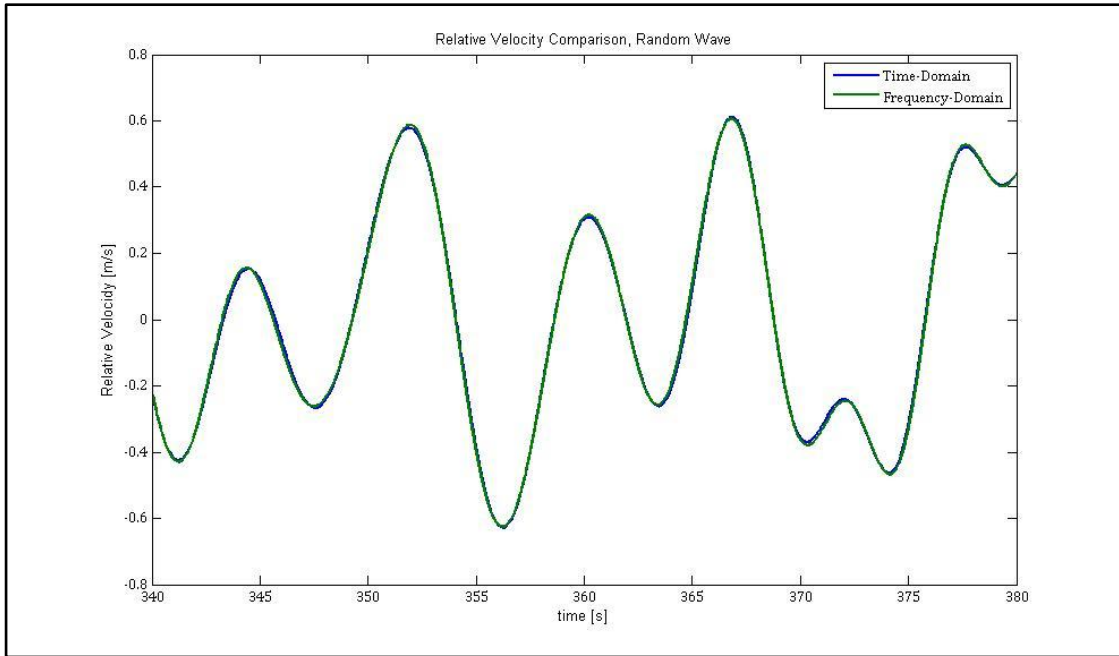


Fig. 5.2: Relative Velocity Comparison, Random Wave

The final constructed plot is a comparison of the per-frequency relative position² to the energy spectra using the frequency-domain results. It is presented in Fig. 5.3. This plot reflects the intuition of the frequency-domain analysis. It provides the developer with a visual understanding of the efficacy of the body design in a particular sea state. And, because the WEC will only present convertible energy in the areas of overlapping frequencies, this plot provides design-modification guidance to the developer.

A frequency-domain approach to simulating wave energy converter hydrodynamics

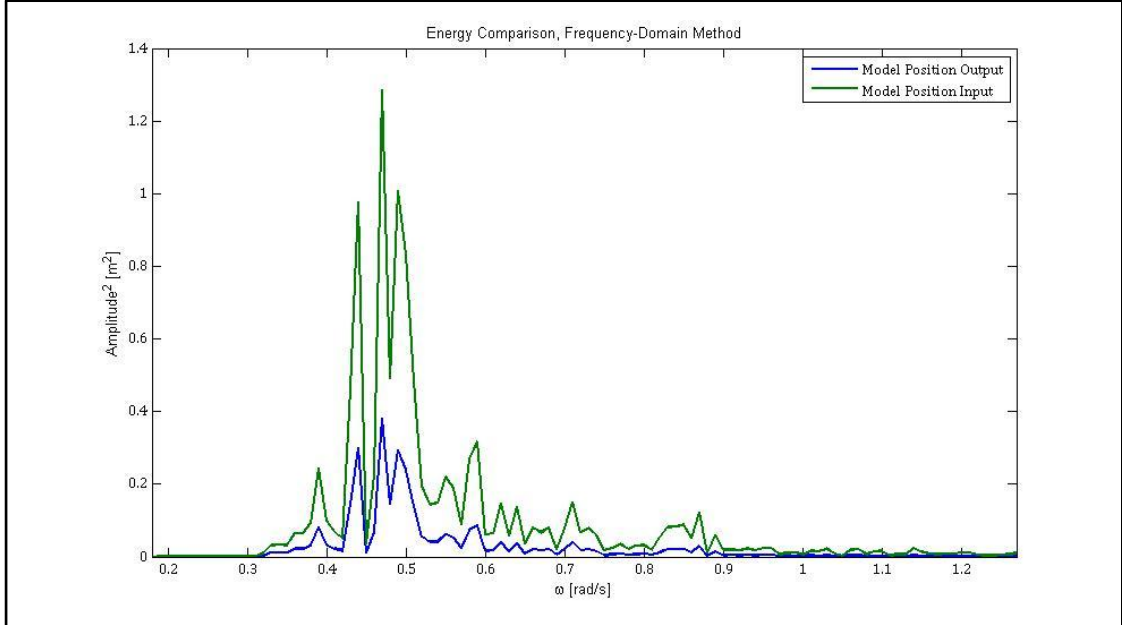


Fig. 5.3: Frequency-Domain Method Input/Output Energy Comparison

5.1.6 WEF Simulation Extrapolation.

Although the research did not include experiments directly related to a WEF simulation, several logical extrapolations are possible. First, the frequency-domain approach enables the simulation of a full, production-sized WEF in statistically-relevant virtual seas. Applying this concept to the methodology presented in [55], an 80x5 WEC array can be simulated in minutes. Not only are the devices in this array modeled for their hydrodynamic responses, the sea-state input for each device are accurately calculated for their relative positions according to Eq. (3-1). Furthermore, while the individual simulation length is constrained by the slowly shifting sea state, the number of consecutive WEF simulations is virtually unlimited. An entire farm of 400 devices can be evaluated for years of ocean states in a few hours.

A frequency-domain approach to simulating wave energy converter hydrodynamics

5.2 Methodology Viability

The research project presented here was designed to be a proof-of-concept project for a frequency-domain simulation methodology in a wave energy development program. The general validity of the frequency approach has been proven for years in the area of communications design. However, applying the concepts from the communications realm to WEC/WEF development is a new investigation. The focus of the investigation was to apply the communications concepts to wave energy development, in enough detail, to prove or disprove the approach. Based on the results of the investigation, it is clear that the methodology is a viable alternative to the traditional time-domain approach.

What may not be evident in the research presented thus far is an assessment of the impact a frequency-domain methodology may have on the WEC and WEF development process. While it has been shown to be a viable alternative to the time-domain approach, this does not ensure that using it provides clear benefits not achievable with the traditional method. A brief commentary on this impact is found in the following sections.

5.2.1 Methodology Advantages

The most obvious advantage of the frequency-domain approach is the amount of time required to simulate the device hydrodynamics. The additional advantages conferred by the short, yet accurate, simulation time are not obvious. The number and variety of simulations that can now be performed lends itself to statistical data processing. A particular body design can now be realistically evaluated over hundreds of hours of realistic sea states. The output data from those simulations can be processed using proven statistical methods and tools. These results, in turn, can be reflected in the design as specifications.

In fact, this methodology enables the developer to evaluate multiple body types in a direct comparison with realistic sea states. This is true as long as all the

A frequency-domain approach to simulating wave energy converter hydrodynamics

simulation environment constraints are met by all of the WEC devices. And because the methodology process is in of the body geometries, evaluating multiple body types is limited to the number of BEM data sets that have been generated.

Another advantage conferred by the methodology is the clean separation of the hydrodynamic response and the electromechanical response of the WEC device. This separation, delineated in the model as F_{PTO} , can now be treated as a specification in the WEC design. In fact, this entire methodology supports a specification-driven development process, simply by the nature of the environment constraints.

In fact, clear identification of F_{PTO} potentially simplifies the design of the electromechanical section. The detailed view provided by the F_{PTO} may be instrumental in the effective application of control processes, especially when controller can only affect one rigid body or can only affect all rigid bodies in same way.

The linearity constraint is, perhaps, the most limiting of the environment constraints faced by the WEC developer. While the methodology requires this constraint, the data organization supports the inclusion of checks on the linearity. These checks are directly tied to the sea-state being simulated, allowing statistical evaluation of sea-state characteristics with respect to device linearity as well as device performance. Such information can enable the developer's efforts in creating a device with good survivability percentages. Additionally, the statistical tools employed in analyzing the output data can identify sea-states that challenge the device operation. Those sea-state sequences can be directly applied to time-domain hydrodynamic models that can reflect the impact of the non-linearity.

A frequency-domain approach to simulating wave energy converter hydrodynamics

5.2.2 Methodology Disadvantages

Just as the research identified additional probable advantages, it also uncovered additional probable disadvantages. And, like the advantages, they were recorded but not explored. Possibly the largest detractor is that the methodology is only fit for a first-level linear assessment. It will not inherently detect system non-linearities. Any level of WEC design that relies on increasing the converted energy by actively controlling the device to force nonlinear responses, such as the amplitude-phase-control method described in [41, ch. 6.3, pp. 207-209], will require unknown modifications to the basic methodology. Neither the depth nor breadth of these modifications has been investigated.

It is likely that the most intimidating disadvantage to the approach is the level of mathematical understanding required to maintain or customize the methodology. This is not an issue for WEC developers who have a solid background in frequency-domain analysis methods bolstered by competency in energy conversion fundamentals and basic knowledge of ocean waves. A possibly substantial learning curve will be required for developers lacking this combination of skills. Especially for those small companies who lack the capital for hiring consultants to complete these tasks.

The final disadvantage identified is that data management may become an issue, especially for any WEF-level simulations. Computer memory itself is not the issue. Rather, the amount of memory available to the base environment, in this case MATLAB™, is the issue. The inherent tool limit has not been investigated, nor have other base environments. The investigation of this issue can likely be an effort that is concurrent with the incorporation of statistical tools.

5.3 Advantage-Driven Benefits

All of the benefits derived from the advantages highlighted in Section 5.2.1 are upon the way the methodology is used by the developer. For example, the

A frequency-domain approach to simulating wave energy converter hydrodynamics

separation of the hydrodynamic and electromechanical models is only a benefit to the developer who can make that advantage work for their development process. Still, a brief discussion of potential benefits may reveal something new to the developer. That change of perception may result in the adoption of the methodology.

The largest positive advantage-driven impact to the WEC developer is the ability to evaluate the hydrodynamics of their design in a statistically-significant number of sea-states. And, it is likely, that those states are developed from a recording station close to the proposed development site. Currently, developers using a time-domain approach can review historical sea state data, even apply statistical analyses to the data, but the harvested power information is one level of estimation removed from the hydrodynamic data. This methodology gives developers the means to virtually prototype their body designs significantly earlier in their development cycles – even before committing capital to building prototypes. Even if the developer is unwilling to change their body designs without real prototyping, application of the methodology may provide guidance as to what sea-states should be investigated. Either of these examples can result in a more focused application of research capital, a vital economic reality for the developer today.

One huge benefit of the methodology that has been identified but not completely investigated is the impact the approach has on WEF development. Utilities and other organizations that support the national grid system currently require farm-level integration studies for any new development proposal. This is also an area of interest to venture capitalists, as the WEF business plan is likely dependant successful grid integration. Methods for providing the data for these studies are rare, with only one public-domain approach currently available [55] [37].

A frequency-domain approach to simulating wave energy converter hydrodynamics

As the extrapolated data presented in Section 5.1.6 indicates, the frequency-domain approach combined with the methodology described in [55] can produce data for WEF integration studies that is directly related to body type. That is, the integration studies can now include a first-level look at the hydrodynamics, bring the WEF-level assessment one step closer to realistic WEF outputs.

5.4 Research Continuation and Expansion

The methodology that was developed in this research satisfies the goals of a proof-of-concept investigation. In keeping with that approach, the methodology deficiencies and remediation recommendations have been documented. Finally, future expansion opportunities for the methodology have also been identified.

5.4.1 Issues to Resolve

The seven modeling issues discussed in Section 4.1 must be resolved before the approach can be used in any meaningful fashion. These issues are summarized, along with recommendations on how to approach their resolution, are below. In addition, descriptions of these issues, and their resolutions, should be forwarded to any current users of the time-domain model. Finally, every resolution should be documented in a revision-controlled location or a bug-tracking database associated with the models.

- Excitation Force Coefficients
 - Verify the AQWA™ amplitude/phase representation with ANSYS.
 - Adjust the $F_{e,p}$ frequency-domain IRF source equations to reflect the accurate amplitudes.
 - Implement the IRF through the use of the full, formal inverse Fourier Transform equation.
- Non-Causality of Excitation Force

A frequency-domain approach to simulating wave energy converter
hydrodynamics

- Determine the correct $F_{e,p}$ amplitude with input from a hydrodynamics expert.
- Implement the correct amplitude in the non-causal/causal filter combination for the time-domain model.
- Implement a correction to the frequency-domain $F_{e,p}$ amplitude source equation if required.
- Radiation Force Coefficients Source Data
 - Verify the relationship between $R(\omega)$ and the AQWA™ output $C(\omega)$ with ANSYS or hydrodynamics expert.
 - Implement the correct relationship in the frequency-domain $F_{r,p}$ source equation.
- Radiation Force Equation
 - Verify the validity of characterizing the ocean as an energy filter with gravity-wave experts.
 - Replace the $k(t)/F'_{r,p}$ formulation with the closed form of $F_{r,p}$, where $Z_p(\omega)$ is the transfer function, in both methodologies.
- Radiation Force Coefficients and Causality
 - Verify the amplitude split of a causal cosine.
 - Confer with experts on how that causal cosine is reflected back into the time-domain.
 - Implement the appropriate amplitude to reflect real physical systems where external amplification is not possible.
- IRF Calculations
 - Investigate the correct frequency range for the energy capture system.
 - Determine the appropriate time-window for the IRF calculation based on the upper end of the correct frequency range.

A frequency-domain approach to simulating wave energy converter hydrodynamics

- Implement the time-window in the IRF calculations.
- Conflicting Sign Conventions
 - Verify that both domains implement the EOMs correctly.
 - Clearly document the form of the EOM employed along with the sign conventions followed for each simulation domain.

It is possible that resolving these seven issues will uncover additional issues.

At a minimum, they should be well documented. Ideally, they would be resolved as well.

The two issues detailed in Section 5.1.2 also need some resolution before the methodology can be expanded. The first of these, the time-domain versus frequency-domain calibration, may be declared a non-issue if developers limit their analyses to the energy-rich frequency range. The issue may be resolved by adding a layer of detail to the frequency-domain approach by more accurately reflecting phase shifts. Or, it may be solved with the resolution of the second issue from that section, the IRF generation. That issue will require some in-depth analysis of how the tool platform is performing the integration steps, and is likely to be a non-trivial effort.

Finally, the coupling, damping and mooring force components should be updated to reflect the current state of public-domain research. At a minimum, the coupling force should be expanded to the original time-domain model equation.

5.4.2 Future Research Topics for this Framework

There are several ways that this methodology can be expanded through additional research. The first, and most obvious, would be to actually demonstrate the methodology in the WEF environment. This effort would be a relatively simple one that could have a high rate of return, because proving the WEF-level application would address a current developmental hole between energy producers and distributors.

A frequency-domain approach to simulating wave energy converter hydrodynamics

A second step would be to expand the correlation efforts to include reality-based experiments, ideally in ocean testing. Even taking a step toward reality by correlating the frequency-domain methodology to tank testing would be a valuable undertaking. Meanwhile, pure virtual enhancements can continue to be developed. The methodology can, and should, be expanded to include at least the non-rotational motion modes. After the methodology is proven to be valid in the WEF setting, developers can begin to address energy attenuation issues.

Finally, although the linear nature of the model may seem restrictive, there are still improvements that can be made within the linear framework. One example would be to approximate the non-linearities by replacing the force components that are functions of one motion vector with a set of components that are a summation of two or all three motion vectors. Experiments in this area may demonstrate that this type of non-linear approximation is more than sufficient for the WEC development process.

5.5 Final Comments

Although it may not be abundantly clear from the evidence presented here, the process of approach a problem from multiple domains, or points of view, leads to a fuller understanding of the both the identified problem and the chosen resolution. This is true for any application. It may also, as was the case in this research, clearly identify issues with implementation of the entrenched methodology. And, since the days when systems were simple enough that they were designed within one discipline, or even by one person, are over, it seems prudent to take advantage of all the different development domains involved in creating a system.

With regard to practical applications, the frequency-domain version of a time-domain process is more intuitive than the time-domain version. This comment is easily supported by reviewing the time-domain and frequency-domain results

A frequency-domain approach to simulating wave energy converter hydrodynamics

presented in Sections 4.3 and 4.4. And, because the domain of electrical communication design frequently uses a frequency-domain approach, there are tools and experts available to jump-start the application of the methodology to the world of hydrodynamics. Especially for the discipline of WEC and WEF design, as there is a more intrinsic overlap between mechanical, hydrodynamic, electrical, and systems engineering than may be found in other areas of ocean device design. The frequency-domain hydrodynamic force coefficients are easier to understand, more intuitive, than the time-domain version. Given current computing power and available algorithms, analysis in the frequency-domain is also computationally easier than in the time-domain. Finally, mathematical manipulations can be reduced from a multiple-step time-domain operation to a single frequency-domain matrix operation, resulting in higher simulation throughputs.

Although the final choice of methodology resides with the individual development teams, the experimental results presented here are sufficiently advantageous to warrant additional development. Especially since this methodology is not a replacement for time-domain simulations, but an adjunct. Hopefully, this initial foray into the WEC development approach will be supplemented by additional research in both public and private arenas.

A frequency-domain approach to simulating wave energy converter
hydrodynamics

6 Appendix A: Time-Domain Model

6.1 Scripts

6.1.1 Define geometry function

```

rho_sw = 1025;      %% density of salt water [kg/m^3]
g = 9.807;          %% acceleration of gravity [m/s/s], match AQWA

%% User Defined Values

fprintf('What Geometry would you like to import?\n\n');
fprintf('\t 1 = Eidsmoen WEC\n');
fprintf('\t 2 = PowerBuoy WEC\n');
fprintf('\t 3 = OSU L10 WEC\n');
fprintf('\t 4 = Eidsmoen PAPER WEC\n\n\t');
answer_1 = input(': ');
fprintf('\n');

%% Import Eidsmoen WEC Geometry
if answer_1 == 1
    load AQWA_data
    % Buoy Values
    B1.D = 3.3;           %% Diameter of Buoy [m]
    B1.A= pi*B1.D^2/4;    %% Area of Buoy [m^2]
    B1.l = 5.1;           %% Length of Buoy [m] *****NOTE: This term
    HIGHLY affects the buoy displacement because it is used to calculate
    mass
    B1.m = 9700;          %% Mass of Buoy [kg] from Eidsmoen (1996)
    B1.am = 9000;          %% From AQWA simulation
    % Spar/Plate Values
    B2.D = 8;              %% Diameter of Plate [m]
    B2.l = .2;             %% Length of Plate [m]
    B2.m = 28000;          %% Mass of Plate [kg] from Eidsmoen (1996)
    B2.Dhs = .4;            %% Wet surface diameter
    B2.A = pi*B2.Dhs^2/4;   %% Area of Spar/Plate [m^2]
    % Import AQWA Buoy and Plate Excitation Data
    B1.Fe = S1.FK;
    B2.Fe = S2.FK;
    % Import AQWA Buoy and Plate Radiation Data
    B1.C = S1.RD11;
    B2.C = S2.RD22;
    % Import Buoy and Plate Added Mass
    B1.AM = S1.AM;
    B2.AM = S2.AM;
    % Mooring Specs
    Moor.Km = 160000;       %% [N/m]

```

A frequency-domain approach to simulating wave energy converter hydrodynamics

```

Moor.Bm = 1e6;           %% Not included in exp testing
% Viscous Damping Coeff (num/exp adjustment)
B1.bv = 507692;          %% Viscous damping coefficient [N/m/s]
B2.bv = B1.bv;
% Damping to match AQWA simulation
damping = 50000;
end

%% Import PowerBuoy WEC Geometry
if answer_1 == 2
    % Buoy Values
    B1.D = 11;             %% Diameter of Buoy [m]
    B1.A= pi*B1.D^2/4;     %% Area of Buoy [m^2]
    B1.l = 3;              %% Length of Bouy [m]
    B1.m = 2.9223E+05;    %% Mass of Buoy [kg] from AQWA
    % Spar/Plate Values
    B2.D = 14;             %% Diameter of Plate [m]
    B2.l = 2;              %% Length of Plate [m]
    B2.m = 5.1045E+05;    %% Mass of Plate [kg] from AQWA
    B2.Dhs = .5;           %% Wet surface diameter
    B2.A= pi*B2.Dhs^2/4;   %% Area of Spar/Plate [m^2]
    % Import AQWA Buoy and Plate Excitation Data
    %     B1.Fe =
    importdata('PowerBuoy_FINAL_Body1_FkDiff_Forces_ZeroDeg.txt');
    %     B2.Fe =
    importdata('PowerBuoy_FINAL_Body2_FkDiff_Forces_ZeroDeg.txt');
    B1.Fe = importdata('PB150_Body1_Froude_Diff.txt');
    B2.Fe = importdata('PB150_Body2_Froude_Diff.txt');
    % Import AQWA Buoy and Plate Radiation Data
    B1.C = importdata('PB150_Body1_Damping.txt');
    B2.C = importdata('PB150_Body2_Damping.txt');
    %     B1.C = importdata('PowerBuoy_FINAL_Body1_RadDamping.txt');
    %     B2.C = importdata('PowerBuoy_FINAL_Body2_RadDamping.txt');

    % Import Buoy and Plate Added Mass
    %     B1.AM = importdata('PowerBuoy_FINAL_Body1_AddedMass.txt');
    %     B2.AM = importdata('PowerBuoy_FINAL_Body2_AddedMass.txt');
    B1.AM = importdata('PB150_Body1_AddedMass.txt');
    B2.AM = importdata('PB150_Body2_AddedMass.txt');
    % Mooring Specs
    Moor.Km = 160000;      %% [N/m]
    Moor.Bm = 1e6;          %% Not included in exp testing
    % Viscous Damping Coeff (num/exp adjustment)
    B1.bv = 507692;          %% Viscous damping coefficient [N/m/s]
    B2.bv = B1.bv;
    % Damping to match AQWA simulation
    damping = 50000;

end

```

A frequency-domain approach to simulating wave energy converter hydrodynamics

```

%% Import OSU L10 WEC Geometry
if answer_1 == 3
    % Buoy Values
    B1.D = 3.5;           %% Diameter of Buoy [m]
    B1.l = 0.76;          %% Length of Bouy [m]
    B1.A= pi*B1.D^2/4;   %% Area of Buoy [m^2]
    B1.m = 2625.3;        %% Mass of Buoy [kg] from AQWA
    % Spar/Plate Values
    B2.D = 1.1;           %% Diameter of Plate [m]
    B2.l = 1.8;           %% Length of Plate [m]
    B2.m = 2650.4;        %% Mass of Plate [kg] from AQWA
    B2.Dhs = .5;          %% Wet surface diameter
    B2.A= pi*B2.Dhs^2/4;  %% Area of Spar/Plate [m^2]

    % Import AQWA Buoy and Plate Excitation Data
    B1.Fe = importdata('L10_FINAL_Body1_FkDiff_Forces_ZeroDeg.txt');
    B2.Fe = importdata('L10_FINAL_Body2_FkDiff_Forces_ZeroDeg.txt');
    % Import AQWA Buoy and Plate Radiation Data
    B1.C = importdata('L10_FINAL_Body1_RadDamping.txt');
    B2.C = importdata('L10_FINAL_Body2_RadDamping.txt');
    % Import Buoy and Plate Added Mass
    B1.AM = importdata('L10_FINAL_Body1_AddedMass.txt');
    B2.AM = importdata('L10_FINAL_Body2_AddedMass.txt');
    % Mooring Specs
    Moor.Km = 160000;     %% [N/m]
    Moor.Bm = 1e5;         %% Not included in exp testing
    % Viscous Damping Coeff (num/exp adjustment)
    B1.bv = 507692;       %% Viscous damping coefficient [N/m/s]
    B2.bv = B1.bv;
    % Damping to match AQWA simulation
    damping = 50000;
end
%% Import Eidsmoen WEC Geometry
if answer_1 == 4
    load AQWA_data
    % Buoy Values
    B1.D = 3.3;           %% Diameter of Buoy [m]
    B1.A= pi*B1.D^2/4;   %% Area of Buoy [m^2]
    B1.l = 5.1;           %% Length of Bouy [m] *****NOTE: This term
    HIGHLY affects the buoy displacement because it is used to calculate
    mass
    B1.m = 9700;          %% Mass of Bouy [kg] from Eidsmoen (1996)
    B1.am = 8700;          %% Added Mass of Bouy [kg] from Eidsmoen (1996)
    % Spar/Plate Values
    B2.D = 8;              %% Diameter of Plate [m]
    B2.l = .2;             %% Length of Plate [m]
    B2.m = 28000;          %% Mass of Plate [kg] from Eidsmoen (1996)
    B2.Dhs = .4;            %% Wet surface diameter
    B2.A = pi*B2.Dhs^2/4;  %% Area of Spar/Plate [m^2]
    % Import AQWA Buoy and Plate Excitation Data

```

A frequency-domain approach to simulating wave energy converter hydrodynamics

```

B1.Fe =
importdata('Eidsmoen_PAPER_Body1_FkDiff_Forces_ZeroDeg.txt');
B2.Fe =
importdata('Eidsmoen_PAPER_Body2_FkDiff_Forces_ZeroDeg.txt');
% Import AQWA Buoy and Plate Radiation Data
B1.C = importdata('Eidsmoen_PAPER_Body1_RadDamping.txt');
B2.C = importdata('Eidsmoen_PAPER_Body2_RadDamping.txt');
% Import Buoy and Plate Added Mass
B1.AM = importdata('Eidsmoen_PAPER_Body1_AddedMass.txt');
B2.AM = importdata('Eidsmoen_PAPER_Body2_AddedMass.txt');
% Mooring Specs
Moor.Km = 160000;      %% [N/m]
Moor.Bm = 1e6;          %% Not included in exp testing
% Viscous Damping Coeff (num/exp adjustment)
B1.bv = 507692;         %% Viscous damping coefficient [N/m/s]
B2.bv = B1.bv;
% Damping to match AQWA simulation
damping = 50000;
end

%% Calculated Values

% Buoy Calculated Values
B1.Khs = rho_sw*g*B1.A;      %% Hydrostatic Stiffness
% Spar Calculated Values
B2.Khs = rho_sw*g*B2.A;      %% Hydrostatic Stiffness

end

```

6.1.2 Impulse response function

```

function [...]
    B1...
    B2...
    Bc...
    tmax...
    omegapos...
    ] = impulserespcalc_rebuild(..., ...
        B1, ...
        B2, ...
        del_t...
    )
    wpos      = B1.Fe(:,2);           % Omega from AQWA.
    omegapos = 0.01:0.01:1.5;        % high-resolution positive omega
    omega     = [-fliplr(omegapos) 0 omegapos];
    tmax     = 31.42;
    t_fe     = -tmax:del_t:tmax;
    t_fr     = 0:del_t:tmax;

```

A frequency-domain approach to simulating wave energy converter
hydrodynamics

```

B1.Fez_amp_raw = B1.Fe(:,7); % Heave excitation amplitude
B1.Fez_phase_raw = B1.Fe(:,8)*pi/180 + 2*pi; % Heave excitation phase
B2.Fez_amp_raw = B2.Fe(:,7); % Heave excitation amplitude
B2.Fez_phase_raw = B2.Fe(:,8)*pi/180 + 2*pi;% Heave excitation phase

% Interpolate to higher resolution
B1.Fez_amp = interp1(wpos,B1.Fez_amp_raw,omegapos,'linear','extrap');
B1.Fez_phase =
interp1(wpos,B1.Fez_phase_raw,omegapos,'linear','extrap');
B2.Fez_amp = interp1(wpos,B2.Fez_amp_raw,omegapos,'linear','extrap');
B2.Fez_phase =
interp1(wpos,B2.Fez_phase_raw,omegapos,'linear','extrap');

% Build the complex F-domain response
B1.Fezpos = B1.Fez_amp.*exp(1i.*B1.Fez_phase);
B2.Fezpos = B2.Fez_amp.*exp(1i.*B2.Fez_phase);

B1.Fez = [conj(fliplr(B1.Fezpos))/2 0 B1.Fezpos/2];
B2.Fez = [conj(fliplr(B2.Fezpos))/2 0 B2.Fezpos/2];

for k = 1:length(t_fe) % Based on AQWA Manual F2T and Falnes
(2002,1995)
    B1.fe(k) =
(1/(2*pi))*trapz(omega,B1.Fez.*exp(1i*omega.*t_fe(k)));
    B2.fe(k) =
(1/(2*pi))*trapz(omega,B2.Fez.*exp(1i*omega.*t_fe(k)));
end

B1.fe_maxImag = abs(max(imag(B1.fe)));
B2.fe_maxImag = abs(max(imag(B2.fe)));

if ((B1.fe_maxImag >= 1e-10) ||...
(B2.fe_maxImag >= 1e-10))
    error('Imaginary part too big')
else
    B1.fez = real(B1.fe);
    B2.fez = real(B2.fe);
end

% Separate Causal from Non-Causal
B1.zeroIndex = find(t_fe >= 0,1); %Find index of zero time element
B2.zeroIndex = find(t_fe >= 0,1); %Find index of zero time element
B1.firCoeffCaus = B1.fez((B1.zeroIndex:end)); %Take the causal part
of sig
B2.firCoeffCaus = B2.fez((B2.zeroIndex:end)); %Take the causal part
of sig
B1.nonCausHorizonTime = -tmax; %Nonzero part of impulse response
time

```

A frequency-domain approach to simulating wave energy converter
hydrodynamics

```

B2.nonCausHorizonTime = -tmax; %Nonzero part of impulse response
time
B1.nonCausHorizonIndex = find(t_fe >= B1.nonCausHorizonTime,1);
%Find index
B2.nonCausHorizonIndex = find(t_fe >= B2.nonCausHorizonTime,1);
%Find index
B1.firCoeffNonCaus = B1.fez(B1.nonCausHorizonIndex:(B1.zeroIndex-1));
%Separate noncausal part
B2.firCoeffNonCaus = B2.fez(B2.nonCausHorizonIndex:(B2.zeroIndex-1));
%Separate noncausal part
% Determines Data Cutoff-> excluding non-causal for eta time-series
caus.largestnonCausHorizonTime=max(abs(B1.nonCausHorizonTime),abs(B2.
nonCausHorizonTime)); %Find index of end of valid data

B1.AMz    = interp1(wpos,B1.AM(:,5),omegapos,'linear','extrap');
B1.AMinf = B1.AMz(end);

B2.AMz    = interp1(wpos,B2.AM(:,5),omegapos,'linear','extrap');
B2.AMinf = B2.AMz(end);

% Coupled added mass estimate
Bc.AM12inf = min([B1.AMinf,B2.AMinf]);
Bc.AM21inf = Bc.AM12inf;
% Interpolate to higher resolution
B1.IM = interp1(wpos,B1.C(:,5),omegapos,'linear','extrap');
B2.IM = interp1(wpos,B2.C(:,5),omegapos,'linear','extrap');

B1.KMpos = (li.*omegapos.* (B1.AMz - B1.AMinf))/4;
B2.KMpos = (li.*omegapos.* (B2.AMz - B2.AMinf))/4;

% Falnes 5.109
B1.KRpos = B1.IM.*omegapos/4;% R matrix from AQWA c
B2.KRpos = B2.IM.*omegapos/4;% R matrix from AQWA c

% Fr check
B1.Zpos = (B1.IM.*omegapos + li.*omegapos.*B1.AMz)/4;
B2.Zpos = (B2.IM.*omegapos + li.*omegapos.*B2.AMz)/4;
%
B1.KR = [fliplr(conj(B1.KRpos)) 0 B1.KRpos];
B2.KR = [fliplr(conj(B2.KRpos)) 0 B2.KRpos];
B1.KM = [fliplr(conj(B1.KMpos)) 0 B1.KMpos];
B2.KM = [fliplr(conj(B2.KMpos)) 0 B2.KMpos];
B1.Z = [fliplr(conj(B1.Zpos)) 0 B1.Zpos];
B2.Z = [fliplr(conj(B2.Zpos)) 0 B2.Zpos];

% Create the time-domain xfer function (filter coefficients) of Eq.
5.112
for k = 1:length(t_fr)

```

A frequency-domain approach to simulating wave energy converter hydrodynamics

```

B1.kr_c(k) =
(1/(2.*pi))*trapz(omega,B1.KR.*exp(1i.*omega.*t_fr(k)));
B2.kr_c(k) =
(1/(2.*pi))*trapz(omega,B2.KR.*exp(1i.*omega.*t_fr(k)));
B1.km_c(k) =
(1/(2.*pi))*trapz(omega,B1.KM.*exp(1i.*omega.*t_fr(k)));
B2.km_c(k) =
(1/(2.*pi))*trapz(omega,B2.KM.*exp(1i.*omega.*t_fr(k)));
B1.z_c(k) =
(1/(2.*pi))*trapz(omega,B1.Z.*exp(1i.*omega.*t_fr(k)));
B2.z_c(k) =
(1/(2.*pi))*trapz(omega,B2.Z.*exp(1i.*omega.*t_fr(k)));
end

B1.kr = real(B1.kr_c);
B2.kr = real(B2.kr_c);
B1.km = real(B1.km_c);
B2.km = real(B2.km_c);
B1.z = real(B1.z_c);
B2.z = real(B2.z_c);

end

```

6.1.3 Simulation run script

```

tic;
clc;
clear all;
close all;
addpath(genpath('PA2BH'));

%% Variable Definitions

Hs      = 2;    % = amplitude of 1, easiest comparison to AQWA results

% universal constants
g = 9.81; % gravity, m/s^2
rho = 1025; % saltwater density kg/m^3
fprintf('\n');

%% Define Hydrodynamics
% Selects the desired geometry and returns constants for simulink
del_t = 0.01;    % Time step - forced by the Rhuel setup

[B1 B2 Moor damping] = definegeometry();

% Calculate impulse response functions from frequency domain data
[B1 B2 Bc tmax w] = impulserespcalc_rebuild(B1,B2,del_t);

```

A frequency-domain approach to simulating wave energy converter
hydrodynamics

```

%% Define the inputs

timestart = -tmax;
timeend = 739.5;% 10min + 10000 cycles window after 40s of pre/post
garbage removed

% Define the time-domain wave
t=timestart:del_t:timeend;
t = t';
mass1 = B1.m;%K
mass2 = B2.m;%K

sumWave = zeros(size(t));

[a b] = size(w);
load 'etaK'
A = Arand(1:150).*exp(li.*P.rand(1:150));

for n = 18:b
    td_simStart = tic;
    regWave =Arand(n)*cos(w(n)*t + P.rand(n));
    sumWave = regWave + sumWave;
    perLength(n) = round((2*pi)/(w(n)*del_t));
    n
    %%
    % Format needed for WEC_MODEL
    eta=[t,regWave]; % time [s], wave surface
    elevation [m]

    % Split into causal/non-causal eta
    % Define shifted input wave elevation for the noncausal
    convolution used by filter
    B1.etaprime = eta;
    B2.etaprime = eta;
    B1.etaprime(:,1) = B1.etaprime(:,1) + B1.nonCausHorizonTime;
    %shift by size of nonzero part of impulse response
    B2.etaprime(:,1) = B2.etaprime(:,1) + B2.nonCausHorizonTime;
    %shift by size of nonzero part of impulse response

    % run the time-domain simulation
    sim('PA2BH_RegWave.mdl');

    % Extract results from simulation record.
    perLength(n) = abs(round((2*pi)/(w(n)*del_t)));
    start_ss = 36000;
    stop_ss = start_ss + perLength(n);

    [input_amp(n), input_idx(n)] = max(regWave(start_ss:stop_ss));
    input_idx(n) = input_idx(n) + start_ss - 1;

```

A frequency-domain approach to simulating wave energy converter
hydrodynamics

```

[B1acc_max(n), B1acc_idx(n)] = (max(z1_acc(start_ss:stop_ss)));
[B1acc_min(n), B1acc_mdx(n)] = (min(z1_acc(start_ss:stop_ss)));
[B2acc_max(n), B2acc_idx(n)] = (max(z2_acc(start_ss:stop_ss)));
[B2acc_min(n), B2acc_mdx(n)] = (min(z2_acc(start_ss:stop_ss)));

[B1vel_max(n), B1vel_idx(n)] = (max(z1_vel(start_ss:stop_ss)));
[B1vel_min(n), B1vel_mdx(n)] = (min(z1_vel(start_ss:stop_ss)));
[B2vel_max(n), B2vel_idx(n)] = (max(z2_vel(start_ss:stop_ss)));
[B2vel_min(n), B2vel_mdx(n)] = (min(z2_vel(start_ss:stop_ss)));

[B1ftot_max(n), B1ftot_idx(n)] = (max(B1ftot(start_ss:stop_ss)));
[B1ftot_min(n), B1ftot_mdx(n)] = (min(B1ftot(start_ss:stop_ss)));
[B2ftot_max(n), B2ftot_idx(n)] = (max(B2ftot(start_ss:stop_ss)));
[B2ftot_min(n), B2ftot_mdx(n)] = (min(B2ftot(start_ss:stop_ss)));

[fe1_max(n), fe1_idx(n)] = (max(fe1(start_ss:stop_ss)));
[fe1_min(n), fe1_mdx(n)] = (min(fe1(start_ss:stop_ss)));
[fe2_max(n), fe2_idx(n)] = (max(fe2(start_ss:stop_ss)));
[fe2_min(n), fe2_mdx(n)] = (min(fe2(start_ss:stop_ss)));

B1vel_idx(n) = input_idx(n) + B1vel_idx(n);
B1vel_mdx(n) = input_idx(n) + B1vel_mdx(n);
B2vel_idx(n) = input_idx(n) + B2vel_idx(n);
B2vel_mdx(n) = input_idx(n) + B2vel_mdx(n);
tdRun(n)=toc(td_simStart);

end

tdRunAve = sum(tdRun)/(b-18);
fe1_phs = 2*pi.*fe1_idx./perLength;
fe2_phs = 2*pi.*fe2_idx./perLength;

%debug stuff
B1vel_amp = (B1vel_max - B1vel_min)./2;
B1acc_amp = (B1acc_max - B1acc_min)./2;
B1ftot_amp = (B1ftot_max - B1ftot_min)./2;

B2vel_amp = (B2vel_max - B2vel_min)./2;
B2acc_amp = (B2acc_max - B2acc_min)./2;
B2ftot_amp = (B2ftot_max - B2ftot_min)./2;
fd_simStart = tic;

load('CalFe.mat');
load('CalFr.mat');

B1FE_amp = abs(B1.Fezpos)/2;% + B1fe_adj_a;
B1FE_phs = angle(B1.Fezpos);

```

A frequency-domain approach to simulating wave energy converter
hydrodynamics

```

B1FE = B1FE_amp.*exp(1i*B1FE_phhs);
B1FE(1:17) = 0;

B2FE_amp = abs(B2.Fezpos)/2;% + B2fe_adj_a;
B2FE_phhs = angle(B2.Fezpos);
B2FE = B2FE_amp.*exp(1i*B2FE_phhs);
B2FE(1:17) = 0;

MoorB = (Moor.Bm);
B2bv = (B2.bv);
B1bv = (B1.bv);
Fpto = (damping);
MoorK = (Moor.Km);
B2khs = B2.Khs;
B1khs = (B1.Khs);

B2KR_amp = (B2.KRpos/2) + B2FrPR_adj_a;
B2KM_amp = (B2.KMpos/2) + B2FrPM_adj_a;

B1KR_amp = (B1.KRpos/2) + B1FrPR_adj_a;
B1KM_amp = (B1.KMpos/2) + B1FrPM_adj_a;

B1KR = B1KR_amp.*exp(1i*0*B1FrPR_phhs);
B1KM = B1KM_amp.*exp(1i*0*B1FrPM_phhs);

B2KR = B2KR_amp.*exp(1i*0*B2FrPR_phhs);
B2KM = B2KM_amp.*exp(1i*0*B2FrPM_phhs);

B1K = B1KR + B1KM;
B2K = B2KR + B2KM;
B1Z = B1K + 1i.*w.*B1.AMinf;
B2Z = B2K + 1i.*w.*B2.AMinf;

BC12K = 0;
BC21K = 0;

%% Model in the Frequency Domain
% Calculate the intermediate values
f = w./(2*pi);

% Coefficients assigned in derived equations (28 A-E)
Co1A = (mass1 - (B1khs./(2.*pi.*f).^2));
Co1BP = (B1Z + B1bv + Fpto)./(2.*pi.*f);
Co1BN = (B1Z + B1bv + Fpto)./(2.*pi.*-f);
Co1C = (B1Z + B1bv + Fpto);
Co1DN = (BC12K - Fpto)./(2.*pi.*-f);
Co1DP = (BC12K - Fpto)./(2.*pi.*f);

```

A frequency-domain approach to simulating wave energy converter
hydrodynamics

```

Co1E = (BC12K - Fpto);

% Coefficients assigned in derived equations (56 A-F)
Co2A = (mass2 - (B2khs + MoorK)./(2.*pi.*f).^2);
Co2BN = (B2Z + MoorB + B2bv - Fpto)./(2.*pi.*f);
Co2BP = (B2Z + MoorB + B2bv - Fpto)./(2.*pi.*f);
Co2C = (B2Z + MoorB + B2bv - Fpto);
Co2D = B2khs + MoorK;
Co2EN = (BC21K + Fpto)./(2.*pi.*f);
Co2EP = (BC21K + Fpto)./(2.*pi.*f);
Co2F = (BC21K + Fpto);

% Derived Equation 70, acceleration, negative frequency delta
Z2a_nf = 2.*A.* (B2FE - (B1FE.*(-Bc.AM21inf + li.*Co2EN)./(Co1A +
1i.*Co1BN))) ...
        ./(Co2A + li.*Co2BN - (-Bc.AM12inf + li.*Co1DN).*(-Bc.AM21inf
+ 1i.*Co2EN)) ...
        ./(Co1A + li.*Co1BN));

Z2a_pf = 2.*A.* (B2FE - (B1FE.*(-Bc.AM21inf - li.*Co2EP)./(Co1A -
1i.*Co1BP))) ...
        ./(Co2A - li.*Co2BP - (-Bc.AM12inf - li.*Co1DP).*(-Bc.AM21inf
- 1i.*Co2EP)) ...
        ./(Co1A - li.*Co1BP));

Z2 = Z2a_pf.*exp(li.*angle(Z2a_pf))/2;

Z1a_nf = 2.*A.* (B1FE)./(Co1A + li.*Co1BN) ...
        - Z2a_nf.*(-Bc.AM12inf + li.*Co1DN)./(Co1A + li.*Co1BN);

Z1a_pf = 2.*A.* (B1FE)./(Co1A - li.*Co1BP) ...
        - Z2a_pf.*(-Bc.AM12inf - li.*Co1DP)./(Co1A - li.*Co1BP);

Z1 = Z1a_pf.*exp(li.*angle(Z1a_pf))/2;
fdRun=toc(fd_simStart);

Z1_err = 100.* (B1acc_amp- abs(Z1))./B1acc_amp;
Z2_err = 100.* (B2acc_amp- abs(Z2))./B2acc_amp;

Z1a_nf(1:17)=0;
Z1a_pf(1:17)=0;

Z2a_nf(1:17)=0;
Z2a_pf(1:17)=0;

Z1v_pf = Z1a_pf./(li.*w);
Z2v_pf = Z2a_pf./(li.*w);
Z1p_pf = Z1v_pf./(li.*w);

```

A frequency-domain approach to simulating wave energy converter
hydrodynamics

```

z2p_pf = z2v_pf./(1i.*w);

t=t';
[n tend] = size(t);
zlaw = zeros(b,tend);
zla = zeros(1,tend);
z2aw = zeros(b,tend);
z2a = zeros(1,tend);

z1vw = zeros(b,tend);
z1v = zeros(1,tend);
z2vw = zeros(b,tend);
z2v = zeros(1,tend);

z1pw = zeros(b,tend);
z1p = zeros(1,tend);
z2pw = zeros(b,tend);
z2p = zeros(1,tend);

tic;
for n=18:b
    fooa = (abs(Z1a_pf(n)) / (2).*cos(w(n).*t + angle(Z1a_pf(n)))); 
    zlaw(n,:) = fooa;
    zla = zla + fooa;
    fooa = (abs(Z2a_pf(n)) / (2).*cos(w(n).*t + angle(Z2a_pf(n)))); 
    z2aw(n,:) = fooa;
    z2a = z2a + fooa;
end

for n=18:b
    foov = (abs(Z1v_pf(n)) / (2).*cos(w(n).*t + angle(Z1v_pf(n)))); 
    z1vw(n,:) = foov;
    z1v = z1v + foov;
    foov = (abs(Z2v_pf(n)) / (2).*cos(w(n).*t + angle(Z2v_pf(n)))); 
    z2vw(n,:) = foov;
    z2v = z2v + foov;
end

for n=18:b
    foop = (abs(Z1p_pf(n)) / (2).*cos(w(n).*t + angle(Z1p_pf(n)))); 
    z1pw(n,:) = foop;
    z1p = z1p + foop;
    foop = (abs(Z2p_pf(n)) / (2).*cos(w(n).*t + angle(Z2p_pf(n)))); 
    z2pw(n,:) = foop;
    z2p = z2p + foop;
end

```

A frequency-domain approach to simulating wave energy converter hydrodynamics

```

fsimTime = toc/3600;

%% Combined Frequency Sim
eta=[t,sumWave]; % time [s], wave surface elevation
[m]

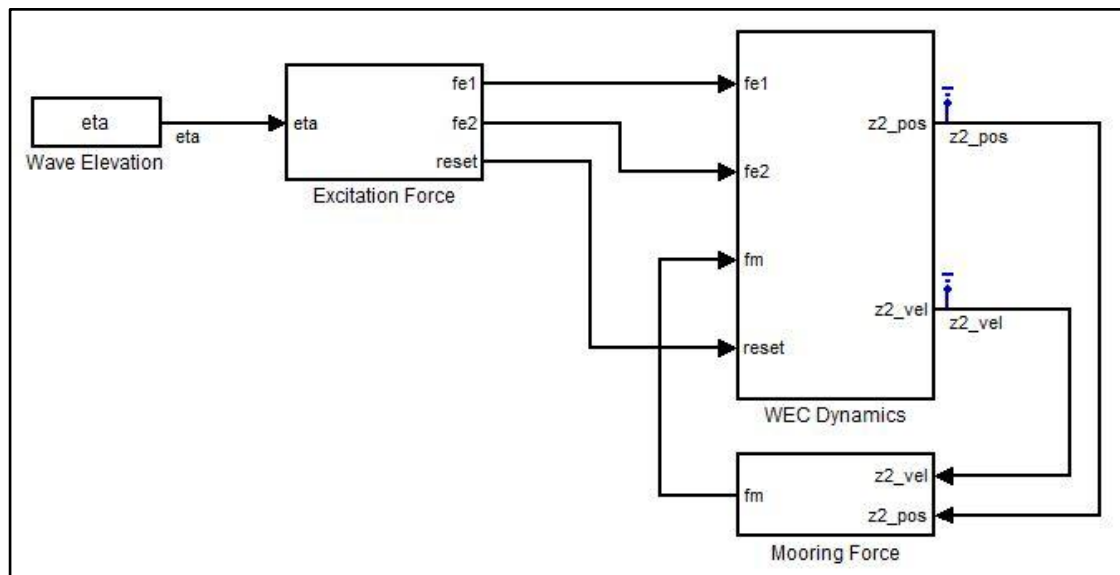
% Split into causal/non-causal eta
% Define shifted input wave elevation for the noncausal convolution
used by filter
B1.etaprime = eta;
B2.etaprime = eta;
B1.etaprime(:,1) = B1.etaprime(:,1) + B1.nonCausHorizonTime; %shift
by size of nonzero part of impulse response
B2.etaprime(:,1) = B2.etaprime(:,1) + B2.nonCausHorizonTime; %shift
by size of nonzero part of impulse response

% run the time-domain simulation
sim('PA2BH_RegWave.mdl');

```

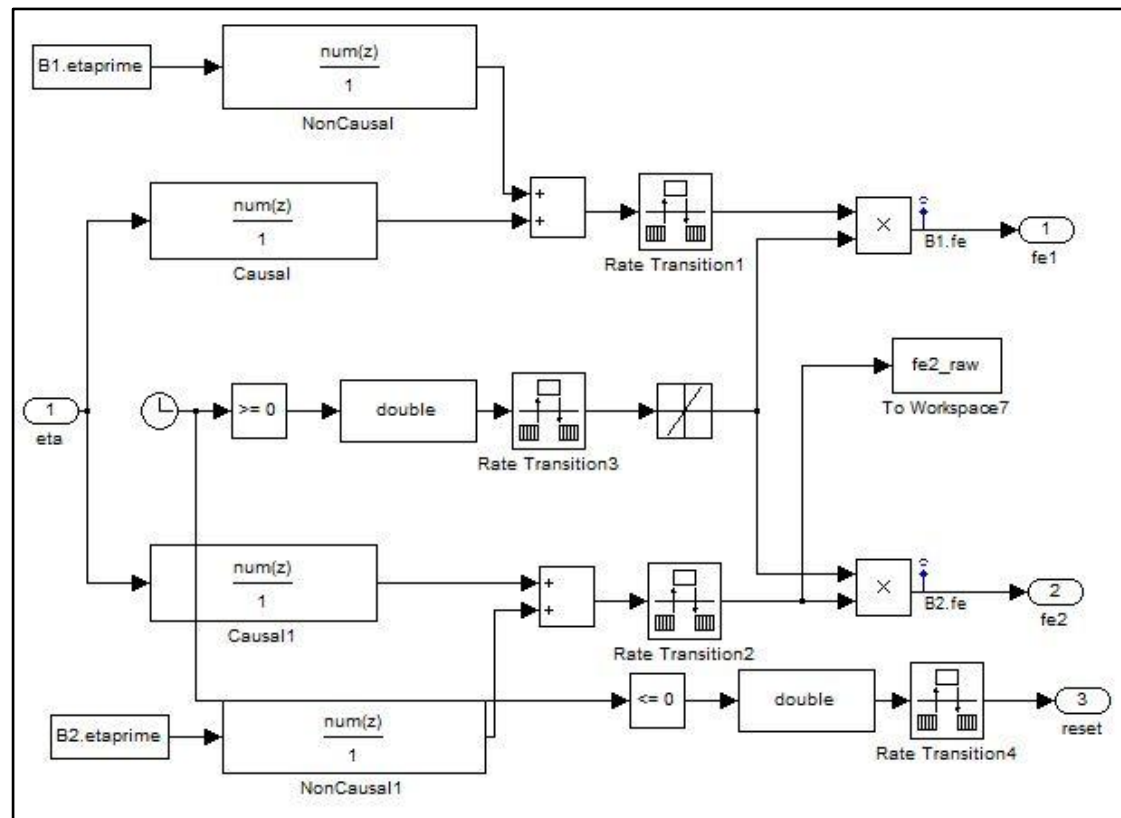
6.2 Schematics

6.2.1 Top Level



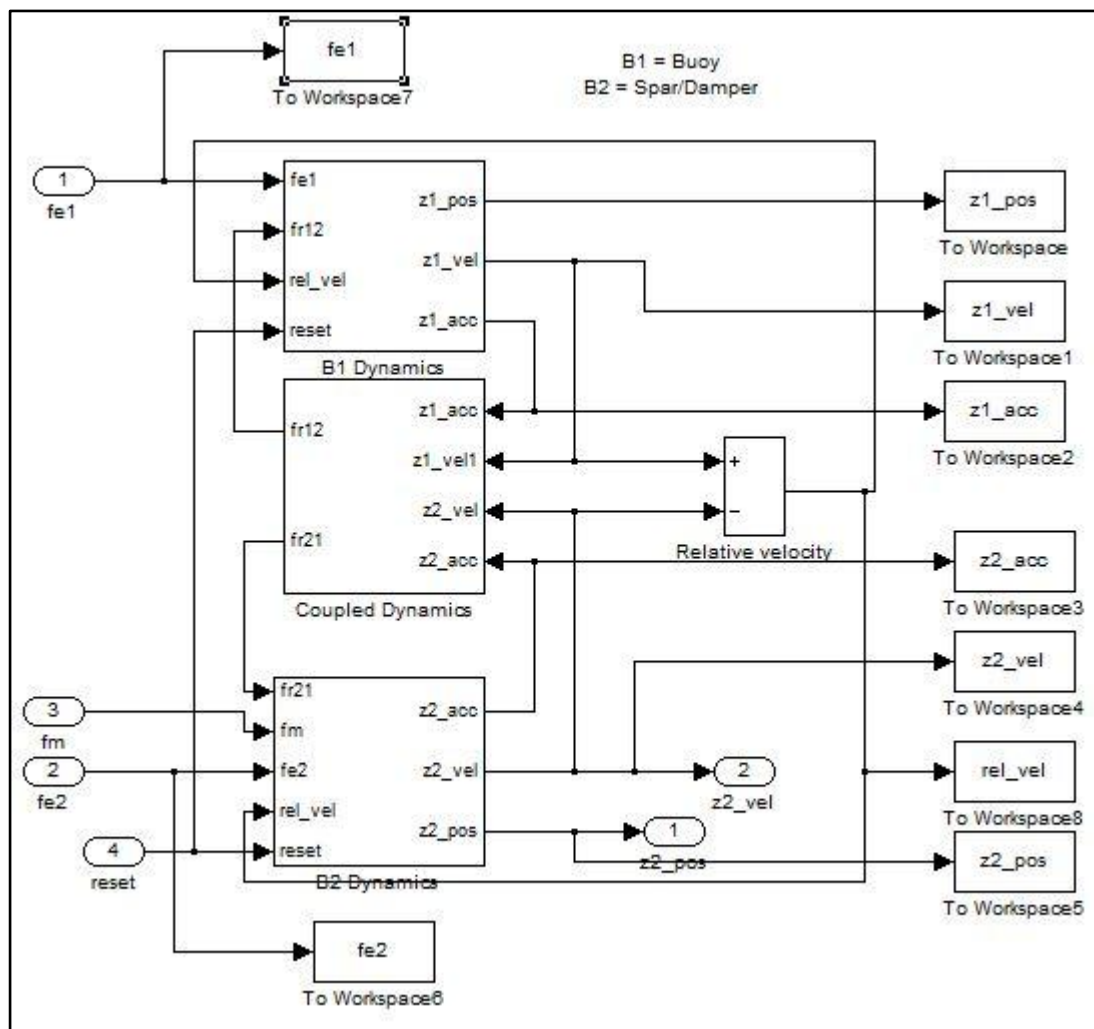
A frequency-domain approach to simulating wave energy converter
hydrodynamics

6.2.2 Excitation



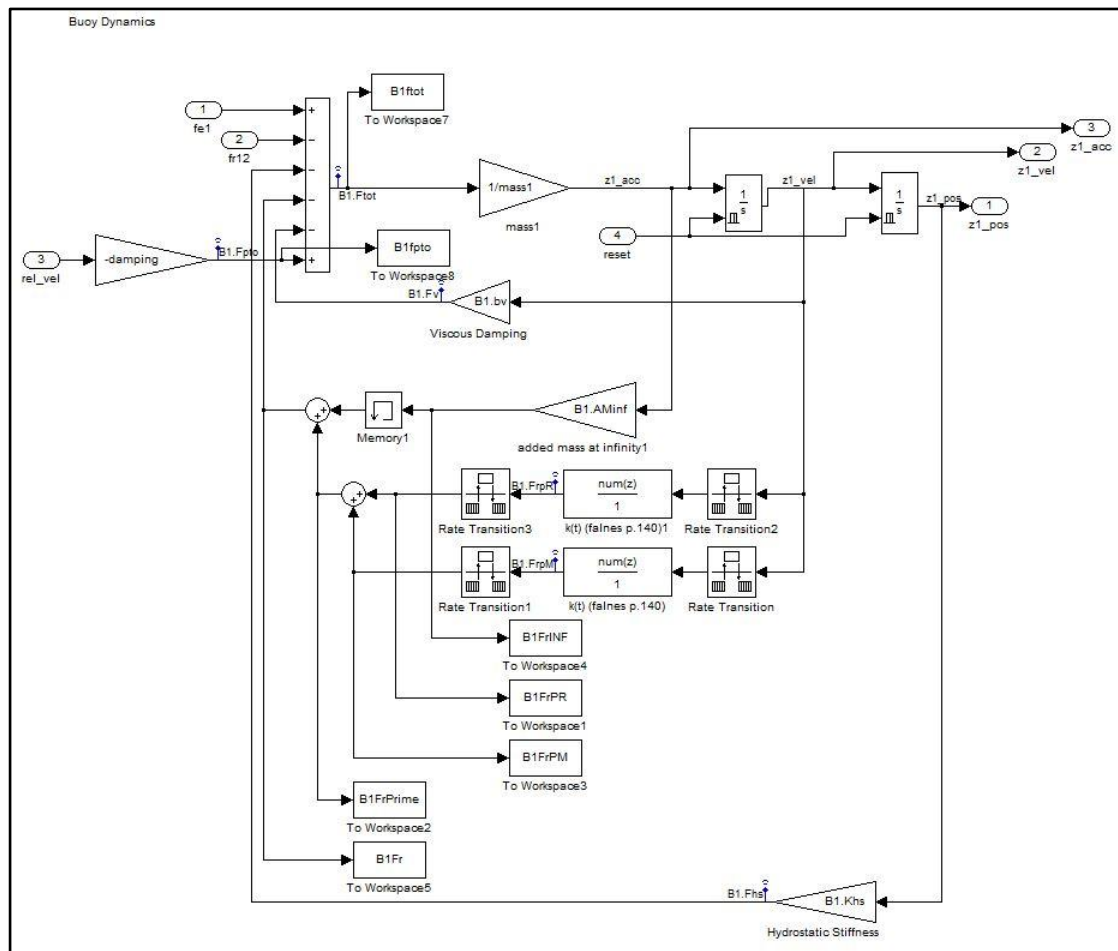
A frequency-domain approach to simulating wave energy converter
hydrodynamics

6.2.3 WEC Dynamics



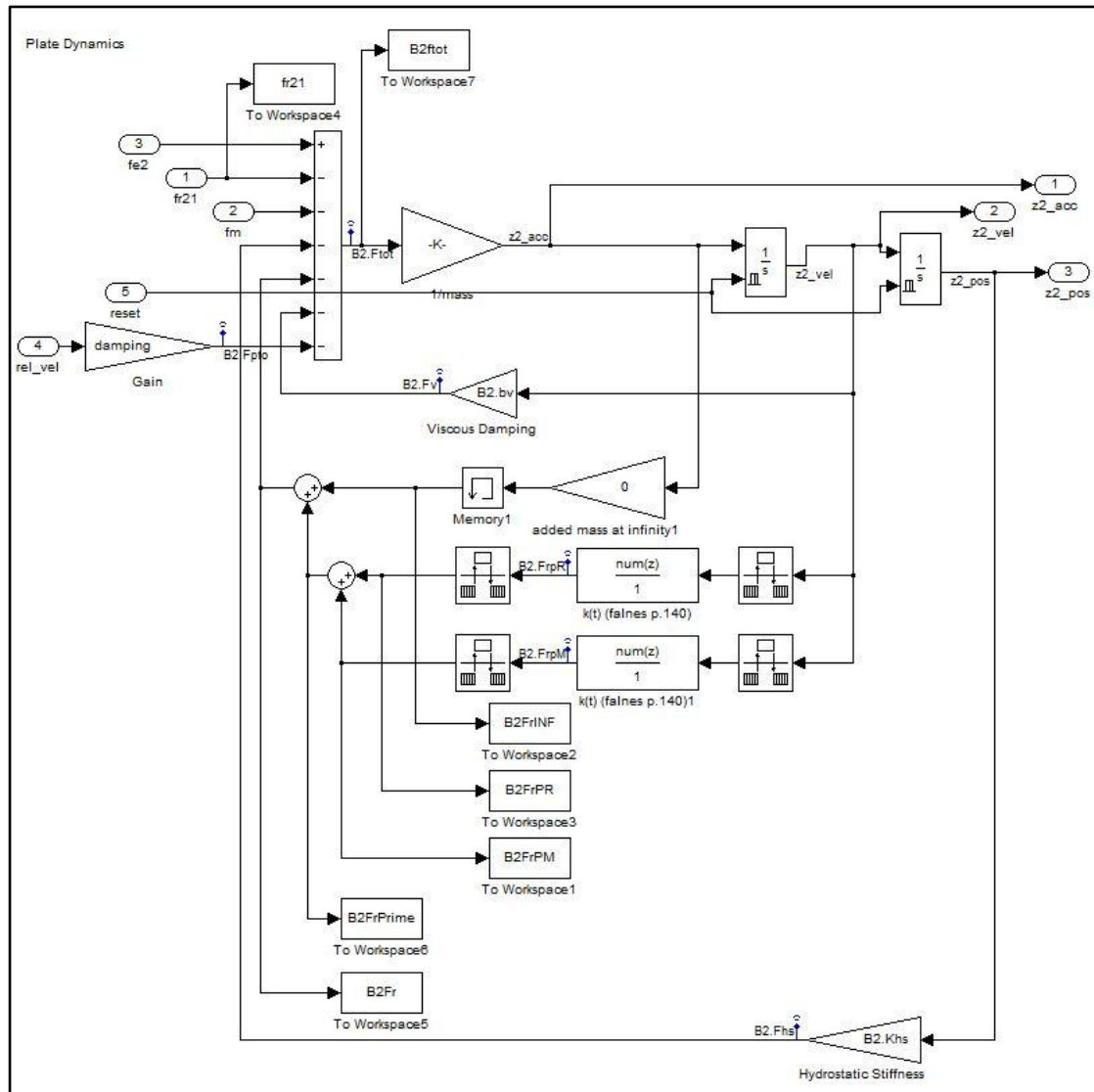
A frequency-domain approach to simulating wave energy converter
hydrodynamics

6.2.4 Body 1 Dynamics



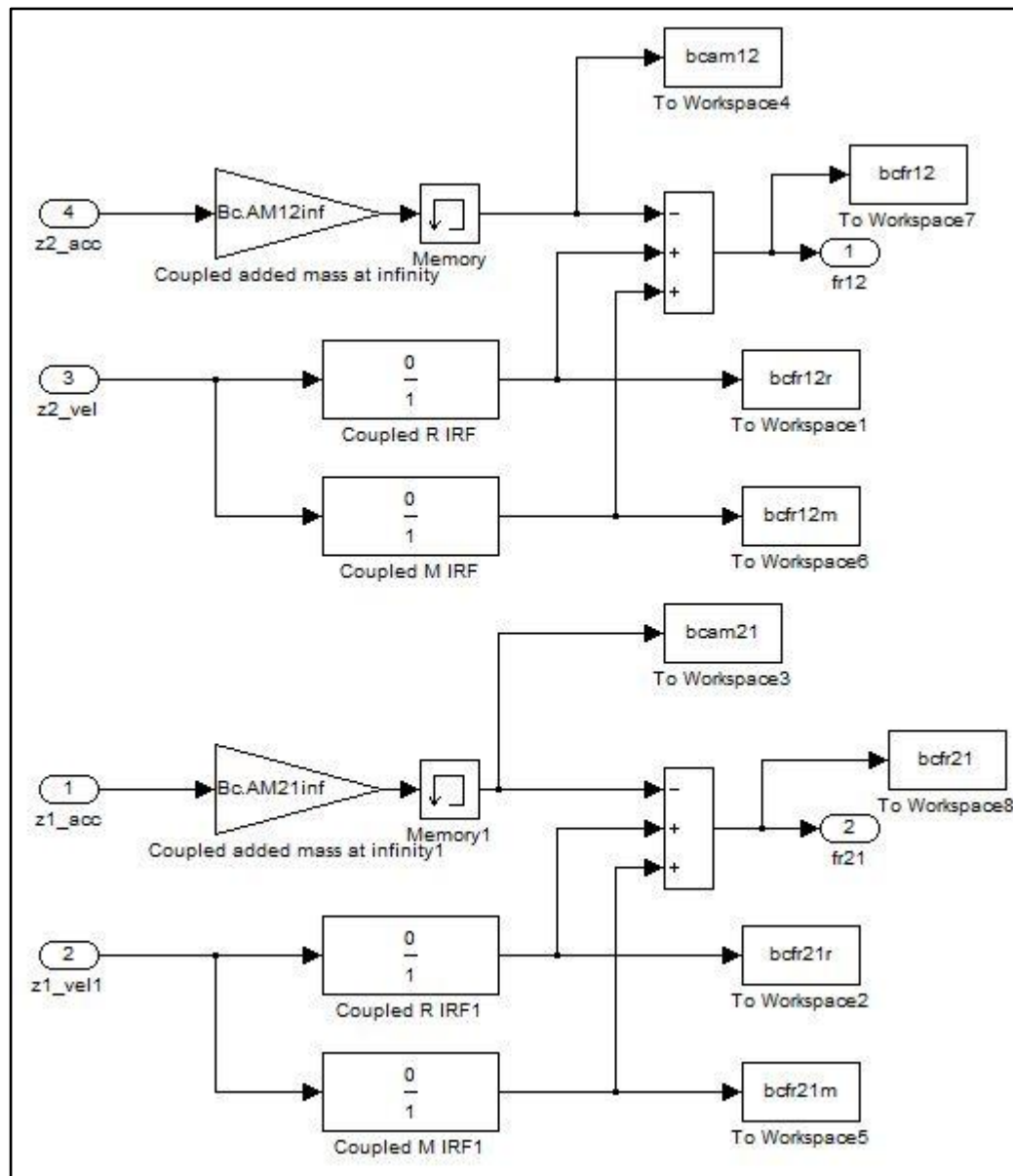
A frequency-domain approach to simulating wave energy converter
hydrodynamics

6.2.5 Body 2 Dynamics



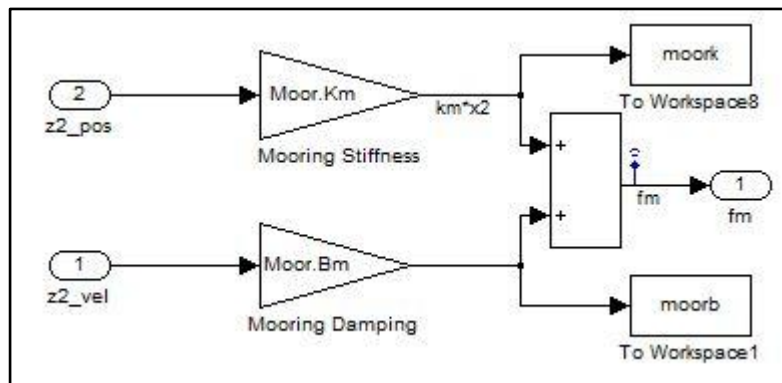
A frequency-domain approach to simulating wave energy converter
hydrodynamics

6.2.6 Coupling



A frequency-domain approach to simulating wave energy converter hydrodynamics

6.2.7 Mooring



A frequency-domain approach to simulating wave energy converter
hydrodynamics

7 Appendix B: Frequency-Domain Model

7.1 Model Derivation

A frequency-domain approach to simulating wave energy converter
hydrodynamics

Equation of Motion (EoM) matches PA-2B-H revision for heave (\dot{z}) direction only. EoM is the sum of forces as functions of time

Body 1 EoM

$$(\text{mass})(\text{acceleration}) = \sum_{\text{all}} f_i(t) = \text{Exitation} - (\text{body 1-2}) - \text{hydrostatic} - \text{radiation} - \text{viscous} + (\text{power take-off})$$

$$(\text{mass})(\dot{z}_1-\text{acc}) = f_{e1} - f_{r12} - f_{ns1} - f_n - f_{v1} + f_{p101} \quad 1$$

where

$$f_{e1} = \text{eta} * [\text{delta t}] \text{B1.f1r Coeff Caus} + \text{B1.e1r prime} * [\text{delta t}] \text{B1.f1r Coeff NonCaus}$$

$$= \text{eta} * \text{B1.f1r.f1H}$$

$$f_{r12} = [(\dot{z}_2 - \text{vel}) \text{B2.AM12.inf}] + (\dot{z}_2 - \text{vel}) * \text{B2.z} \quad 2$$

$$f_{ns1} = [(\dot{z}_1 - \text{pos}) \text{B1.Kns}] u(t) \quad 4$$

$$f_n = [(\dot{z}_1 - \text{vel}) * \text{B1.z}] u(t) \quad 5$$

$$f_{v1} = [(\dot{z}_1 - \text{vel}) \text{B1.bv}] u(t) \quad 6$$

$$f_{p101} = [(\text{rel.vel}) (-\text{damping})] u(t) \quad 7$$

$$= [(\dot{z}_1 - \text{vel}) - \text{eq.vel}] (-\text{damping}) u(t) \quad 8$$

$$= [(\dot{z}_2 - \text{vel}) - \text{z1.vel}] \text{damping} u(t)$$

Substitute EQ 2-7 into EQ 1

$$(\text{mass})(\dot{z}_1 - \text{acc}) = \text{eta} * \text{B1.f1r.f1H} + \{ (+)[(\dot{z}_2 - \text{acc}) \text{B2.AM12.inf}] + (\dot{z}_2 - \text{vel}) * \text{B2.z} \} - (\dot{z}_1 - \text{pos}) \text{B1.Kns}$$

$$- (\dot{z}_1 - \text{vel}) * \text{B1.z} - (\dot{z}_1 - \text{vel}) \text{B1.bv} + (\dot{z}_2 - \text{vel}) \text{damping} - (\dot{z}_1 - \text{vel}) \text{damping} \} u(t) \quad 8$$

A frequency-domain approach to simulating wave energy converter
hydrodynamics

According to Linear Systems Theory, the output waveform of a linear system will have the same shape and frequency as the input waveform. For this system, the input waveform is described by Svendsen, pg 114, eq 34.36 as:

$$\eta_{in}(t) = \sum_{n=1}^{\infty} A_n \cos(\omega_n t + \phi_n); \quad \omega_n = 2\pi f_n \Rightarrow \eta_{in}(t) = \sum_{n=1}^{\infty} A_n \cos(2\pi f_n t + \phi_n)$$

The acceleration output of the system can be described in a similar manner:

$$\ddot{z}_B \text{acc}(t) = \sum_{n=1}^{\infty} z_B^n \cos(2\pi f_n t + z_B \phi_n)$$

10

The system input is non-causal, so the cosine in (9) is ideal.

The system output is causal, so the cosine function in (10) is modified by the unit step function, $u(t)$. This results in a right-sided cosine.

A frequency-domain approach to simulating wave energy converter
hydrodynamics

Rewrite (8) isolating z_1 terms to left side of the equation:

$$(mass)(z_1\text{-acc})u(t) + (B_1)K_{ns}(z_1\text{-pos})u(t) + [z_1\text{-vel})u(t)] * B_1.z + [z_1\text{-vel})u(t)] B_1.b_n$$

+ $(z_1\text{-vel})u(t)$ damping

$$= c_{ta} * B_1.f_e \int_0^t u(t) dt - (z_2\text{-acc})u(t)B_2.Am12inf$$

$$- [z_2\text{-vel})u(t)] * B_2.z + (z_2\text{-vel})u(t) damping$$

Write velocity and position terms as functions of acceleration terms:

$$\begin{aligned} (z_2\text{-vel})u(t) &= \int (z_2\text{-acc})u(t) dt = \int_{-\infty}^{\infty} z_2 B_n \cos(2\pi f_n t + z_2 s_n) u(t) dt \\ &= \sum_{n=1}^{\infty} z_2 B_n \left[\int_{-\infty}^0 \cos(2\pi f_n t + z_2 s_n) dt + \int_0^{\infty} \cos(2\pi f_n t + z_2 s_n) dt \right] \\ &= \sum_{n=1}^{\infty} z_2 B_n \left[\frac{1}{2\pi f_n} \right] \sin(2\pi f_n t + z_2 s_n) + C_B V_n \end{aligned}$$

12

$$\begin{aligned} (z_2\text{-pos})u(t) &= \int (z_2\text{-vel})u(t) dt \\ &= \int_{-\infty}^{\infty} z_2 B_n \left[\frac{1}{2\pi f_n} \right] \sin(2\pi f_n t + z_2 s_n) + C_B V_n u(t) dt \\ &= \sum_{n=1}^{\infty} z_2 B_n \left[\int_{-\infty}^0 \frac{1}{2\pi f_n} dt + \left(\frac{1}{2\pi f_n} \right) \int_0^{\infty} \sin(2\pi f_n t + z_2 s_n) dt + C_B V_n \int_0^{\infty} dt \right] \\ &= \sum_{n=1}^{\infty} z_2 B_n \left[\frac{-1}{2\pi f_n} \cos(2\pi f_n t + z_2 s_n) + C_B V_n t + C_B P_n \right] u(t) \end{aligned}$$

13

3

9/22

9/7

A frequency-domain approach to simulating wave energy converter
hydrodynamics

Substitute (10, 12, 13) into (11)

8/22
9/4

$$\begin{aligned}
 & \sum_{n=1}^{\infty} z_{1n} \left[(\text{Mass}_1) \cos(2\pi f_n t + 21\delta_n) u(t) + [B1, K] \cos\left(\frac{-1}{(2\pi f_n)^2} \cos(2\pi f_n t + 21\delta_n) + C1 V_n t + C1 P_n\right) u(t) \right. \\
 & \quad \left. + \left[\frac{1}{2\pi f_n}\right] \sin(2\pi f_n t + 21\delta_n) + C1 V_n\right] u(t) * B1, z \\
 & + [B1, bV + \text{damping}] \left[\left[\frac{1}{2\pi f_n}\right] \sin(2\pi f_n t + 21\delta_n) + C1 V_n \right] u(t) \\
 & = \\
 & \sum_{n=1}^{\infty} A_n \cos(2\pi f_n t + \delta_n) * B1, f_e - f_1 t \\
 & - \sum_{n=1}^{\infty} z_{2n} \left[(B2, AM1, Z1, m) \cos(2\pi f_n t + 22\delta_n) u(t) + \left[\frac{1}{2\pi f_n}\right] \sin(2\pi f_n t + 22\delta_n) + C2 V_n\right] u(t) * B2, z \\
 & - \text{damping} \left[\left[\frac{1}{2\pi f_n}\right] \sin(2\pi f_n t + 22\delta_n) + C2 V_n \right] u(t)
 \end{aligned}$$

14

A frequency-domain approach to simulating wave energy converter
hydrodynamics

Convert (14) from Time-domain to Frequency-domain with
a Fourier Transform.

$$\begin{aligned}
 & \sum_{n=1}^{\infty} z_n \left[(\text{mass}) \mathcal{F} \{ \cos(2\pi f_n t + 2j\delta_n) u(t) \} - \frac{B_1 K_{ns}}{(2\pi f_n)^2} \mathcal{F} \{ \cos(2\pi f_n t + 2j\delta_n) u(t) \} \right. \\
 & + (B_1 K_{ns}) (C_1 V_n) \mathcal{F} \{ t u(t) \} + (B_1 K_{ns}) (C_1 R_n) \mathcal{F} \{ u(t) \} \\
 & + \left[\left(\frac{1}{2\pi f_n} \right) \mathcal{F} \{ \sin(2\pi f_n t + 2j\delta_n) u(t) \} + C_1 V_n \mathcal{F} \{ u(t) \} \right] \# \{ B_1 \cdot z \} \\
 & + \left. \left(\frac{B_1 b_n + \text{damping}}{2\pi f_n} \mathcal{F} \{ \sin(2\pi f_n t + 2j\delta_n) u(t) \} + (B_1 b_n + \text{damping})(C_1 V_n) \mathcal{F} \{ u(t) \} \right) \right] \\
 & = \sum_{n=1}^{\infty} A_n \mathcal{F} \{ \cos(2\pi f_n t + \delta_n) \} \mathcal{F} \{ B_1 \cdot f_n \cdot f_1 \cdot z \} \\
 & - \sum_{n=1}^{\infty} z_n \left[(B_1 A M_1 / 2 \pi f_n) \mathcal{F} \{ \cos(2\pi f_n t + 22\delta_n) u(t) \} \right. \\
 & + \left. \left[\left(\frac{1}{2\pi f_n} \right) \mathcal{F} \{ \sin(2\pi f_n t + 22\delta_n) u(t) \} + (C_2 V_n) \mathcal{F} \{ u(t) \} \right] \# \{ B_1 \cdot z \} \right] \\
 & - \text{damping} \left[\left(\frac{1}{2\pi f_n} \right) \mathcal{F} \{ \sin(2\pi f_n t + 22\delta_n) u(t) \} + (C_2 V_n) \mathcal{F} \{ u(t) \} \right]
 \end{aligned}$$

8/22

9/2

5

A frequency-domain approach to simulating wave energy converter
hydrodynamics

$$\begin{aligned}
 & \mathcal{F} \left\{ \cos(2\pi f_0 t) \right\} = \frac{1}{2} \left[S(f + f_0) + S(f - f_0) \right] \quad \text{Loftus \& Ding, 107} \\
 & \mathcal{F} \left\{ \sin(2\pi f_0 t) \right\} = \frac{1}{2} (i) \left[S(f + f_0) - S(f - f_0) \right] \\
 & \mathcal{F} \left\{ \cos(2\pi f_0 t) u(t) \right\} = \frac{1}{4} \left[S(f - f_0) + S(f + f_0) \right] + \frac{i 2\pi f}{(2\pi f_0)^2 - (2\pi f)^2} \\
 & \mathcal{F} \left\{ \sin(2\pi f_0 t) u(t) \right\} = \left(\frac{1}{4i} \right) \left[S(f - f_0) - S(f + f_0) \right] + \frac{2\pi f_0}{(2\pi f_0)^2 - (2\pi f)^2} \\
 & \mathcal{F} \left\{ \cos(2\pi f_0 t + \alpha_n) \right\} = \mathcal{F} \left\{ \cos(2\pi f_0 t) \cos(\alpha_n) - \sin(2\pi f_0 t) \sin(\alpha_n) \right\} \\
 & = \cos(\alpha_n) \mathcal{F} \left\{ \cos(2\pi f_0 t) \right\} - \sin(\alpha_n) \mathcal{F} \left\{ \sin(2\pi f_0 t) \right\} \\
 & = \frac{\cos(\alpha_n)}{2} \left[S(f + f_0) + S(f - f_0) \right] - \frac{i \sin(\alpha_n)}{2} \left[S(f + f_0) - S(f - f_0) \right] \quad \text{Anton, 112} \\
 & \mathcal{F} \left\{ \cos(2\pi f_0 t + \alpha_n) u(t) \right\} = \mathcal{F} \left\{ \cos(2\pi f_0 t) \cos(\alpha_n) u(t) \right\} - \mathcal{F} \left\{ \sin(2\pi f_0 t) \sin(\alpha_n) u(t) \right\} \\
 & = \cos(\alpha_n) \mathcal{F} \left\{ \cos(2\pi f_0 t) u(t) \right\} - \sin(\alpha_n) \mathcal{F} \left\{ \sin(2\pi f_0 t) u(t) \right\} \\
 & = \cos(\alpha_n) \left[\frac{1}{4} \left(S(f - f_0) + S(f + f_0) \right) + \frac{i 2\pi f}{(2\pi f_0)^2 - (2\pi f)^2} \right] \\
 & \quad - \sin(\alpha_n) \left[\frac{1}{4} \left(S(f - f_0) - S(f + f_0) \right) + \frac{2\pi f_0}{(2\pi f_0)^2 - (2\pi f)^2} \right] \quad \text{Loftus \& Ding, 107}
 \end{aligned}$$

18

Loftus \& Ding, 107

16

8/25
9/4

A frequency-domain approach to simulating wave energy converter
hydrodynamics

$$\mathcal{F} \left\{ \sin(2\pi f_0 t + \phi_n) u(t) \right\} = \mathcal{F} \left\{ \sin(2\pi f_0 t) \cos(\phi_n) u(t) \right\} + \mathcal{F} \left\{ \cos(2\pi f_0 t) \sin(\phi_n) u(t) \right\}$$

8/25 9/12
Andon, 4/12

$$= \cos(\phi_n) \left[\left(\frac{1}{i\pi} (\delta(f-f_0) - \delta(f+f_0)) \right) + \frac{2\pi f_0}{(2\pi f_0)^2 - (2\pi f)^2} \right] \\ + \sin(\phi_n) \left[\left(\frac{1}{i\pi} (\delta(f-f_0) + \delta(f+f_0)) \right) + \frac{i2\pi f}{(2\pi f_0)^2 - (2\pi f)^2} \right]$$

Lat. & Ding, 10/7
19

$$\mathcal{F} \left\{ x^n h(x), n=0,1,\dots \right\} = \frac{\sin(f)}{2(-2\pi i)^n} + \frac{n!}{(2\pi i f)^{n+1}}$$

where $h(x)$ is the heaviside step function.

Kammler, A-6

20

$$\therefore \mathcal{F} \left\{ t u(t) \right\} = \frac{\mathcal{S}'(f)}{2(-2\pi i)^1} + \frac{1!}{(2\pi i f)^{1+1}} = \frac{(+1)(+i)\mathcal{S}'(f)}{4\pi} + \frac{1}{-1(2\pi f)^2}$$

21

$$= \frac{\mathcal{S}'(f)}{4\pi} - \frac{1}{(2\pi f)^2}$$

Lat. & Ding, 10/7

22

$$\text{And } \mathcal{F} \left\{ u(t) \right\} = \frac{\mathcal{S}(f)}{2} - \frac{i}{2\pi f}$$

A frequency-domain approach to simulating wave energy converter
hydrodynamics

Finally, define the transforms of the forces that are time-domain functions.

8/25
9/7

$$\mathcal{F} \left\{ B\beta \cdot f_{e-f_H}(t) \right\} = B\beta \cdot F_e$$

$$\mathcal{F} \left\{ B\beta \cdot f_{r-f_H}(t) \right\} = B\beta \cdot F_r$$

where β represents the body number (1,2) or the body-body coupling (c)

These forces are output of hydrodynamic modeling software. They are delivered in a table format, with one constant per frequency. The constant is complex

24

23

A frequency-domain approach to simulating wave energy converter
hydrodynamics

Rewrite (15), grouping constants and like terms.

$$\begin{aligned}
 & \sum_{n=1}^{\infty} zl_n \left[\frac{(\text{mass})}{(2\pi f_n)^2} \right] \cos(2\pi f_n t + 21\delta_n) u(t) + (B1.K_{ns})(C1V_n) \cancel{\int t \cdot u(t)} + (B1.K_{ns})(C1P_n) \cancel{\int u(t)} \\
 & + \sum_{n=1}^{\infty} zl_n \left[\left(\frac{1}{2\pi f_n} \right) \cancel{\int} \sin(2\pi f_n t + 21\delta_n) u(t) \right] + (C1V_n) \cancel{\int u(t)} + [B1.z] \\
 & + \sum_{n=1}^{\infty} zl_n \left[(B1.bv + \text{damping}) \left(\frac{1}{2\pi f_n} \right) \cancel{\int} \sin(2\pi f_n t + 21\delta_n) u(t) \right] + (B1.bv + \text{damping}) C1V_n \cancel{\int u(t)} \\
 & = \sum_{n=1}^{\infty} A_n \cancel{\int} \cos(2\pi f_n t + \delta_n) \cancel{\int} B1.f_{c-n} f_{1t} \\
 & - \sum_{n=1}^{\infty} zl_n (B1.Am)(2\pi f_n) \cancel{\int} \cos(2\pi f_n t + 22\delta_n) u(t) \\
 & - \sum_{n=1}^{\infty} zl_n \left[\left(\frac{1}{2\pi f_n} \right) \cancel{\int} \sin(2\pi f_n t + 22\delta_n) u(t) \right] + (C2V_n) \cancel{\int u(t)} + [B2.c.z]
 \end{aligned}$$

A frequency-domain approach to simulating wave energy converter
hydrodynamics

Substitute $(16 - 24)$ into 25

$$\begin{aligned}
 & \sum_{n=1}^{\infty} Z_n \left\{ \left[\text{mass} - \frac{B1.Khs}{(2\pi f_n)^2} \right] \cos(2f_n s_n) \left[\frac{1}{4} \left(\delta(f-f_n) + \delta(f+f_n) \right) + \frac{i 2\pi f}{(2\pi f_n)^2 - (2\pi f)^2} \right] \right. \\
 & - \left(\text{mass} - \frac{B1.Khs}{(2\pi f_n)^2} \right) \sin(2f_n s_n) \left[\frac{1}{4i} \left(\delta(f-f_n) - \delta(f+f_n) \right) + \frac{2\pi f_n}{(2\pi f_n)^2 - (2\pi f)^2} \right] \\
 & + (B1.Kns) C1 V_n \left(\frac{s'_n f}{2\pi} - \frac{i}{2\pi f} \right) + (B1.Kns) C1 P_n \left(\frac{\delta f_n}{2} - \frac{i}{2\pi f} \right) \} \\
 & + \sum_{n=1}^{\infty} Z_n \left\{ \left(\frac{1}{2\pi f_n} \right) \cos(2f_n s_n) \left[\frac{1}{4i} \left(\delta(f-f_n) - \delta(f+f_n) \right) + \frac{2\pi f_n}{(2\pi f_n)^2 - (2\pi f)^2} \right] \right. \\
 & + \left(\frac{1}{2\pi f_n} \right) \sin(2f_n s_n) \left[\frac{1}{4} \left(\delta(f-f_n) + \delta(f+f_n) \right) + \frac{i 2\pi f}{(2\pi f_n)^2 - (2\pi f)^2} \right] - \\
 & \left. + (C1 V_n) \left(\frac{\delta f_n}{2} - \frac{i}{2\pi f} \right) \right\} B1 \cdot Z_n \\
 & + \sum_{n=1}^{\infty} Z_n \left\{ (B1.bv + \text{damping}) \left(\frac{1}{2\pi f_n} \right) \cos(2f_n s_n) \left[\frac{1}{4i} \left(\delta(f-f_n) - \delta(f+f_n) \right) + \frac{2\pi f_n}{(2\pi f_n)^2 - (2\pi f)^2} \right] \right. \\
 & + (B1.bv + \text{damping}) \left(\frac{1}{2\pi f_n} \right) \sin(2f_n s_n) \left[\frac{1}{4} \left(\delta(f-f_n) + \delta(f+f_n) \right) + \frac{i 2\pi f}{(2\pi f_n)^2 - (2\pi f)^2} \right] \\
 & \left. + (B1.bv + \text{damping}) C1 V_n \left(\frac{\delta f_n}{2} - \frac{i}{2\pi f} \right) \right\}
 \end{aligned}$$

Continued

A frequency-domain approach to simulating wave energy converter
hydrodynamics

Continued

11
9/2

$$\begin{aligned}
 &= \sum_{n=1}^{\infty} A_n \left(\frac{1}{2} \right) \cos(\delta_n) \left[S(f+f_n) + S(f-f_n) \right] B_{L,FE,n} - i \sum_{n=1}^{\infty} A_n \left(\frac{1}{2} \right) \sin(\delta_n) \left[S(f+f_n) - S(f-f_n) \right] B_{L,FE,n} \\
 &\quad - \sum_{n=1}^{\infty} 2\alpha_n \left\{ \beta_c \cdot AMR_{inf} \cos(2\delta_n) \left[\frac{1}{4} \left(S(f-f_n) + S(f+f_n) \right) + \frac{i(2\pi f)}{(2\pi f_n)^2 - (2\pi f)^2} \right] \right. \\
 &\quad \left. - (\beta_c \cdot AMR_{inf}) \sin(2\delta_n) \left[\frac{1}{4i} \left(S(f-f_n) - S(f+f_n) \right) + \frac{2\pi f_n}{(2\pi f_n)^2 - (2\pi f)^2} \right] \right\} \\
 &\quad - \sum_{n=1}^{\infty} 2\alpha_n \left\{ \left(\frac{1}{2\pi f_n} \right) \cos(2\delta_n) \left[\frac{1}{4i} \left(S(f-f_n) - S(f+f_n) \right) + \frac{2\pi f_n}{(2\pi f_n)^2 - (2\pi f)^2} \right] \right. \\
 &\quad \left. + \left(\frac{1}{2\pi f_n} \right) \sin(2\delta_n) \left[\frac{1}{4} \left(S(f-f_n) + S(f+f_n) \right) + \frac{i(2\pi f)}{(2\pi f_n)^2 - (2\pi f)^2} \right] \right. \\
 &\quad \left. + (C_d V_n) \left(\frac{S(f)}{2} - \frac{i}{2\pi f} \right) \right\} \beta_c Z \\
 &\quad + \sum_{n=1}^{\infty} 2\alpha_n (\text{damping}) \left\{ \left(\frac{1}{2\pi f_n} \right) \cos(2\delta_n) \left[\frac{1}{4i} \left(S(f-f_n) - S(f+f_n) \right) + \frac{2\pi f_n}{(2\pi f_n)^2 - (2\pi f)^2} \right] \right. \\
 &\quad \left. + \left(\frac{1}{2\pi f_n} \right) \sin(2\delta_n) \left[\frac{1}{4} \left(S(f-f_n) + S(f+f_n) \right) + \frac{i(2\pi f)}{(2\pi f_n)^2 - (2\pi f)^2} \right] \right. \\
 &\quad \left. + (C_d V_n) \left(\frac{S(f)}{2} - \frac{i}{2\pi f} \right) \right\}
 \end{aligned}$$

A frequency-domain approach to simulating wave energy converter
hydrodynamics

Rotational, Denominators of (26). Put all $\delta(f)$ grouped into same order: $\delta(f + f_n) \pm \delta(f - f_n)$

$$\begin{aligned}
 & \sum_{n=1}^{\infty} Z_{1n} \left\{ \left(\text{mass} \right) - \frac{\beta l K_{ns}}{(2\pi f_n)^2} \cos(2l\delta_n) \left[\frac{1}{4} \left(\delta(f + f_n) + \delta(f - f_n) \right) + \frac{i 2\pi f}{(2\pi f_n)^2 - (2\pi f)^2} \right] \right. \\
 & - \left(\text{mass} \right) - \frac{\beta l K_{ns}}{(2\pi f_n)^2} \sin(2l\delta_n) \left[\frac{1}{4} \left(\frac{i}{2} \right) (-1) \left(\delta(f + f_n) - \delta(f - f_n) \right) + \frac{2\pi f_n}{(2\pi f_n)^2 - (2\pi f)^2} \right] \\
 & + (\beta l K_{ns}) C_1 V_n \left(\frac{\delta'(t)}{4\pi} - \frac{i}{2\pi f_n} \right) + (\beta l K_{ns}) C_1 P_n \left(\frac{\delta(t)}{2} - \frac{i}{2\pi f_n} \right) \\
 & + \sum_{n=1}^{\infty} Z_{1n} (\beta l Z_n) \left\{ \left(\frac{1}{2\pi f_n} \right) \cos(2l\delta_n) \left[\frac{1}{4} \left(\frac{i}{2} \right) (-1) \left(\delta(f + f_n) - \delta(f - f_n) \right) + \frac{2\pi f_n}{(2\pi f_n)^2 - (2\pi f)^2} \right] \right. \\
 & + \left(\frac{1}{2\pi f_n} \right) \sin(2l\delta_n) \left[\frac{1}{4} \left(\delta(f + f_n) + \delta(f - f_n) \right) + \frac{i 2\pi f_n}{(2\pi f_n)^2 - (2\pi f)^2} \right] \\
 & \left. + \left(C_1 V_n \right) \left(\frac{\delta'(t)}{2} - \frac{i}{2\pi f} \right) \right\} (\beta l, b_v + \text{damping})
 \end{aligned}$$

Continued

A frequency-domain approach to simulating wave energy converter
hydrodynamics

Continued

13

9/2

$$\begin{aligned}
 &= \sum_{n=1}^{\infty} A_n (B_L, F_n) \left(\frac{1}{2} \right) \left\{ \cos(\delta_n) [S(f+f_n) + S(f-f_n)] - i \sin(\delta_n) [S(f+f_n) - S(f-f_n)] \right\} \\
 &- \sum_{n=1}^{\infty} 2Z_n (B_L, A_M, f_{ref}) \left\{ \cos(2Z_n) \left[\frac{1}{4} (S(f+f_n) + S(f-f_n)) + \frac{i 2\pi f}{(2\pi f_n)^2 - (2\pi f)^2} \right] \right. \\
 &\quad \left. - \sin(2Z_n) \left[\frac{1}{4} (S(f+f_n) - S(f-f_n)) + \frac{2\pi f_n}{(2\pi f_n)^2 - (2\pi f)^2} \right] \right\} \\
 &- \sum_{n=1}^{\infty} 2Z_n \left\{ \left(\frac{1}{2\pi f_n} \right) \cos(2Z_n) \left[\frac{1}{4} \left(\frac{f}{f_n} \right) (-1) (S(f+f_n) - S(f-f_n)) + \frac{i 2\pi f_n}{(2\pi f_n)^2 - (2\pi f)^2} \right] \right. \\
 &\quad \left. + \left(\frac{1}{2\pi f_n} \right) \sin(2Z_n) \left[\left(\frac{f}{f_n} \right) (S(f+f_n) - S(f-f_n)) + \frac{i 2\pi f}{(2\pi f_n)^2 - (2\pi f)^2} \right] \right. \\
 &\quad \left. + (C_D V_n) \left(\frac{S(f)}{2} - \frac{i}{2\pi f} \right) \right\} (B_L, Z_n - \text{damping})
 \end{aligned}$$

24

Define variables for coefficients of (27): (COM number) (Term # in order of appearance)

$$C_0 A = \frac{\text{mass}}{\text{mass}} - \frac{B_L K_{hs}}{(2\pi f_n)^2}$$

$$C_0 D = \frac{B_L Z_n - \text{damping}}{2\pi f_n}$$

$$C_0 B = \frac{B_L Z_n + B_L b_{hv} + \text{damping}}{2\pi f_n}$$

$$C_0 E = B_L Z_n - \text{damping}$$

$$C_0 C = B_L Z_n + B_L b_{hv} + \text{damping}$$

A frequency-domain approach to simulating wave energy converter
hydrodynamics

Substitute (28 A-E) into (27)

$$\begin{aligned}
 & \sum_{n=1}^{\infty} (\bar{z}_n)(C_0)A \left\{ \cos(2\pi f_n) \left[\frac{1}{4} (\delta(f+f_n) + \delta(f-f_n)) + \frac{i 2\pi f}{(2\pi f_n)^2 - (2\pi f)^2} \right] \right. \\
 & \quad \left. - \sin(2\pi f_n) \left[\left(\frac{1}{4}\right) i (\delta(f+f_n) - \delta(f-f_n)) + \frac{2\pi f_n}{(2\pi f_n)^2 - (2\pi f)^2} \right] \right\} + B_1 K_{ns} \sum_{n=1}^{\infty} (C_n V_n) \\
 & \quad + B_1 K_{ns} \sum_{n=1}^{\infty} 2k_n \left[C_n V_n \left(\frac{\delta'(f)}{4\pi} - \frac{i}{(2\pi f)^2} \right) + C_1 P_n \left(\frac{\delta(f)}{2} - \frac{i}{2\pi f} \right) \right] \\
 & + \sum_{n=1}^{\infty} (\bar{z}_n)(C_0)B \left\{ \cos(2\pi f_n) \left[\frac{1}{4} i (\delta(f+f_n) - \delta(f-f_n)) + \frac{2\pi f_n}{(2\pi f_n)^2 - (2\pi f)^2} \right] \right. \\
 & \quad \left. + \sin(2\pi f_n) \left[\left(\frac{1}{4}\right) i (\delta(f+f_n) + \delta(f-f_n)) + \frac{i 2\pi f}{(2\pi f_n)^2 - (2\pi f)^2} \right] \right\}
 \end{aligned}$$

Continued.

A frequency-domain approach to simulating wave energy converter
hydrodynamics

Continued

$$\begin{aligned}
 &= \sum_{n=1}^{\infty} (A_n) (B_{1,F,E_n}) \left(\frac{1}{2}\right) \left\{ \cos(f_n) [S(f+f_n) + S(f-f_n)] - i \sin(f_n) [S(f+f_n) - S(f-f_n)] \right\} \\
 &- \sum_{n=1}^{\infty} (22_n) (B_{2,A,M,I2,n,f}) \left\{ \cos(22_n) \left[\frac{i}{4} (\delta(f+f_n) + \delta(f-f_n)) + \frac{i 2\pi f}{(2\pi f_n)^2 - (2\pi f)^2} \right] \right. \\
 &\quad \left. - \sin(22_n) \left[\left(\frac{i}{4} \right) \left(\frac{i}{4} \right) \left(\delta(f+f_n) - \delta(f-f_n) \right) \right] + \frac{2\pi f_n}{(2\pi f_n)^2 - (2\pi f)^2} \right\} \\
 &- \sum_{n=1}^{\infty} (22_n) (C_{0,1,D}) \left\{ \cos(22_n) \left[\left(\frac{i}{4} \right) \left(\frac{i}{4} \right) \left(\delta(f+f_n) - \delta(f-f_n) \right) + \frac{2\pi f_n}{(2\pi f_n)^2 - (2\pi f)^2} \right] \right. \\
 &\quad \left. + \sin(22_n) \left[\left(\frac{i}{4} \right) \left(\frac{i}{4} \right) \left(\delta(f+f_n) + \delta(f-f_n) \right) + \frac{i 2\pi f}{(2\pi f_n)^2 - (2\pi f)^2} \right] \right\} \\
 &- \sum_{n=1}^{\infty} (22_n) (C_{0,1,E}) (22_n) \left(\frac{df}{2} \right) - \frac{i}{2\pi f}
 \end{aligned}$$

29

Drop summation sign. Keep 'n' subscript as summation reminder.

Separate (29) into 4 equations:

1. $f = -f_n$
2. $f = f_n$
3. $f = 0$

4. $-\infty \leq f \leq \infty$

15

9/2

A frequency-domain approach to simulating wave energy converter
hydrodynamics

$$f = -f_n \int \delta(f + f_n) \cdot$$

16 7/2

$$(21_n)(C_0 A) \left[\frac{1}{4} \right] \cos(21\omega_n) - i \sin(21\omega_n) \delta(f + f_n) + (21_n)(C_0 B) \left[\frac{1}{4} \right] i \cos(21\omega_n) + \sin(21\omega_n) \delta(f + f_n)$$

$$= (A_n)(B1.FE_n) \left[\frac{1}{2} \right] \cos(\omega_n) - i \sin(\omega_n) \delta(f + f_n) -$$

$$- (22_n)(Bc.Am12.inf) \left[\frac{1}{4} \right] \cos(22\omega_n) - i \sin(22\omega_n) \delta(f + f_n)$$

$$- (22_n)(C_0 D) \left[\frac{1}{4} \right] [i \cos(22\omega_n) + \sin(22\omega_n)] \delta(f + f_n)$$

30

$$\text{now } \cos \alpha - i \sin \alpha = \cos(\omega) + i \sin(-\omega) = \cos(-\alpha) + i \sin(-\alpha) = \exp(-i\omega)$$

$$i \cos \alpha + \sin \alpha = i \cos(\omega) + (i)(i)(-1) \sin(\omega) = i(\cos \alpha + i \sin(-\omega)) = i(\cos \alpha + i \sin(\omega)) = i \exp(i\omega)$$

Substitute 31a-b into 30. Multiply 30 by 4

$$(21_n)(C_0 A) \left[\frac{1}{4} \right]^1 \exp(-i21\omega_n) \delta(f + f_n) + (21_n)(C_0 B) \left[\frac{1}{4} \right]^1 i \exp(-i21\omega_n) \delta(f + f_n)$$

$$= A_n(B1.FE_n) \left[\frac{1}{2} \right]^2 \exp(-i\omega_n) \delta(f + f_n) - 22_n(Bc.Am12.inf) \left[\frac{1}{4} \right]^1 \exp(-i22\omega_n) \delta(f + f_n) - (22_n)(C_0 D) \left[\frac{1}{4} \right]^1 \exp(-i22\omega_n) \delta(f + f_n)$$

32

Factor Main Variables

$$(21_n) \exp(-i21\omega_n) \delta(f + f_n) [C_0 A + i C_0 B] =$$

$$= (A_n) \exp(-i\omega_n) \delta(f + f_n) (B1.FE_n) (2)$$

33

A frequency-domain approach to simulating wave energy converter
hydrodynamics

$$f = -\int_n f \delta(f + f_n)$$

16 7/2

$$\begin{aligned}
 & (21_n)(C_0 A) \left[\frac{1}{4} \right] [\cos(21\omega_n) - i \sin(21\omega_n)] \delta(f + f_n) + (21_n)(C_0 B) \left[\frac{1}{4} \right] [i \cos(21\omega_n) + \sin(21\omega_n)] \delta(f + f_n) \\
 & = (A_n)(B1.FE_n) \left[\frac{1}{2} \right] [\cos(\omega_n) - i \sin(\omega_n)] \delta(f + f_n) - \\
 & - (22_n)(Bc.Am12.inf) \left[\frac{1}{4} \right] [\cos(21\omega_n) - i \sin(21\omega_n)] \delta(f + f_n) \\
 & - (22_n)(C_0 D) \left[\frac{1}{4} \right] [i \cos(22\omega_n) + \sin(22\omega_n)] \delta(f + f_n)
 \end{aligned}$$

30

$$\begin{aligned}
 \text{now } \cos \alpha - i \sin \alpha &= \cos(\omega) + i \sin(-\omega) = \cos(-\omega) + i \sin(-\omega) = \exp(-i\omega) \\
 \cos \omega + \sin \omega &= i \cos(\omega) + (i)(i)(-1) \sin(\omega) = i(\cos(\omega) + i \sin(-\omega)) = i \exp(i\omega)
 \end{aligned}$$

\hookrightarrow best write $31.a-b$ into 30. Multiply 30 by 4

$$\begin{aligned}
 & (21_n)(C_0 A) \left[\frac{1}{4} \right]^1 \exp(-i21\omega_n) \delta(f + f_n) + (21_n)(C_0 B) \left[\frac{1}{4} \right]^1 (i) \exp(-i21\omega_n) \delta(f + f_n) \\
 & = A_n(B1.FE_n) \left[\frac{1}{2} \right]^2 \exp(-i\omega_n) \delta(f + f_n) \\
 & - 22_n(Bc.Am12.inf) \left[\frac{1}{4} \right]^1 \exp(-i22\omega_n) \delta(f + f_n) - (22_n)(C_0 D) \left[\frac{1}{4} \right]^1 \exp(-i22\omega_n) \delta(f + f_n)
 \end{aligned}$$

31.a-b

$$\begin{aligned}
 & (Z1_n) \exp(-i21\omega_n) \delta(f + f_n) [C_0 A + i C_0 B] = \\
 & = (A_n) \exp(-i\omega_n) \delta(f + f_n) (B1.FE_n) (2) \\
 & - (22_n) \exp(-i22\omega_n) \delta(f + f_n) [Bc.Am12.inf + i C_0 D]
 \end{aligned}$$

32

33

Factor Main Variables

A frequency-domain approach to simulating wave energy converter
hydrodynamics

Use sinusoid identities to convert to exponential form
 $\cos\alpha + i\sin\alpha = \exp(i\alpha)$

$$(-1)(i)\cos\alpha + \sin\alpha = (-1)i\cos\alpha + (i)(i)(-1)\sin\alpha = -i[\cos\alpha + i\sin\alpha] = -i\exp(i\alpha)$$

Substitute $(34_{a,b})$ into (36)

$$\begin{aligned} & (Z_1n) \exp(iZ_1\delta_n) \delta(f-f_n) (C_0 A) + (Z_1n)(-i) \exp(iZ_1n) \delta(f-f_n) (C_0 B) \\ & = (Z_1n) \exp(i\delta_n) \delta(f-f_n) B_1 F_{E,n} - (Z_2n) \exp(iZ_2\delta_n) \delta(f-f_n) B_2 A M_1 Z_{1nf} \\ & \quad - (Z_2n)(-i) \exp(iZ_2n) \delta(f-f_n) C_0 D \end{aligned}$$

38

Factor out main variables

$$(Z_1n) \exp(iZ_1\delta_n) \delta(f-f_n) [C_0 A - iC_0 B]$$

$$= (Z_1n) \exp(i\delta_n) \delta(f-f_n) B_1 F_{E,n} - (Z_2n) \exp(iZ_2\delta_n) \delta(f-f_n) [B_2 A M_1 Z_{1nf} - iC_0 D]$$

39

Solve for $(Z_1n) \exp(iZ_1\delta_n) \delta(f-f_n)$

$$\begin{aligned} (Z_1n) \exp(iZ_1\delta_n) \delta(f-f_n) &= (Z_1n) \exp(i\delta_n) \delta(f-f_n) \frac{B_1 F_{E,n}}{C_0 A - iC_0 B} \\ & \quad - (Z_2n) \exp(iZ_2\delta_n) \delta(f-f_n) \frac{B_2 A M_1 Z_{1nf} - iC_0 D}{C_0 A - iC_0 B} \end{aligned}$$

40

A frequency-domain approach to simulating wave energy converter
hydrodynamics

Body R EqM

(mass2)Acceleration = Excitation - $\frac{(\text{body}^2 - 1)}{\text{radiation}}$ - hydrostatic - radiation - mooring - viscous - $\frac{(\text{Power} - \text{take-off})}{\text{take-off}}$

$$\text{mass2}(z2_acc) = f_{ez} - f_{rz1} - f_{ns2} - f_{rz} - f_m - f_{vz} - f_{mo2}$$

where

f_{ez}

$=$

$$= \text{eta} * \text{B2}.f_e * f_{14}$$

$$f_{rz1} = [(\bar{z1}\text{-}acc)/Bc, Amplitude] + (\bar{z1}\text{-vel}) * Bc, z u(t)$$

43

$$f_{ns2} = (z2\text{-pos})(B2.K_{ns}) u(t)$$

44

$$f_{rz} = [(z2\text{-vel}) * (B2.z)] u(t)$$

45

$$f_m = [(z2\text{-vel})(Moor.Bm) + (z2\text{-pos})(Moor.Km)] u(t)$$

46

$$f_{vz} = [(\bar{z2}\text{-vel})(B2.bv)] u(t)$$

47

$$f_{mo2} = [(\bar{z1}\text{-vel})(damping)] u(t)$$

48

$$= (\bar{z1}\text{-vel} - z2\text{-vel})(damping) u(t)$$

49

Substitute (42-49) into 41

$$(\text{mass2})(z2_acc) = \text{eta} * B2.f_e f_{14} - [(\bar{z1}\text{-acc})(Bc, Amplitude)] + (\bar{z1}\text{-vel}) * Bc, z u(t)$$

$$- (z2\text{-pos})(B2.K_{ns}) u(t) - [(\bar{z2}\text{-vel}) * (B2.z)] u(t)$$

$$- [(\bar{z2}\text{-vel})(Moor.bm) + (z2\text{-pos})(Moor.Km)] u(t) - (\bar{z2}\text{-vel})(B2.bv) u(t)$$

$$- (\bar{z1}\text{-vel} - z2\text{-vel})(damping) u(t)$$

49

19

9/9

A frequency-domain approach to simulating wave energy converter
hydrodynamics

Rewrite (49) isolating Z_2 terms to left of equation

$$\begin{aligned}
 & (\text{mass}_2)(Z_2_{\text{acc}}) + (Z_2_{\text{-pos}})(B_2, K_{ns}) u(t) + [Z_2_{\text{-vel}}] * (B_2, z) u(t) + (Z_2_{\text{-vel}})(M_{\text{oar}}, B_m) u(t) \\
 & + (Z_2_{\text{-pos}})(M_{\text{oar}}, K_m) u(t) + (Z_2_{\text{-vel}})(B_2, b_z) u(t) - (Z_2_{\text{-vel}})(\text{damping}) u(t) \\
 & = (\text{cto})(B_2, f_{e, f, l} t) - (Z_1_{\text{acc}})(B_u, A M Z_{l, \text{inf}}) u(t) \\
 & - (Z_1_{\text{-vel}}) * (B_c, z) u(t) - (Z_1_{\text{-vel}})(\text{damping}) u(t)
 \end{aligned}$$

Substitute (10, 12, 13) in 40 (50)

$$\begin{aligned}
 & (\text{mass}_2) \sum_{n=1}^{\infty} Z_2 n \cos(2\pi f_n t + Z_2 \delta_n) + \sum_{n=1}^{\infty} Z_2 n \left[\frac{-1}{(Z_m f_n)^2} \cos(2\pi f_n t + Z_2 \delta_n) + (C_2 V_n) t + (C_2 P_n) \right] (B_2, K_{ns}) u(t) \\
 & + \sum_{n=1}^{\infty} Z_2 n \left[\frac{1}{Z_m f_n} \sin(2\pi f_n t + Z_2 \delta_n) + C_2 V_n \right] u(t) * B_2, z + \sum_{n=1}^{\infty} Z_2 n \left[\frac{1}{Z_m f_n} \sin(2\pi f_n t + Z_2 \delta_n) + C_2 V_n \right] u(t) M_{\text{oar}}, B_m \\
 & + \sum_{n=1}^{\infty} Z_2 n \left[\frac{-1}{(Z_m f_n)^2} \cos(2\pi f_n t + Z_2 \delta_n) + (C_2 V_n) t + (C_2 P_n) \right] u(t) (M_{\text{oar}}, K_m) \\
 & + \sum_{n=1}^{\infty} Z_2 n \left[\frac{1}{Z_m f_n} \sin(2\pi f_n t + Z_2 \delta_n) + C_2 V_n \right] u(t) (B_2, b_z) - \sum_{n=1}^{\infty} Z_2 n \left[\frac{1}{Z_m f_n} \sin(2\pi f_n t + Z_2 \delta_n) + C_2 V_n \right] u(t) (\text{damping}) \\
 & = \sum_{n=1}^{\infty} A_n \cos(2\pi f_n t + \delta_n) * B_2, f_{e, f, l} t - \sum_{n=1}^{\infty} Z_1 n \cos(2\pi f_n t + Z_1 \delta_n) u(t) (B_c, A M Z_{l, \text{inf}}) \\
 & - \sum_{n=1}^{\infty} Z_1 n \left[\frac{1}{Z_m f_n} \sin(2\pi f_n t + Z_1 \delta_n) + C_1 V_n \right] u(t) * B_c, z - \sum_{n=1}^{\infty} Z_1 n \left[\frac{1}{Z_m f_n} \sin(2\pi f_n t + Z_1 \delta_n) + C_1 V_n \right] u(t) \text{damping}
 \end{aligned}$$

50

51

A frequency-domain approach to simulating wave energy converter
hydrodynamics

Write (51) with common terms collected

$$\begin{aligned}
 & \sum_{n=1}^{\infty} Z_{1n} \left[(\text{mass}_2) \cos(2\pi f_n t + 2\beta_{6n}) - \frac{1}{(2\pi f_n)^2} \cos(2\pi f_n t + 2\beta_{6n}) \text{Moor. } k_m \right] u(t) \\
 & + \sum_{n=1}^{\infty} Z_{2n} \left[((C_2 V_n)/B_2, K_{ns})(t) u(t) + ((C_2 P_n)(B_2, K_{ns}) u(t) + (C_2 \sqrt{n})(\text{Moor. } K_m)(t) u(t) + (C_2 P_n)(\text{Moor. } k_m) u(t) \right] \\
 & + \frac{1}{2\pi f_n} \sum_{n=1}^{\infty} Z_{2n} \left[\sin(2\pi f_n t + 2\beta_{6n}) u(t) * B_2 z + \sin(2\pi f_n t + 2\beta_{6n}) u(t) \text{ Moor. } b_m + \sin(2\pi f_n t + 2\beta_{6n}) u(t) B_2 b_n \right. \\
 & \left. - \sin(2\pi f_n t + 2\beta_{6n}) u(t) \text{ damping} \right] + \sum_{n=1}^{\infty} Z_{2n} \left[((C_2 V_n) u(t) * B_2 z + (C_2 V_n)(\text{Moor. } B_m + B_2 b_n) - \text{damping}) u(t) \right] \\
 & = \sum_{n=1}^{\infty} A_n \cos(2\pi f_n t + \zeta_n) * B_2 f_n - \sum_{n=1}^{\infty} Z_{1n} \cos(2\pi f_n t + 2\beta_{6n}) u(t) (\text{Moor. } f) \\
 & - \frac{1}{2\pi f_n} \sum_{n=1}^{\infty} Z_{1n} \left[\sin(2\pi f_n t + 2\beta_{6n}) u(t) * B_2 z - \sin(2\pi f_n t + 2\beta_{6n}) u(t) \text{ damping} \right] \\
 & - \sum_{n=1}^{\infty} Z_{1n} \left[((C_1 V_n) u(t) * B_2 z + (C_1 V_n) u(t) \text{ damping} \right]
 \end{aligned}$$

52

A frequency-domain approach to simulating wave energy converter
hydrodynamics

Convert (52) from time-domain to Frequency domain by applying Fourier Transforms. 22
Collect terms where possible

$$\begin{aligned}
 & \sum_{n=1}^{\infty} Z_n^{2n} [(m_{ns}) - \frac{1}{(2\pi f_n)^2} (B2.K_{ns} + M_{ns}.K_{ns})] \hat{f}_2^2 \cos(2\pi f_n t + 2\pi s_n u(t)) \\
 & + \sum_{n=1}^{\infty} Z_n \left[(C2V_n) B2.K_{ns} + (C2V_n)(M_{ns}.K_{ns}) \right] \hat{f}_2^2 t \cdot u(t) + \frac{1}{2\pi f_n} \sum_{n=1}^{\infty} Z_n \hat{f}_2^2 \sin(2\pi f_n t + 2\pi s_n u(t)) \hat{f}_2^2 B2.z \\
 & + \frac{1}{2\pi f_n} \sum_{n=1}^{\infty} Z_n \left[(C2R_n)(B2.K_{ns}) + (C2R_n)(M_{ns}.K_{ns}) + (C2V_n)M_{ns}.B_m + (C2V_n)(B2.bv) - \text{damping} \right] \hat{f}_2^2 \sin(2\pi f_n t + 2\pi s_n u(t)) + \sum_{n=1}^{\infty} Z_n (C2V_n) \hat{f}_2^2 u(t) \hat{f}_2^2 B2.z \\
 & + \sum_{n=1}^{\infty} Z_n \left[(C2R_n)(B2.K_{ns}) + (C2R_n)(M_{ns}.K_{ns}) + (C2V_n)M_{ns}.B_m + (C2V_n)(B2.bv) - (C2V_n) \text{damping} \right] \hat{f}_2^2 u(t) \\
 & = \sum_{n=1}^{\infty} A_n \left\{ \cos(2\pi f_n t + s_n) \hat{f}_2^2 B2.f_e.s_n \right\} - \sum_{n=1}^{\infty} (2I_n) \left\{ B2.Am21.n \right\} \hat{f}_2^2 \cos(2\pi f_n t + 21.s_n) u(t) \\
 & - \frac{1}{2\pi f_n} \sum_{n=1}^{\infty} (2I_n) \hat{f}_2^2 S_n (2\pi f_n t + 21.s_n) u(t) \hat{f}_2^2 B2.z - \frac{1}{2\pi f_n} \sum_{n=1}^{\infty} (2I_n) \text{damping} \hat{f}_2^2 \sin(2\pi f_n t + 21.s_n) u(t) \\
 & - \sum_{n=1}^{\infty} Z_n \left\{ (C2V_n) \hat{f}_2^2 u(t) \right\} \hat{f}_2^2 B2.z - \sum_{n=1}^{\infty} Z_n \left\{ (C2V_n) (\text{damping}) \hat{f}_2^2 u(t) \right\}
 \end{aligned}$$

A frequency-domain approach to simulating wave energy converter
hydrodynamics

Rewrite (53) using the transform pairs identified in (16-24)

23

99

$$\begin{aligned}
 & \sum_{n=1}^{\infty} 2\alpha_n \left[\text{mass}_2 - \frac{i}{(2\pi f_n)^2} (\text{B2.K}_{ns} + \text{Moor.K}_{ns}) \right] \cos(2\pi f_n t) \left\{ \frac{1}{4} (\delta(f-f_n) + \delta(f+f_n)) + \frac{i 2\pi f}{(2\pi f_n)^2 - (2\pi f)^2} \right\} \\
 & - \left\{ \text{mass}_2 - \frac{i}{(2\pi f_n)^2} (\text{B2.K}_{ns} + \text{Moor.K}_{ns}) \right\} \sin(2\pi f_n t) \left\{ \frac{1}{4\pi} (\delta(f-f_n) - \delta(f+f_n)) + \frac{2\pi f_n}{(2\pi f_n)^2 - (2\pi f)^2} \right\} \\
 & + \sum_{n=1}^{\infty} 2\alpha_n (\text{C2V}_n) \left[\text{B2.K}_{ns} + \text{Moor.K}_{ns} \right] \left[\frac{\delta'(t)}{4\pi} - \frac{i}{(2\pi f)^2} \right] \\
 & + \frac{1}{2\pi f_n} \sum_{n=1}^{\infty} (2\alpha_n) (\text{B2.Z}_n) \left[\cos(2\pi f_n t) \left\{ \frac{1}{4\pi} (\delta(f-f_n) - \delta(f+f_n)) + \frac{2\pi f_n}{(2\pi f_n)^2 - (2\pi f)^2} \right\} \right. \\
 & \quad \left. + \sin(2\pi f_n t) \left\{ \frac{1}{4} (\delta(f-f_n) + \delta(f+f_n)) + \frac{i 2\pi f}{(2\pi f_n)^2 - (2\pi f)^2} \right\} \right] [\text{Moor.B}_m + \text{B2.b}_m - \text{damping}] \\
 & + \sum_{n=1}^{\infty} 2\alpha_n (\text{C2P}_n) \left[\text{B2.K}_{ns} + \text{Moor.K}_{ns} \right] \left[\frac{\delta(t)}{2} - \frac{i}{2\pi f} \right] \\
 & + \sum_{n=1}^{\infty} 2\alpha_n (\text{C2V}_n) \left[\text{B2.K}_{ns} + \text{Moor.K}_{ns} \right] \left[\frac{\delta(t)}{2} - \frac{i}{2\pi f} \right]
 \end{aligned}$$

Continued

A frequency-domain approach to simulating wave energy converter
hydrodynamics

continued

24

9/9

$$\begin{aligned}
 &= \sum_{n=1}^{\infty} (A_n) (B_2 T_n) \left(\frac{1}{2}\right) \left[\cos(\xi_m) (\delta(f + f_n) + \delta(f - f_n)) - i \sin(\xi_m) (\delta(f + f_n) - \delta(f - f_n)) \right] \\
 &- \sum_{n=1}^{\infty} (Z_n) (B_c A_n W) \left\{ \cos(2\xi_n) \left[\frac{1}{4i} (\delta(f - f_n) + \delta(f + f_n) + \frac{i 2\pi f}{(2\pi f_n)^2 - (2\pi f)^2}) \right] \right. \\
 &\quad \left. - \sin(2\xi_n) \left[\frac{1}{4i} (\delta(f - f_n) - \delta(f + f_n)) + \frac{2\pi f_n}{(2\pi f_n)^2 - (2\pi f)^2} \right] \right\} \\
 &- \left(\frac{1}{2\pi f_n} \right) \sum_{n=1}^{\infty} Z_n (B_c T_n + \text{damping}) \left\{ \cos(2\xi_n) \left[\frac{1}{4i} (\delta(f - f_n) - \delta(f + f_n) + \frac{2\pi f_n}{(2\pi f_n)^2 - (2\pi f)^2}) \right] \right. \\
 &\quad \left. + \sin(2\xi_n) \left[\frac{1}{4i} (\delta(f - f_n) + \delta(f + f_n)) + \frac{i 2\pi f}{(2\pi f_n)^2 - (2\pi f)^2} \right] \right\} \\
 &- \sum_{n=1}^{\infty} Z_n (B_c T_n + \text{damping}) \left[\frac{\delta(f)}{2} - \frac{i}{2\pi f} \right]
 \end{aligned}$$

54

A frequency-domain approach to simulating wave energy converter
hydrodynamics

Rearrange denominators of (54). Put all selected $\delta(f)$ groups into same order; $\delta(f+f_n) \pm \delta(f-f_n)$

25

9/9

$$\begin{aligned}
 & \sum_{n=1}^{\infty} 2\pi n \left[\text{Mass}_2 - \frac{B2.K_{ns} + \text{Moor.}K_{ns}}{(2\pi f_n)^2} \right] \left\{ \cos(2\pi n) \left[\frac{1}{4} (\delta(f+f_n) + \delta(f-f_n)) + \frac{i2\pi f}{(2\pi f_n)^2 - (2\pi f)^2} \right] \right. \\
 & \quad \left. - \sin(2\pi n) \left[\frac{1}{4} (\delta(f+f_n) - \delta(f-f_n)) + \frac{2\pi f_n}{(2\pi f_n)^2 - (2\pi f)^2} \right] \right\} \\
 & + \frac{1}{2\pi f_n} \sum_{n=1}^{\infty} 2\pi n \left[B2.Z_m + \text{Moor.}B_m + B2.b_n - \text{damping} \right] \left\{ \cos(2\pi n) \left[\frac{1}{4} (\delta(f+f_n) - \delta(f-f_n)) + \frac{2\pi f_n}{(2\pi f_n)^2 - (2\pi f)^2} \right] \right. \\
 & \quad \left. + \sin(2\pi n) \left[\frac{1}{4} (\delta(f+f_n) + \delta(f-f_n)) + \frac{i2\pi f}{(2\pi f_n)^2 - (2\pi f)^2} \right] \right\} \\
 & + \sum_{n=1}^{\infty} 2\pi n \left[(2\pi n) [B2.Z_m + \text{Moor.}B_m + B2.b_n - \text{damping}] \left[\frac{\delta(t)}{2} - \frac{i}{2\pi f} \right] \right. \\
 & \quad \left. + \sum_{n=1}^{\infty} 2\pi n \left[(2\pi n) [B2.K_{ns} + \text{Moor.}K_{ns}] \left[\frac{\delta'(t)}{4\pi} - \frac{1}{(2\pi f_n)^2} \right] \right. \right. \\
 & \quad \left. \left. + \sum_{n=1}^{\infty} 2\pi n \left[(2\pi n) [B2.K_{ns} + \text{Moor.}K_{ns}] \left[\frac{\delta(t)}{2} - \frac{i}{2\pi f} \right] \right. \right]
 \end{aligned}$$

Continued

A frequency-domain approach to simulating wave energy converter
hydrodynamics

Continued

16

9/9

$$\begin{aligned}
 &= \sum_{n=1}^{\infty} (A_n)(B_2, i\mathbb{F}_n) \left[\frac{1}{2} \right] [\cos(\omega_n) \left[\frac{1}{4} \right] (\delta(f+f_n) + \delta(f-f_n)) - i \sin(\omega_n) \left[\frac{1}{2} \right] (\delta(f+f_n) - \delta(f-f_n))] \\
 &\quad - \sum_{n=1}^{\infty} (Z_n)(B_2, M\mathbb{F}_n) \left\{ \cos(\omega_n) \left[\frac{1}{4} \right] \left[\frac{i}{4} \right] (\delta(f+f_n) + \delta(f-f_n)) + \frac{i 2\pi f}{(2\pi f_n)^2 - (2\pi f_n)^2} \right. \\
 &\quad \left. - \sin(\omega_n) \left[\frac{1}{4} \right] \left[\frac{i}{4} \right] (-1) \left[\frac{i}{4} \right] (\delta(f+f_n) - \delta(f-f_n)) + \frac{2\pi f}{(2\pi f_n)^2 - (2\pi f_n)^2} \right\} \\
 &\quad - \sum_{n=1}^{\infty} Z_n (B_2, Z_n + \text{damping}) \left\{ \cos(\omega_n) \left[\frac{1}{4} \right] \left[\frac{i}{4} \right] (-1) \delta(f+f_n) - \delta(f-f_n) \right. \\
 &\quad \left. + \frac{i 2\pi f}{(2\pi f_n)^2 - (2\pi f_n)^2} \right\} \\
 &\quad + \sin(\omega_n) \left[\frac{1}{4} \right] \left[\frac{i}{4} \right] (\delta(f+f_n) + \delta(f-f_n)) + \frac{i 2\pi f}{(2\pi f_n)^2 - (2\pi f_n)^2} \left. \right\}
 \end{aligned}$$

$$- \sum_{n=1}^{\infty} Z_n (B_2, Z_n + \text{damping}) \left[\frac{\delta(f)}{2} - \frac{i}{2\pi f} \right]$$

Define variables for coefficients of (55) using convention defined on pg 13 (9/2)

$$C_{02A} = \frac{\text{mass}}{(2\pi f_n)^2} - \frac{B_2, K_{ns} + \text{Moor}, K_{ns}}{(2\pi f_n)^2}$$

$$C_{02B} = \frac{1}{2\pi f_n} (B_2, Z_n + \text{Moor}, B_m + B_2, b_v - \text{damping})$$

$$C_{02F} = B_2, Z_n + \text{damping}$$

$$C_{02D} = B_2, Z_n + \text{Moor}, B_m + B_2, b_v - \text{damping}$$

A frequency-domain approach to simulating wave energy converter
hydrodynamics

$$\begin{aligned}
 & \text{Sobstydiale } (56 A - F) \rightarrow (55) \\
 & \sum_{n=1}^{\infty} z_{2n} (C_0 2A) \left\{ \cos(2z_{2n}) \left[\frac{1}{4} (\delta(f+f_n) + \delta(f-f_n)) + \frac{i 2\pi f}{(2\pi f_n)^2 - (2\pi f)^2} \right] \right. \\
 & \quad \left. - \sin(2z_{2n}) \left[\frac{1}{4} (\delta(f+f_n) - \delta(f-f_n)) + \frac{2\pi f_n}{(2\pi f_n)^2 - (2\pi f)^2} \right] \right\} \\
 & \quad + \sum_{n=1}^{\infty} z_{2n} (C_0 2B) \left\{ \cos(2z_{2n}) \left[\frac{1}{4} (\delta(f) + \delta(f+f_n) - \delta(f-f_n)) + \frac{2\pi f_n}{(2\pi f_n)^2 - (2\pi f)^2} \right] \right. \\
 & \quad \left. + 5m(2z_{2n}) \left[\frac{1}{4} (\delta(f+f_n) + \delta(f-f_n)) + \frac{i 2\pi f}{(2\pi f_n)^2 - (2\pi f)^2} \right] \right\} \\
 & \quad + \sum_{n=1}^{\infty} z_{2n} (C_2 R_n) (C_0 2C) \left[\frac{\delta'(f)}{2} - \frac{i}{2\pi f} \right] + \sum_{n=1}^{\infty} z_{2n} (C_2 V_n) (C_0 2D) \left[\frac{\delta'(f)}{4\pi} - \frac{i}{(2\pi f)^2} \right] \\
 & \quad + \sum_{n=1}^{\infty} z_{2n} (C_2 R_n) (C_0 2D) \left[\frac{\delta'(f)}{2} - \frac{i}{2\pi f} \right] \\
 & = \sum_{n=1}^{\infty} (A_n) \left[B_2, fE_n \right] \left[\cos(z_n) (\delta(f+f_n) + \delta(f-f_n)) - i \sin(z_n) (\delta(f+f_n) - \delta(f-f_n)) \right] \\
 & \quad - \sum_{n=1}^{\infty} z_{2n} (B_2, A M_{2n}, f) \left\{ \cos(2z_{2n}) \left[\frac{1}{4} (\delta(f+f_n) + \delta(f-f_n)) + \frac{i 2\pi f}{(2\pi f_n)^2 - (2\pi f)^2} \right] \right. \\
 & \quad \left. - \sin(2z_{2n}) \left[\frac{1}{4} (\delta(f+f_n) - \delta(f-f_n)) + \frac{2\pi f_n}{(2\pi f_n)^2 - (2\pi f)^2} \right] \right\}
 \end{aligned}$$

(continued)

A frequency-domain approach to simulating wave energy converter
hydrodynamics

Continued

28

9/9

$$\begin{aligned}
 & - \sum_{n=1}^{\infty} z \ln(c_0 2F) \left\{ \cos(z \ln) \left[\frac{i}{4} \right] (i) \left[\frac{J(f+f_n)}{f-f_n} - \frac{J(f-f_n)}{(2\pi f_n)^2} \right] \right. \\
 & + \sin(z \ln) \left[\frac{i}{4} \right] \left(J(f+f_n) + J(f-f_n) \right) + \left. \frac{i 2\pi f}{(2\pi f_n)^2 - (2\pi f)^2} \right\}
 \end{aligned}$$

$$= \sum_{n=1}^{\infty} z \ln(c_0 2F) \left[\frac{J(f)}{2} - \frac{i}{2\pi F} \right] W_n$$

Drop summation sign, keeping 'n' subscript as reminder.
 Separate (57) into 4 equations:

1. $f = -f_n$
2. $f = f_n$
3. $f = 0$
4. $-\infty \leq f \leq \infty$

57

A frequency-domain approach to simulating wave energy converter
hydrodynamics

$$f = -f_n; \quad S(f + f_n)$$

29

9/9

$$(Z_{2n})(c_{0.2}A) \left[\cos(22\delta_n) \left(\frac{1}{4}\right) S(f + f_n) - i \sin(22\delta_n) \left(\frac{1}{4}\right) S(f + f_n) \right] \\ + (Z_{2n})(c_{0.2}B) \left[i \cos(\delta_n) S(f + f_n) + \sin(22\delta_n) \left(\frac{1}{4}\right) S(f + f_n) \right]$$

$$= A_n \left(\frac{1}{2}\right) (B2FE_n) \left[\cos(\delta_n) S(f + f_n) - i \sin(\delta_n) S(f + f_n) \right]$$

$$- Z_{1n} (Bc, AM2)_{inf} \left[\cos(\delta_n) \left(\frac{1}{4}\right) S(f + f_n) - i \sin(\delta_n) \left(\frac{1}{4}\right) S(f + f_n) \right]$$

$$- Z_{1n} (c_{0.2}E) \left[i \cos(\delta_n) \left(\frac{1}{4}\right) S(f + f_n) + \sin(\delta_n) \left(\frac{1}{4}\right) S(f + f_n) \right]$$

58

Multiply (58) by 4. Factor main variables.

$$(Z_{2n})(c_{0.2}A) S(f + f_n) \left[\cos(22\delta_n) - i \sin(22\delta_n) \right] + Z_{2n}(c_{0.2}B) S(f + f_n) \left[i \cos(22\delta_n) + \sin(22\delta_n) \right] \\ = 2(A_n) S(f + f_n) B2FE_n \left[\cos(\delta_n) - i \sin(\delta_n) \right] - (Z_{1n}) S(f + f_n) (Bc, AM2)_{inf} \left[\cos(\delta_n) - i \sin(\delta_n) \right] \\ - (Z_{1n}) S(f + f_n) (c_{0.2}E) \left[i \cos(\delta_n) + \sin(\delta_n) \right]$$

59

Substitute (31a-b) into (59)

$$(Z_{2n}) \exp(-i22\delta_n) S(f + f_n) (c_{0.2}A) + Z_{2n}(i) \exp(-i22\delta_n) S(f + f_n) (c_{0.2}B) \\ = 2(A_n) \exp(-i\delta_n) S(f + f_n) B2FE_n - (Z_{1n}) \exp(-i2\delta_n) S(f + f_n) (Bc, AM2)_{inf} \\ - (Z_{1n})(i) \exp(-i2\delta_n) S(f + f_n) (c_{0.2}E)$$

60

A frequency-domain approach to simulating wave energy converter
hydrodynamics

factor like terms in (60)

$$(Z_{2n}) \exp(-iZ_{2n}) \delta(f+f_n) [C_{02A} + iC_{02B}] = 2(A_n) \exp(-i\delta_n) \delta(f+f_n) B_{2,FE_n}$$

$$- (Z_{1n}) \exp(-iZ_{1n}) \delta(f+f_n) [B_{c,AMZ1,inf} + iC_{02E}]$$

Substitute (34) into (61)

$$(Z_{2n}) \exp(-iZ_{2n}) \delta(f+f_n) [C_{02A} + iC_{02B}] = 2(A_n) \exp(-i\delta_n) \delta(f+f_n) B_{2,FE_n}$$

$$- \frac{2(A_n) \exp(-i\delta_n) \delta(f+f_n) (B_{1,FE_n}) [B_{c,AMZ1,inf} + iC_{02E}]}{C_{01A} + iC_{01B}}$$

$$+ (Z_{2n}) \exp(-iZ_{2n}) \delta(f+f_n) [B_{c,AMZ1,inf} + iC_{01D}] [B_{c,AMZ1,inf} + iC_{02E}]$$

$$C_{01A} + iC_{01B}$$

Move $(Z_{2n}) \exp(-iZ_{2n}) \delta(f+f_n)$ term to left side of equation.

$$(Z_{2n}) \exp(-iZ_{2n}) \delta(f+f_n) \left[C_{02A} + iC_{02B} - \frac{[B_{c,AMZ1,inf} + iC_{01D}] [B_{c,AMZ1,inf} + iC_{02E}]}{C_{01A} + iC_{01B}} \right]$$

$$= 2(A_n) \exp(-i\delta_n) \delta(f+f_n) \left[B_{2,FE_n} - \frac{B_{1,FE_n} [B_{c,AMZ1,inf} + iC_{02E}]}{C_{01A} + iC_{01B}} \right]$$

30

9/9

A frequency-domain approach to simulating wave energy converter
hydrodynamics

Excitation force and Radiation force transfer function values are complex numbers. Make all complex numbers explicit.

3

%

%

A

B

C

D

E

F

G

H

I

J

K

L

M

N

O

P

Q

R

S

T

U

V

W

X

Y

Z

$$R_{1FF_n} = \operatorname{RE}\{B1,1FF_n\}, \quad |1FF_n| = \operatorname{M}\{B1,1FF_n\}$$

$$R_{2FF_n} = \operatorname{RE}\{B2,1FF_n\}, \quad |2FF_n| = \operatorname{M}\{B2,1FF_n\}$$

$$R_{1Z_n} = \operatorname{RE}\{B1,Z_n\}, \quad |1Z_n| = \operatorname{M}\{B1,Z_n\}$$

$$R_{2Z_n} = \operatorname{RE}\{B2,Z_n\}, \quad |2Z_n| = \operatorname{M}\{B2,Z_n\}$$

$$C_0/A = \frac{\text{Mass}}{(2\pi f_n)^2}$$

$$R_{10}B = \operatorname{RE}\{C_0B\} = \frac{R_{1Z_n} + B.bv + \text{damping}}{2\pi f_n}, \quad |C_0B| = \operatorname{M}\{C_0B\} = \frac{|1Z_n|}{2\pi f_n}$$

$$R_{10}C = \operatorname{RE}\{C_0C\} = R_{1Z_n} + B.bv + \text{damping}, \quad |C_0C| = \operatorname{M}\{C_0C\} = |1Z_n|$$

$$R_{20}Z_n = \operatorname{RE}\{B2,Z_n\}, \quad |C_0Z_n| = \operatorname{M}\{B2,Z_n\}$$

$$R_{10}D = \operatorname{RE}\{C_0D\} = \frac{R_{1Z_n} - \text{damping}}{2\pi f_n}, \quad |C_0D| = \operatorname{M}\{C_0D\} = \frac{|1Z_n|}{2\pi f_n}$$

$$R_{10}E = \operatorname{RE}\{C_0E\} = R_{1Z_n} - \text{damping}, \quad |C_0E| = \operatorname{M}\{C_0E\} = |1Z_n|$$

$$R_{10}B = \operatorname{RE}\{C_0B\} = \frac{R_{1Z_n} + \text{Mass} + B.bv - \text{damping}}{2\pi f_n}, \quad |C_0B| = \operatorname{M}\{C_0B\} = \frac{|1Z_n|}{2\pi f_n}$$

A frequency-domain approach to simulating wave energy converter
hydrodynamics

$$RC_{02C} = RE\{C_{02C}\} = RZ_n + M_{02Bm} + \beta_2 b_n - \text{damping}; \quad |C_{02C}| = IM\{C_{02C}\} = 12Z_n$$

$$RC_{02E} = RE\{C_{02E}\} = \frac{RZ_n + \text{damping}}{2n_f}; \quad |C_{02E}| = IM\{C_{02E}\} = \frac{|C_{02C}|}{2n_f}$$

$$RC_{02F} = RE\{C_{02F}\} = RZ_n + \text{damping}; \quad |C_{02F}| = IM\{C_{02F}\} = |C_{02C}|$$

Rewrite (63) with explicit complex numbers identified in (64 A-N)

$$\begin{aligned} & \left[\frac{(Z_n) \exp(-iZ_n f_n) S(f_n)}{[ColA + i(RC_{02B} + i(C_{02B})][ColA + i(RC_{01B} + i(C_{01B})] \right] \\ & - \left[\frac{[B_{c, AM1, inf} + i(RC_{01D} + i(C_{01D})][B_{c, AM2, inf}]^T + i(RC_{02E} + i(C_{02E})]}{[ColA + i(RC_{01B} + i(C_{01B}))} \right] \\ & = 2(A_n) \exp(-iZ_n f_n) S(f_n) \left[\frac{[RZ_n E_n + i(2FE_n)] [ColA + i(RC_{01B} + i(C_{01B}))]}{[ColA + i(RC_{01B} + i(C_{01B}))} \right. \\ & \quad \left. - \frac{[RFF_n + i(12FF_n)][B_{c, AM2, inf} + i(RC_{02E} + i(C_{02E})]}{[ColA + i(RC_{01B} + i(C_{01B}))]} \right] \end{aligned}$$

65

A frequency-domain approach to simulating wave energy converter
hydrodynamics

Expand imaginary terms, then group Real and Imaginary Parts.

33

 η_{II}

$$\begin{aligned}
 & (\underline{\mathbf{E}}_{2n}) \exp(-i\underline{\mathbf{E}}_{2n}) S(f_+ f_n) \left[\frac{[(C_{02A} - 1C_{02B}) + iR C_{02B}] [(C_{01A} - 1C_{01B}) + iR C_{01B}]}{(C_{01A} - 1C_{01B}) + iR C_{01B}} \right. \\
 & \quad \left. - \frac{[(B_{c, AM2, inf} - 1C_{01D}) + iR C_{01D}] [(B_{c, AM2, inf} - 1C_{02E}) + iR C_{02E}]}{(C_{01A} - 1C_{01B}) + iR C_{01B}} \right] \\
 & = 2(A_n) \exp(-i\omega_n) S(f_+ f_n) \left[\frac{[R_2 F_{E_n} + iI_2 F_{E_n}] [(C_{01A} - 1C_{01B}) + iR C_{01B}]}{(C_{01A} - 1C_{01B}) + iR C_{01B}} \right. \\
 & \quad \left. - \frac{[R_1 F_{E_n} + iI_1 F_{E_n}] [(B_{c, AM2, inf} - 1C_{02E}) + iR C_{02E}]}{(C_{01A} - 1C_{01B}) + iR C_{01B}} \right] \\
 & \quad \text{Perform multiplication of numerator terms} \\
 & (\underline{\mathbf{E}}_{2n}) \exp(-i\underline{\mathbf{E}}_{2n}) S(f_+ f_n) \left[\frac{[(C_{02A} - 1C_{02B})(C_{01A} - 1C_{01B}) - (R C_{02B})(R C_{01B}) + i[(C_{02A} - 1C_{02B})(R C_{01B}) + (R C_{02B})(C_{01A} - 1C_{01B})]}{(C_{01A} - 1C_{01B}) + iR C_{01B}} \right. \\
 & \quad \left. - \frac{[(B_{c, AM2, inf} - 1C_{01D})(B_{c, AM2, inf} - 1C_{02E}) - (R C_{01D})(R C_{02E}) + i[(B_{c, AM2, inf} - 1C_{01D})(R C_{02E}) + (R C_{01D})(B_{c, AM2, inf} - 1C_{02E})]}{(C_{01A} - 1C_{01B}) + iR C_{01B}} \right. \\
 & \quad \left. - \frac{[(R_2 F_{E_n})(C_{01A} - 1C_{01B}) - (I_2 F_{E_n})(R C_{01B}) + i[(R_2 F_{E_n})(R C_{01B}) + (I_2 F_{E_n})(C_{01A} - 1C_{01B})]}{(C_{01A} - 1C_{01B}) + iR C_{01B}} \right. \\
 & \quad \left. - \frac{[(R_1 F_{E_n})(B_{c, AM2, inf} - 1C_{02E}) - (I_1 F_{E_n})(R C_{02E}) + i[(R_1 F_{E_n})(R C_{02E}) + (I_1 F_{E_n})(B_{c, AM2, inf} - 1C_{02E})]}{(C_{01A} - 1C_{01B}) + iR C_{01B}} \right]
 \end{aligned}$$

67

A frequency-domain approach to simulating wave energy converter
hydrodynamics

Define Coefficients :

R_{f1} , N/p , 'Body#', 'order of appearance'

log 34

A

B

C

D

E

F

G

H

I

J

K

L

M

N

O

P

Q

R

S

T

U

V

W

X

Y

Z

AA

BB

CC

DD

EE

FF

GG

HH

II

JJ

KK

LL

MM

NN

OO

PP

QQ

RR

TT

UU

VV

WW

XX

YY

ZZ

AA

BB

CC

DD

EE

FF

GG

HH

II

JJ

KK

LL

MM

NN

OO

PP

QQ

RR

TT

UU

VV

WW

XX

YY

ZZ

AA

BB

CC

DD

EE

FF

GG

HH

II

JJ

KK

LL

MM

NN

OO

PP

QQ

RR

TT

UU

VV

WW

XX

YY

ZZ

AA

BB

CC

DD

EE

FF

GG

HH

II

JJ

KK

LL

MM

NN

OO

PP

QQ

RR

TT

UU

VV

WW

XX

YY

ZZ

AA

BB

CC

DD

EE

FF

GG

HH

II

JJ

KK

LL

MM

NN

OO

PP

QQ

RR

TT

UU

VV

WW

XX

YY

ZZ

AA

BB

CC

DD

EE

FF

GG

HH

II

JJ

KK

LL

MM

NN

OO

PP

QQ

RR

TT

UU

VV

WW

XX

YY

ZZ

AA

BB

CC

DD

EE

FF

GG

HH

II

JJ

KK

LL

MM

NN

OO

PP

QQ

RR

TT

UU

VV

WW

XX

YY

ZZ

AA

BB

CC

DD

EE

FF

GG

HH

II

JJ

KK

LL

MM

NN

OO

PP

QQ

RR

TT

UU

VV

WW

XX

YY

ZZ

AA

BB

CC

DD

EE

FF

GG

HH

II

JJ

KK

LL

MM

NN

OO

PP

QQ

RR

TT

UU

VV

WW

XX

YY

ZZ

AA

BB

CC

DD

EE

FF

GG

HH

II

JJ

KK

LL

MM

NN

OO

PP

QQ

RR

TT

UU

VV

WW

XX

YY

ZZ

AA

BB

CC

DD

EE

FF

GG

HH

II

JJ

KK

LL

MM

NN

OO

PP

QQ

RR

TT

UU

VV

WW

XX

YY

ZZ

AA</

A frequency-domain approach to simulating wave energy converter
hydrodynamics

Solve (64) for $(\tilde{Z}_{2n}) \exp(-i\tilde{Z}_{2n}) S(f_n f_n)$. Denominators cancel.

35 9/11

$$\begin{aligned}
 & (\tilde{Z}_{2n}) \exp(-i\tilde{Z}_{2n}) S(f_n f_n) \\
 &= \frac{i(\tilde{f}_n) \exp(i\tilde{f}_n) S(f_n)}{\frac{[(R_{AC} - R_{AD}) + i(N_{AC} - N_{AD})]}{(R_{AA} - R_{AB}) + i(N_{AA} - N_{AB})}}
 \end{aligned}$$

70

A frequency-domain approach to simulating wave energy converter
hydrodynamics

$$f = f_n; \quad S(f - f_n)$$

36 9/11

$$\begin{aligned}
 & (Z_{2n})(C_02A) [\cos(2\delta_n)(\frac{1}{4}) \delta(f - f_n)] - i \sin(2\delta_n)(\frac{1}{4})(-i) \delta(f - f_n) \\
 & + (Z_{2n})(C_02B) [\cos(2\delta_n)(\frac{1}{4})(i)(-i) \delta(f - f_n) + \sin(2\delta_n)(\frac{1}{4}) \delta(f - f_n)] \\
 & = (A_n)(\frac{1}{2})(B_2, F_{E_n}) [\cos(\delta_n) \delta(f - f_n) - i \sin(\delta_n)(-i) \delta(f - f_n)] \\
 & - (Z_{1n})(B_2, A M 2, \inf) [\cos(2\delta_n)(\frac{1}{4}) \delta(f - f_n) - i \sin(2\delta_n)(\frac{1}{4})(-i) \delta(f - f_n)] \\
 & - (Z_{1n})(C_02E) [\cos(2\delta_n)(\frac{1}{4})(i)(-i) \delta(f - f_n) + \sin(2\delta_n)(\frac{1}{4}) \delta(f - f_n)]
 \end{aligned}$$

Multiply (71) by 4. Factor main variables

$$\begin{aligned}
 & (Z_{2n})(C_02A) \delta(f - f_n) [\cos(2\delta_n) + i \sin(2\delta_n)] + (Z_{2n})(C_02B) \delta(f - f_n) [-i \cos(2\delta_n) + \sin(2\delta_n)] \\
 & = 2(A_n)(B_2, F_{E_n}) \delta(f - f_n) [\cos(\delta_n) + i \sin(\delta_n)] \\
 & - (Z_{1n})(B_2, A M 2, \inf) \delta(f - f_n) [\cos(2\delta_n) + i \sin(2\delta_n)] \\
 & - (Z_{1n})(C_02E) \delta(f - f_n) [-i \cos(2\delta_n) + \sin(2\delta_n)]
 \end{aligned}$$

Substitute (37a-b) into (72)

$$\begin{aligned}
 & (Z_{2n})(C_02A) \delta(f - f_n) \exp(i2\delta_n) + (Z_{2n})(C_02B) \delta(f - f_n) (-i) \exp(i2\delta_n) \\
 & = (2)(A_n)(B_2, F_{E_n}) \delta(f - f_n) \exp(i2\delta_n) \\
 & - (Z_{1n})(B_2, A M 2, \inf) \delta(f - f_n) \exp(i2\delta_n) - (Z_{1n})(C_02E) \delta(f - f_n) (-i) \exp(i2\delta_n)
 \end{aligned}$$

72

73

A frequency-domain approach to simulating wave energy converter
hydrodynamics

Rewrite (73) factoring like terms

$$(Z_{2n}) \exp(iZ_{2\delta_n}) \delta(f-f_n) [C_{02A} - iC_{02B}] = 2(A_n) \exp(i\delta_n) \delta(f-f_n) (B_{2,FE_n})$$

$$- (Z_{1n}) \exp(iZ_1\delta_n) \delta(f-f_n) [B_{c,AM2,inf} - iC_{02E}]$$

Substitute (40) into (74)

$$(Z_{2n}) \exp(iZ_{2\delta_n}) \delta(f-f_n) [C_{02A} - iC_{02B}] = 2(A_n) \exp(i\delta_n) \delta(f-f_n) (B_{2,FE_n})$$

$$- 2(A_n) \exp(i\delta_n) \delta(f-f_n) \left[\frac{B_{1,FE_n}}{C_{0A} - iC_{0B}} \right] [B_{c,AM2,inf} - iC_{02E}]$$

$$+ (Z_{2n}) \exp(iZ_{2\delta_n}) \delta(f-f_n) \left[\frac{[B_{c,AM2,inf} - iC_{0D}]}{C_{0A} - iC_{0B}} \right] [B_{c,AM2,inf} - iC_{02E}]$$

75

Move (Z_{2n}) \exp(iZ_{2\delta_n}) \delta(f-f_n) to left side of equation

$$(Z_{2n}) \exp(iZ_{2\delta_n}) \delta(f-f_n) \left[[C_{02A} - iC_{02B}] - \frac{[B_{c,AM2,inf} - iC_{0D}][B_{c,AM2,inf} - iC_{02E}]}{C_{0A} - iC_{0B}} \right]$$

$$= 2(A_n) \exp(i\delta_n) \delta(f-f_n) \left[B_{2,FE_n} - \frac{[B_{1,FE_n}][B_{c,AM2,inf} - iC_{02E}]}{C_{0A} - iC_{0B}} \right]$$

76

74

37

9/11

A frequency-domain approach to simulating wave energy converter
hydrodynamics

Rewrite (76) with explicit complex numbers identified in (64 A-N)

38

91

$$\begin{aligned}
 & (\mathcal{Z}_n) \exp(i\mathcal{Z}_{S_n}) S(f-f_n) \left[C_{02A} - i(R_{C02B} + iC_{02B}) \right] [C_{01A} - i(R_{C01B} + iC_{01B})] \\
 & \quad - \left[\frac{[B_{c,AM}12_{inf} - i(R_{C01D} + iC_{01D})]}{C_{01A} - i(R_{C01B} + iC_{01B})} \right] \left[\frac{[B_{c,AM}2_{inf} - i(R_{C02E} + iC_{02E})]}{C_{02A} - i(R_{C02B} + iC_{02B})} \right] \\
 & = 2(A_n) \exp(i\mathcal{Z}_{S_n}) S(f-f_n) \left[\frac{[R_{2FF_n} + i12_{FE_n}]}{C_{01A} - i(R_{C01B} + iC_{01B})} \right] \\
 & \quad - \left[\frac{[R_{1FF_n} + i11_{FE_n}]}{C_{01A} - i(R_{C01B} + iC_{01B})} \right] \left[\frac{[B_{c,AM}2_{inf} - i(R_{C02E} + iC_{02E})]}{C_{02A} - i(R_{C02B} + iC_{02B})} \right]
 \end{aligned}$$

Expand imaginary terms, Then group Real & Imaginary Parts.

$$\begin{aligned}
 & (\mathcal{Z}_n) \exp(i\mathcal{Z}_{S_n}) S(f-f_n) \left[\frac{[(C_{02A} + iC_{02B}) - iR_{C02B}]}{(C_{01A} + iC_{01B}) - iR_{C01B}} \right] \\
 & \quad - \left[\frac{[(B_{c,AM}12_{inf} + iL_{01D}) - iR_{C01D}]}{(C_{01A} + iC_{01B}) - iR_{C01B}} \right] \left[\frac{[(B_{c,AM}2_{inf} + iC_{02E}) - iR_{C02E}]}{(C_{02A} + iC_{02B}) - iR_{C02B}} \right] \\
 & = 2(A_n) \exp(i\mathcal{Z}_{S_n}) S(f-f_n) \left[\frac{[R_{2FF_n} + i12_{FE_n}]}{(C_{01A} + iC_{01B}) - iR_{C01B}} \right] \\
 & \quad - \left[\frac{[R_{1FF_n} + i11_{FE_n}]}{(C_{01A} + iC_{01B}) - iR_{C01B}} \right] \left[\frac{[(B_{c,AM}2_{inf} + iC_{02E}) - iR_{C02E}]}{(C_{02A} + iC_{02B}) - iR_{C02B}} \right]
 \end{aligned}$$

78

77

A frequency-domain approach to simulating wave energy converter
hydrodynamics

Perform Multiplication of Numerator Terms

$$(Z_{2n}) \exp(i2\omega_n) S(f, f_n) \left[\frac{[(C_{02A} + iC_{02B})(C_{01A} + iC_{01B}) - (RC_{02B})(RC_{01B})] - i[(C_{02A} + iC_{02B})(RC_{01B}) + (RC_{02B})(C_{01A} + iC_{01B})]}{(C_{01A} - iC_{01B}) - iRC_{01B}} \right]$$

$$= \frac{[(R_{1FFn})(B_{c, AM21}^{inf} + iC_{02D})(B_{c, AM21}^{inf} + iC_{02E}) - (RC_{01D})(RC_{02E})] - i[(B_{c, AM21}^{inf} + iC_{0D})(RC_{02E}) + (RC_{01D})(B_{c, AM21}^{inf} + iC_{02E})]}{(C_{01K} - iC_{01B}) - iRC_{01B}}$$

$$= R_{1FFn} \exp(i\omega_n) S(f - f_n) \left[\frac{[(R_{2FFn})(C_{01A} + iC_{01B}) + (i2FFn)(RC_{01B}) + (i2FE_n)(RC_{02E})] - i[(R_{2FFn})(RC_{01B}) - (i2FE_n)(C_{01A} + iC_{01B})]}{(C_{01A} - iC_{01B}) - iRC_{01B}} \right] \quad 79$$

$$\text{Define Coefficients, using "rules" applied to (68)} \quad 80$$

$$RP2A = [C_{02A} + iC_{02B})(C_{01A} + iC_{01B}) - (RC_{02B})(RC_{01B})]$$

$$RP2A = [(C_{02A} + iC_{02B})(RC_{01B}) + (RC_{02B})(C_{01A} + iC_{01B})]$$

$$RP2B = [(B_{c, AM21}^{inf} + iC_{01D})(B_{c, AM21}^{inf} + iC_{02E}) - (RC_{01D})(RC_{02E})]$$

$$RP2B = [(B_{c, AM21}^{inf} + iC_{0D})(RC_{02E}) + (RC_{01D})(B_{c, AM21}^{inf} + iC_{02E})]$$

$$RP2C = [(R_{2FFn})(C_{01A} + iC_{01B}) + (i2FFn)(RC_{01B})]$$

$$RP2C = [(R_{2FFn})(RC_{01B}) - (i2FFn)(C_{01A} + iC_{01B})]$$

$$RP2D = [(R_{1FFn})(B_{c, AM21}^{inf} + iC_{02E}) + (iFFn)(RC_{02E})]$$

$$RP2D = [(R_{1FFn})(RC_{02E}) - (iFFn)(B_{c, AM21}^{inf} + iC_{02E})]$$

C
D
E
F

5
6
7
8

A frequency-domain approach to simulating wave energy converter
hydrodynamics

Substitute (80 A-H) into (79)

$$(Z_{2n}) \exp(iZ_2 s_n) \delta(f - f_n) \left[\frac{R_{P2A} - iR_{P2A} - R_{P2B} + iR_{P2B}}{(C_{oA} - iC_{oB}) - iR_{CoIB}} \right]$$

$$= 2(A_n) \exp(iS_n) \delta(f - f_n) \left[\frac{R_{P2C} - iR_{P2C} - R_{P2D} + iR_{P2D}}{(C_{oA} - iC_{oB}) - iR_{CoIB}} \right]$$

Solve for $(Z_{2n}) \exp(iZ_2 s_n) \delta(f - f_n)$

$$(Z_{2n}) \exp(iZ_2 s_n) \delta(f - f_n) = 2(A_n) \exp(iS_n) \delta(f - f_n) \frac{[R_{P2C} - R_{P2D}] - i[R_{P2C} - iR_{P2D}]}{[R_{P2A} - R_{P2B}] - i[R_{P2A} - iR_{P2B}]}$$

A frequency-domain approach to simulating wave energy converter
hydrodynamics

7.2 Calibration

7.2.1 Excitation Force Calibration Script

```

tic;
clc;
clear all;
close all;
addpath(genpath('PA2BH'));

% universal constants
g = 9.81; % gravity, m/s^2
rho = 1025; % saltwater density kg/m^3
fprintf('\n');

%% Define Hydrodynamics
% Selects the desired geometry and returns constants for simulink
del_t = 0.01; % Time step - forced by the Rhuel setup

[B1 B2 Moor damping] = definegeometry();

% Calculate impulse response functions from frequency domain data
[B1 B2 Bc tmax w] = impulserespcalc_rebuild(B1,B2,del_t);

%% Define the inputs

timestart = -tmax;
timeend = 639.5;%  

% Define the time-domain simulation resolution
t=timestart:del_t:timeend;
t = t';
[a b] = size(w);

for n = 18:b
    n
    regWave = cos(w(n)*t);

    % time [s], wave surface elevation [m]
    eta = [t,regWave];

    % Split into causal/non-causal eta
    % Define shifted input wave elevation for the noncausal
    convolution used by filter
    B1.etaprime = eta;
    B2.etaprime = eta;
    B1.etaprime(:,1) = B1.etaprime(:,1) + B1.nonCausHorizonTime;
    %shift by size of nonzero part of impulse response

```

A frequency-domain approach to simulating wave energy converter hydrodynamics

```

B2.etaprime(:,1) = B2.etaprime(:,1) + B2.nonCausHorizonTime;
%shift by size of nonzero part of impulse response

sim('CalibrateFeModel.mdl');

% Extract results from simulation record.
perLength(n) = abs(round((2*pi)/(w(n)*del_t)));
stop_ss = t(end)/del_t - 3*perLength(n);
start_ss = stop_ss - perLength(n);

% inputs
[z_acc_max(n), z_acc_idx(n)] = max(unitCos(start_ss:stop_ss));
z_acc_idx(n) = z_acc_idx(n) + start_ss;

% Excitation Forces
[B1fe_max(n), B1fe_idx(n)] =
max(real(B1fe(z_acc_idx(n):z_acc_idx(n) + perLength(n)*3)));
[B2fe_max(n), B2fe_idx(n)] =
max(real(B2fe(z_acc_idx(n):z_acc_idx(n) + perLength(n)*3)));

end

%% Amplitude Calibration
B1fe_adj_a = (B1fe_max) - abs(B1.Fezpos)/2;
B2fe_adj_a = (B2fe_max) - abs(B2.Fezpos)/2;

% Error as a percentage of time-domain solution
B1fe_amp_e = 100*(B1fe_adj_a./B1fe_max);
B2fe_amp_e = 100*(B2fe_adj_a./B2fe_max);

%% Phase Calibration
% T-domain steps into rads
B1fe_ang = -(2.*pi.* (B1fe_idx))./perLength;
B2fe_ang = -(2.*pi.* (B2fe_idx))./perLength;

B1fe_adj_p = B1fe_ang - B1.Fez_phase;
B2fe_adj_p = B2fe_ang - B2.Fez_phase;

% Error as a percentage of period
B1fe_ang_e = 100*(B1fe_adj_p./(2*pi));
B2fe_ang_e = 100*(B2fe_adj_p./(2*pi));

FeCalTime = toc/3600;
save('CalFe', 'B1fe_adj_a', 'B1fe_adj_p', ...
      'B2fe_adj_a', 'B2fe_adj_p',...
      'FeCalTime');

```

A frequency-domain approach to simulating wave energy converter
hydrodynamics

7.2.2 Radiation Force Calibration Script

```

tic;
clc;
clear all;
close all;
addpath(genpath('PA2BH'));

% universal constants
g = 9.81; % gravity, m/s^2
rho = 1025; % saltwater density kg/m^3
fprintf('\n');

%% Define the inputs

del_t = 0.01; % Time step - forced by the Rhuel setup

[B1 B2 Moor damping] = definegeometry();

% Calculate impulse response functions from frequency domain data
[B1 B2 Bc tmax w] = impulserespcalc_rebuild(B1,B2,del_t);

%% Define the inputs

timestart = -tmax;
timeend = 639.5 + 800

t=timestart:del_t:timeend;
t = t';
mass1 = B1.m;
mass2 = B2.m;

%% Perform simulation and calculate offsets
[a b] = size(w);

for n = 18:b
    regWave = sin(w(n)*t);
n
    % time [s], wave surface elevation [m]
    eta = [t,regWave];

    sim('CalibrateFrModel.mdl');

    % Extract results from simulation record.
    perLength(n) = abs(round((2*pi)/(w(n)*del_t)));
    start_ss = 36000;
    stop_ss = start_ss + perLength(n);

```

A frequency-domain approach to simulating wave energy converter hydrodynamics

```
% inputs

[B1vel_max(n), B1vel_idx(n)] = max(z1_vel(start_ss:stop_ss));
B1vel_idx(n) = B1vel_idx(n) + start_ss;
[z1_vel_min(n), z1_vel_mdx(n)] = min(z1_vel(start_ss:stop_ss));

[B2vel_max(n), B2vel_idx(n)] = max(z2_vel(start_ss:stop_ss));
B2vel_idx(n) = B2vel_idx(n) + start_ss;
[z2_vel_min(n), z2_vel_mdx(n)] = min(z2_vel(start_ss:stop_ss));

[B1FrZ_max(n), B1FrZ_idx(n)] =
(max(B1FrZ(B1vel_idx(n):B1vel_idx(n)+perLength(n)))) ;
[B2FrZ_max(n), B2FrZ_idx(n)] =
(max(B2FrZ(B2vel_idx(n):B2vel_idx(n)+perLength(n)))) ;
[B1FrPM_max(n), B1FrPM_idx(n)] =
(max(B1FrPM(B1vel_idx(n):B1vel_idx(n)+perLength(n)))) ;
[B2FrPM_max(n), B2FrPM_idx(n)] =
(max(B2FrPM(B2vel_idx(n):B2vel_idx(n)+perLength(n)))) ;
[B1FrPR_max(n), B1FrPR_idx(n)] =
(max(B1FrPR(B1vel_idx(n):B1vel_idx(n)+perLength(n)))) ;
[B2FrPR_max(n), B2FrPR_idx(n)] =
(max(B2FrPR(B2vel_idx(n):B2vel_idx(n)+perLength(n)))) ;

end
save CalFrAll.mat;

z1_vel_amp = (B1vel_max - z1_vel_min)/2;
z2_vel_amp = (B2vel_max - z2_vel_min)/2;

B1FrPM_amp = B1FrPM_max;
B2FrPM_amp = B2FrPM_max;
B1FrPR_amp = B1FrPR_max;
B2FrPR_amp = B2FrPR_max;

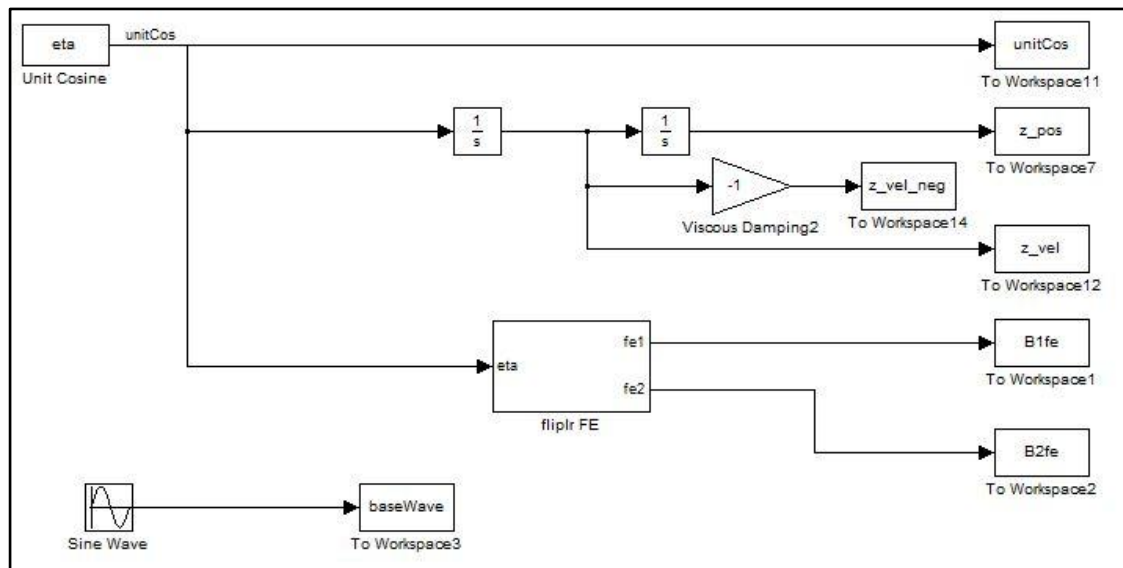
B1FrPR_adj_a = B1FrPR_amp - B1.KRpos/2;
B2FrPR_adj_a = B2FrPR_amp - B2.KRpos/2;
B1FrPM_adj_a = 1i*B1FrPM_amp - B1.KMpos/2;
B2FrPM_adj_a = 1i*B2FrPM_amp - B2.KMpos/2;

FrCalTime = toc/3600;

%% Output variables
save('CalFr', 'B1FrPR_adj_a',...
      'B2FrPR_adj_a',...
      'B1FrPM_adj_a',...
      'B2FrPM_adj_a',...
      'FrCalTime');
```

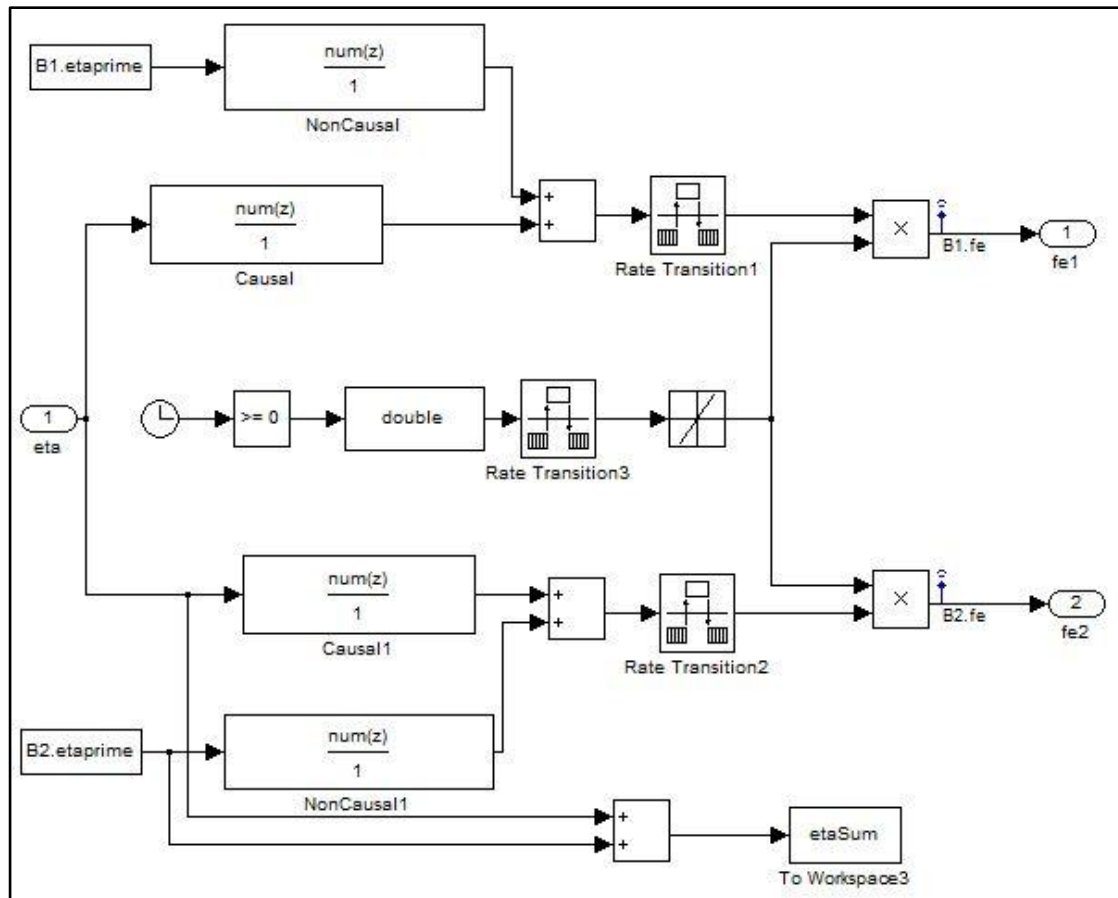
A frequency-domain approach to simulating wave energy converter
hydrodynamics

7.2.3 Excitation Force Calibration Schematic



Top Level

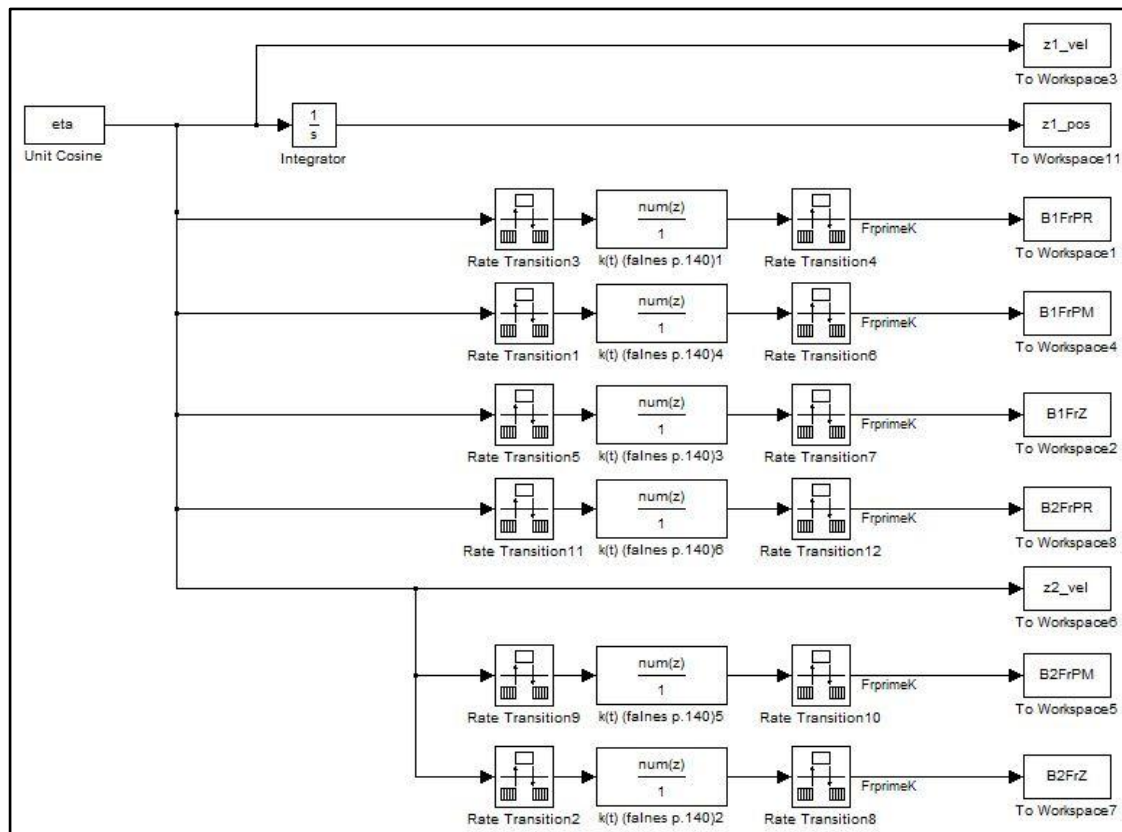
A frequency-domain approach to simulating wave energy converter hydrodynamics



Fliplr FE block

A frequency-domain approach to simulating wave energy converter
hydrodynamics

7.2.4 Radiation Force Calibration Schematic



A frequency-domain approach to simulating wave energy converter
hydrodynamics

A frequency-domain approach to simulating wave energy converter
hydrodynamics

8 References

- [1] J. Cruz, R. Sykes, P. Siddorn, and R. E. Taylor, "Estimating the loads and energy yield of arrays of wave energy converters under realistic seas," *Renewable Power Generation, IET*, vol. 4, pp. 488-497, 06/11/2010 2010.
- [2] M. E. McCormick, *Ocean Wave Energy Conversion*, Dover ed. Mineola: Dover Publications, 2007.
- [3] A. Babarit, "Impact of long separating distances on the energy production of two interacting wave energy converters," *Ocean Engineering*, vol. 37, pp. 718-729, 2010.
- [4] K. Thorburn, H. Bernhoff, and M. Leijon, "Wave energy transmission system concepts for linear generator arrays," *Ocean Engineering*, vol. 31, pp. 1339-1349, 2004.
- [5] I. t. Joint Technical Committee ISO/IEC JTC 1 and S. a. s. e. Subcommittee SC 7, "Systems and software engineering -- Vocabulary," *International Standards*, pp. 1-418, 2010-12-15 2010.
- [6] I. A. Svendsen, *Introduction to Nearshore Hydrodynamics*, xxi, 722 p ed. Hackensack, NJ: World Scientific, 2006.
- [7] I. R. Young, *Wind generated ocean waves*. Amsterdam; New York: Elsevier, 1999.
- [8] M. R. Belmont, J. M. K. Horwood, R. W. F. Thurley, and J. Baker, "Filters for linear sea-wave prediction," *Ocean Engineering*, vol. 33, pp. 2332-2351, 11/18/2005 2006.
- [9] J. R. Halliday, D. G. Dorrell, and A. R. Wood, "An application of the Fast Fourier Transform to the short-term prediction of sea wave behaviour," *Renewable Energy*, vol. 36, pp. 1685-1692, 29 November 2010 2011.
- [10] F. De Serio and M. Mossa, "Experimental study on the hydrodynamics of regular breaking waves," *Coastal Engineering*, vol. 53, pp. 99-113, 2006.
- [11] D. Millar, H. Smith, and D. Reeve, "Modelling analysis of the sensitivity of shoreline change to a wave farm," *Ocean Engineering*, vol. 34, pp. 884-901, 2007.
- [12] A. Van Dongeren, A. Reniers, J. Battjes, and I. Svendsen, "Numerical modeling of infragravity wave response during DELILAH," *J. Geophys. Res.*, vol. 108, p. 3288, 5 September 2003. 2003.
- [13] L. Cavaleri, J. H. G. M. Alves, F. Arduin, A. Babanin, M. Banner, K. Belibassakis, *et al.*, "Wave modelling - The state of the art," *Progress In Oceanography*, vol. 75, pp. 603-674, 23 May 2007 2007.
- [14] H. L. Tolman, B. Balasubramaniyan, L. D. Burroughs, D. V. Chalikov, Y. Y. Chao, H. S. Chen, *et al.*, "Development and Implementation of Wind-

A frequency-domain approach to simulating wave energy converter
hydrodynamics

Generated Ocean Surface Wave Modelsat NCEP*, "Weather and Forecasting, vol. 17, pp. 311-333, 13 April 2001 2002.

- [15] E. B. Agamloh, A. K. Wallace, and A. von Jouanne, "Application of fluid-structure interaction simulation of an ocean wave energy extraction device," *Renewable Energy*, vol. 33, pp. 748-757, 2008.
- [16] C. Beels, P. Troch, G. De Backer, M. Vantorre, and J. De Rouck, "Numerical implementation and sensitivity analysis of a wave energy converter in a time-dependent mild-slope equation model," *Coastal Engineering*, vol. 57, pp. 471-492, 16 November 2009 2010.
- [17] C. Beels, P. Troch, K. De Visch, J. P. Kofoed, and G. De Backer, "Application of the time-dependent mild-slope equations for the simulation of wake effects in the lee of a farm of Wave Dragon wave energy converters," *Renewable Energy*, vol. 35, pp. 1644-1661, 1 December 2009 2010.
- [18] J. M. B. P. Cruz and A. J. N. A. Sarmento, "Sea state characterisation of the test site of an offshore wave energy plant," *Ocean Engineering*, vol. 34, pp. 763-775, 26 April 2006 2007.
- [19] P. C. Vicente, A. F. de O. Falcão, L. M. C. Gato, and P. A. P. Justino, "Dynamics of arrays of floating point-absorber wave energy converters with inter-body and bottom slack-mooring connections," *Applied Ocean Research*, vol. 31, pp. 267-281, 2009.
- [20] J. Cruz, *Ocean wave energy : current status and future perspectives [i.e. perspectives]*. Berlin: Springer, 2008.
- [21] F. Iov and F. Blaabjerg, "Power electronics for renewable energy systems," in *Power Engineering, Energy and Electrical Drives, 2009. POWERENG '09. International Conference on*, 2009, pp. 9-12.
- [22] B. S. Lamb and K. Rhinefrank. (2011, 07/13/2011) Catch the Next Wave: Hydrodynamic simulation from ANSYS helps to deliver two- to three-times wave power efficiency improvement for Columbia Power Technologies. *Industry Today*. Available: http://www.industrytoday.co.uk/energy_and_environment/catch-the-next-wave-hydrodynamic-simulation-from-ansys-helps-to-deliver-two--to-three-times-wave-power-efficiency-improvement-for-columbia-power-technologies/5804
- [23] C. Yicheng, P. Pillay, and A. Khan, "PM wind generator topologies," *IEEE Trans. Ind. Appl.*, vol. 41, pp. 1619-1626, 2005.
- [24] T. K. A. Brekken, A. von Jouanne, and H. Han, "Ocean wave energy overview and research at Oregon State University," 2009, pp. 1-7.

A frequency-domain approach to simulating wave energy converter
hydrodynamics

- [25] E. A. Amon, A. A. Schacher, and T. K. A. Brekken, "A novel maximum power point tracking algorithm for ocean wave energy devices," in *Energy Conversion Congress and Exposition, 2009. ECCE 2009. IEEE*, 2009, pp. 2635-2641.
- [26] A. Babarit and A. H. Clément, "Optimal latching control of a wave energy device in regular and irregular waves," *Applied Ocean Research*, vol. 28, pp. 77-91, 26 May 2006
- 2006.
- [27] P. B. Garcia-Rosa, J. P. V. S. Cunha, and F. Lizarralde, "Turbine speed control for an ocean wave energy conversion system," in *American Control Conference, 2009. ACC '09.*, 2009, pp. 2749-2754.
- [28] J. K. H. Shek, D. E. Macpherson, M. A. Mueller, and J. Xiang, "Reaction force control of a linear electrical generator for direct drive wave energy conversion," *Renewable Power Generation, IET*, vol. 1, pp. 17-24, 13 February 2007 2007.
- [29] J. K. H. Shek, D. E. Macpherson, and M. A. Mueller, "Phase and amplitude control of a linear generator for wave energy conversion," in *Power Electronics, Machines and Drives, 2008. PEMD 2008. 4th IET Conference on*, 2008, pp. 66-70.
- [30] H. Bailey and I. Bryden, "Nonlinear Modelling of Power Take Off Systems," in *OCEANS 2007 - Europe*, 2007, pp. 1-5.
- [31] A. F. de O. Falcão, "Modelling and control of oscillating-body wave energy converters with hydraulic power take-off and gas accumulator," *Ocean Engineering*, vol. 34, pp. 2021-2032, 7 February 2007
- 2007.
- [32] N. M. Kimoulakis and A. G. Kladas, "Modeling and control of a coupled electromechanical system exploiting heave motion, for energy conversion from sea waves," in *PESC 2008. IEEE*, 2008, pp. 3850-3853.
- [33] A. El Marjani, F. Castro Ruiz, M. A. Rodriguez, and M. T. Parra Santos, "Numerical modelling in wave energy conversion systems," *Energy*, vol. 33, pp. 1246-1253, 31 July 2007 2008.
- [34] M. Folley and T. Whittaker, "Spectral modelling of wave energy converters," *Coastal Engineering*, vol. 57, pp. 892-897, 12 May 2010
- 2010.
- [35] A. E. Kiprakis, A. J. Nambiar, D. Forehand, and A. R. Wallace, "Modelling arrays of wave energy converters connected to weak rural electricity networks," in *Sustainable Power Generation and Supply, 2009. SUPERGEN '09. International Conference on*, 2009, pp. 1-7.
- [36] M. Leijon, C. Boström, O. Danielsson, S. Gustafsson, K. Haikonen, O. Langhamer, *et al.*, "Wave Energy from the North Sea: Experiences from the

A frequency-domain approach to simulating wave energy converter
hydrodynamics

Lysekil Research Site," *Surveys in Geophysics*, vol. 29, pp. 221-240, 23 September 2008 2008.

- [37] S. McArthur and T. K. A. Brekken, "Ocean wave power data generation for grid integration studies," in *Power and Energy Society General Meeting, 2010 IEEE*, 2010, pp. 1-6.
- [38] M. Huang and G. Aggidis, "Developments, expectations of wave energy converters and mooring anchors in the UK," *Journal of Ocean University of China (English Edition)*, vol. 7, pp. 10-16, 2008.
- [39] D. Stewart and D. Hallenbeck, "Three case histories of virtual prototypes to support concurrent engineering," in *Electronics Industries Forum of New England, 1997. Professional Program Proceedings*, 1997, pp. 85-96.
- [40] R. G. Dean and R. A. Dalrymple, *Water wave mechanics for engineers and scientists*. Singapore ; Teaneck, NJ: World Scientific, 1991.
- [41] J. Falnes, *Ocean Waves and Oscillating Systems - Linear Interactions Including Wave-Energy Extraction*: Cambridge University Press.
- [42] R. H. Stewart. (2008, 04/28/2011). *Introduction to Physical Oceanography* [PDF]. Available: http://oceanworld.tamu.edu/resources/ocng_textbook/PDF_files/book.pdf
- [43] R. G. Dean and R. A. Dalrymple, *Coastal Processes with Engineering Applications*. Cambridge: Cambridge University Press, 2004.
- [44] J. Andrews and N. A. Jolley, *Energy science : principles, technologies, and impacts*. Oxford ; New York: Oxford University Press, 2007.
- [45] N. D. B. C. NDBC. (2008, 10/31). *NDBC Virtual Tour* [SHTML]. Available: <http://www.ndbc.noaa.gov/tour/virtr1.shtml>
- [46] N. D. B. C. NDBC, "Handbook of Automated Data Quality Control Checks and Procedures," NDBC, Ed., August 2009 ed. Stennis Space Center: NDBC, 2009, p. 78.
- [47] D. W. Kammler, *A First Course in Fourier Analysis*: Cambridge University Press, 2007.
- [48] F. Hensler, "AQWA ", A. Simmons, Ed., ed, 2011.
- [49] webmaster@wamit.com. (2008, 30 April). *Company Info* [HTML]. Available: <http://www.wamit.com/companyinfo.htm>
- [50] G. Thomas, "The Theory Behind the Conversion of Ocean Wave Energy: a Review," in *Ocean wave energy : current status and future perspectives [i.e. perspectives]*, J. Cruz, Ed., ed Berlin: Springer, 2008, pp. 41-91.
- [51] R. Shaw, *Wave energy : a design challenge*. Chichester, West Sussex New York: E. Horwood ; Halsted Press, 1982.

A frequency-domain approach to simulating wave energy converter
hydrodynamics

- [52] T. A. K. Brekken, "Dynamics of Electromechanical Energy Conversion," ed. Corvallis, Oregon: Oregon State University, Department of Electrical and Computer Engineering, 2009.
- [53] K. Ruehl, "Time-Domain Modeling of Heaving Point Absorber Wave Energy Converters, Including Power Take-Off and Mooring," Master of Science, Mechanical Engineering, Mechanical Engineering, Oregon State University, Corvallis, 2011.
- [54] E. Bouws, H. Günther, W. Rosenthal, and C. Vincent " Similarity of the Wind Wave Spectrum in Finite Depth Water 1. Spectral Form," *J. Geophys. Res.*, vol. 90, p. 11, January 20, 1985 1985.
- [55] T. K. A. Brekken, H. T. Özkan-Haller, and A. Simmons, "Title," unpublished].
- [56] E. F. Thompson, D. United States. Army. Corps of Engineers. Pacific Ocean, U. S. A. E. W. E. Station, and C. Coastal Engineering Research, *Wave response of Kahului Harbor, Maui, Hawaii*. Vicksburg, Miss.: U.S. Army Engineer Waterways Experiment Station, 1996.
- [57] ANSYS. (2012). *AQWA Reference Manual* [PDF].
- [58] H. Anton, *Calculus with Analytic Geometry*, 2nd ed. New York: Wiley & Sons, 1984.
- [59] B. P. a. Z. D. Lathi, *Modern Digital and Analog Communication Systems*, 4th ed. xix, 1004 p ed. New York: Oxford University Press, 2009.
- [60] M. Tucker, P. Challenor, and D. Carter, "Numerical simulation of a random sea: a common error and its effect upon wave group statistics," *Applied Ocean Research*, vol. 6, pp. 118-122, 1984.
- [61] M. J. H. A.L. Silver, R.E. Conrad, S.S. Lee, J.T. Klamo, J.T. Park, "Evaluation of Multi-Vessel Ship Motion Prediction Codes," Hydromechanics, Ed., ed. West Bethesda, MD 20817-5700: Navel Surface Warfare Center Carderock Division, 2008.